

ISTANBUL TECHNICAL UNIVERSITY ★ GRADUATE SCHOOL OF SCIENCE
ENGINEERING AND TECHNOLOGY

**STUDY AND DESIGN OF CIRCULARLY POLARIZED ANTENNAS FOR
WIRELESS APPLICATIONS**

M.Sc. THESIS

Sasan AHDI REZAEIEH

Department of Electrical and Electronics Engineering

Telecommunication Engineering Programme

Thesis Advisor: Prof. Dr. Ibrahim AKDUMAN

JANUARY 2012

ISTANBUL TECHNICAL UNIVERSITY ★ GRADUATE SCHOOL OF SCIENCE
ENGINEERING AND TECHNOLOGY

**STUDY AND DESIGN OF CIRCULARLY POLARIZED ANTENNAS FOR
WIRELESS APPLICATIONS**

M.Sc. THESIS

Sasan AHDI REZAEIEH
(504091395)

Department of Electrical and Electronics Engineering

Telecommunication Engineering Programme

Thesis Advisor: Prof. Dr. Ibrahim AKDUMAN

JANUARY 2012

İSTANBUL TEKNİK ÜNİVERSİTESİ ★ FEN BİLİMLERİ ENSTİTÜSÜ

**KABLOSUZ UYGULAMALAR İÇİN DAİRESEL POLARİZE ANTENLERİN
TASARIM VE ARAŞTIRMASI**

YÜKSEK LİSANS TEZİ

**Sasan AHDI REZAEIEH
(504091395)**

Elektrik ve Elektronik Mühendisliği Anabilim Dalı

Telekomünikasyon Mühendisliği Programı

Tez Danışmanı: Prof. Dr. İbrahim AKDUMAN

OCAK 2012

Sasan ahdi rezaeieh, a **M.Sc.** student of **ITU Graduate School of Science Engineering and Technology** student ID **504091395**, successfully defended the thesis entitled “**Study and design of circularly polarized antennas for wireless applications**”, which he prepared after fulfilling the requirements specified in the associated legislations, before the jury whose signatures are below.

Thesis Advisor : **Prof. Dr.** **Ibrahim AKDUMAN**
İstanbul Technical University

Jury Members : **Prof. Dr. Ibrahim AKDUMAN**
İstanbul Technical University

Doc. Dr. Ali YAPAR
İstanbul Technical University

Doc. Dr. Ahmet KIZILAY
Yıldız Technical University

Date of Submission : 19 December 2011
Date of Defense : 24 January 2012

To my parents ZIBA & ALIREZA,

My sister SAMAN

and my sweetheart NEGIN

FOREWORD

I would like to express my deepest appreciation and gratitude to my academic and research advisor, Professor Dr. Ibrahim AKDUMAN for his advice and invaluable guidance throughout my research. This work would have been impossible without his precious support and encouragement. I would also want to thank PhD student Mehmet Abbak for his great help in constructing and measurement of the antennas in electromagnetic laboratory of Istanbul technical University. After all my great thanks to my father ALIREZA which this work was not possible without his support and to my mother ZIBA which I had always felt her prays with me.

November 2011

Sasan AHDI REZAEIEH

TABLE OF CONTENTS

	<u>Page</u>
FOREWORD	ix
TABLE OF CONTENTS	xi
ABBREVIATIONS	xiii
LIST OF TABLES	xv
LIST OF FIGURES	xvii
SUMMARY	xix
ÖZET	xxi
1. INTRODUCTION	25
1.1 Purpose of Thesis	26
2. ANTENNA THEORY AND BASIC PARAMETERS OF AN ANTENNA	29
2.1 Antenna	29
2.2 Field Regions of Antenna.....	30
2.2.1 Far field region.....	30
2.2.2 Reactive near field region	30
2.2.3 Near field (Frensel) region	31
2.3 Radiation Pattern	32
2.4 Polarization of an Antenna	32
3. OVERVIEW OF CIRCULARLY POLARIZED ANTENNAS	35
3.1 Advantages Of Circularly Polarized Antennas	35
3.1.1 Reflectivity.....	35
3.1.2 Absorption.....	35
3.1.3 Phasing issues	35
3.1.4 Multi path.....	36
3.1.5 Inclement weather	36
3.1.6 Line of sight	36
3.1.7 Power loss	36
3.2 Circularly Polarized Square Slot Antennas	37
3.3 Annular Ring Slot Antennas	40
3.4 Overview of Microstrip Antennas.....	41
3.4.1 Direct feed.....	42
3.4.2 Inset feed	42
3.4.3 Gap coupled	42
3.4.4 Proximity coupled feeding	43
3.4.5 Microstrip circularly polarized.....	44
4. DESIGN OF CIRCULARLY POLARIZED ANTENNAS	45
4.1 A New Triple Band Circularly Polarized Square Slot Antenna Design with Crooked T and F-Shape Strips for Wireless Applications	45
4.1.1 Introduction.....	45
4.1.2 Antenna design.....	46

4.1.3 Parametric study of the antenna	49
4.1.3.1 Studying effects of L_{16}	51
4.1.3.2 Studying effects of W_7	52
4.1.3.1 Studying effects of L_6 and L_{10}	53
4.2 Dual Band Dual Sense Circularly Polarized Monopole Antenna For GPS And WLAN Applications.....	59
4.2.1 Antenna design.....	59
4.2.2 Parametric study of the antenna	60
4.3 Abroadband Asymmetric CPW Fed Circularly Polarized Antenna With Defected Substrate.....	63
4.3.1 Introduction	63
4.3.2 Antenna design.....	64
4.3.3 Design procedures	65
4.3.3.1 Effects of L_h on CP	69
4.3.3.2 Effects of L_{h2} and L_{h3} on CP band.....	70
4.3.3.3 Effects of L_{x1} and R on CP	71
4.3.3.4 Further design verifications.....	72
4.3.4 Measured results.....	72
4.3.5 Conclusion.....	75
4.4 Broadband CPW-Fed Circularly Polarized Square Slot Antenna with Inverted L-strips for Wireless Applications.....	78
4.4.1 Antenna design.....	78
4.4.2 Parametric study.....	79
5. CONCLUSIONS AND RECOMMENDATIONS	87
REFERENCES	88
CURRICULUM VITAE.....	93

ABBREVIATIONS

CP	: Circular Polarization
CPSSA	: Circularly Polarized Square Slot Antenna
AR	: Axial Ratio
ARBW	: Axial Ratio Bandwidth
FCPBW	: Fractional Circular Polarization Bandwidth

LIST OF TABLES

	<u>Page</u>
Table 4.1 : Measured S_{11} and 3dB ARBW _s of CPSS antennas	59
Table 4.2 : Parameters and performance of three antennas under investigation.....	60
Table 4.3 : Measured 3-Db Arbws, And Measured Vswr<2 Impedance Bandwidths Of Antennas 1–4 (F_c Is The Center Frequency Of Vswr<2) (Unit: mm) 75	75
Table 4.4 : Measured Performances Of The Proposed Antenna In The Development Process; $\epsilon_r=4.4$, $\tan \delta=0.02$, $H=0.8$, $G=60$, $L=28$, $W_f=3$, $G=0.3$ (F_c Is The Center Frequency Of Vswr<2)(Unit: mm)	77
Table 4.5 : Measured performances of the proposed antennas with different substratethicknesses (F_c is the cented frequency of the VSWR<2)(unit:mm)	77
Table 4.6 : Comparison of characteristics of some CPSS antennas reported with the proposed antenna in this work	84
Table 4.7 : Summary of measured and simulated characteristics of some CPSS antennas. The impedance bandwidth is the frequency range where the VSWR is equal to or less than 2 ($\epsilon_r=4.4$, $\tan \delta=0.024$, $H=0.8$, $G=40$, $L=28$, $G=0.3$, $W=3$, $L_f = 6$, $L_t =3.5$, $W_x=6.25$, $L_h=10$) (Unit: mm).....	85

LIST OF FIGURES

	<u>Page</u>
Figure 2.1 : Reactive near field, Near field and far field of an antenna.....	31
Figure 2.2 : The Rays from any Point on the Antenna	31
Figure 2.3 : Radiation pattern of a typical dipole	32
Figure 2.4 : Polarization Coordinates	33
Figure 2.5 : Polarization as a Function of E_y/E_x and Phase angle	33
Figure 2.6 : Circular Polarization - E Field.....	34
Figure 3.1 : Polarization ellipse illustrating the parameters associated with polarized electromagnetic wave propagation	37
Figure 3.2 : Typical square slot antenna structure	38
Figure 3.3 : Antenna presented in [4]	39
Figure 3.4 : (a) square slot with crisscross patch, (b) inverted-L conducting strip slot	40
Figure 3.5 : Different feeds for annular ring antennas	40
Figure 3.6 : Direct microstrip feed line.....	42
Figure 3.7 : Gap-coupled microstrip feed line	42
Figure 3.8 : Inset microstrip feed line	43
Figure 3.9 : Proximity coupled microstrip feeding.....	43
Figure 3.10 : Different microstrip circularly polarized antenna configurations	44
Figure 4.1 : Geometry of the proposed CP triple band antenna.....	47
Figure 4.2 : Four improved prototypes of the antenna.....	49
Figure 4.3 : Improved S_{11} of the antenna	49
Figure 4.4 : S_{11} of the proposed antennas in figure 4.2	50
Figure 4.5 : Axial ratio of the proposed antennas in figure 4.2	51
Figure 4.6 : S_{11} for different iterations of L_{16}	51
Figure 4.7 : Axial Ratio for different iterations of L_{16}	52
Figure 4.8 : S_{11} for different iterations of W_7	52
Figure 4.9 : Axial Ratio for different iterations of W_7	53
Figure 4.10 : S_{11} for different iterations of L_6	54
Figure 4.11 : Axial Ratio for different iterations of L_6	54
Figure 4.12 : Axial Ratio for different iterations of L_{10}	54
Figure 4.13 : Distribution of the surface current on the feed and ground of the CPSS antenna at 5.4 GHz in 0° , 90° , 180° , and 270° phase.....	56
Figure 4.14 : Measured radiation patterns of the antenna at 4.8GHz (Left) and 5.3GHz (Right) at (a) $\varphi=0^\circ$, (b) $\varphi=90^\circ$	56
Figure 4.15 : Photograph of the four prototypes of CPSS antennas	57
Figure 4.16 : Measured and simulated (a) impedance matching and 3dB axial ratio bandwidths of the proposed CPSSA with frequency and (b) different φ angles at sample frequency of 5GHz.....	57

Figure 4.17 : Measured group delay of the antenna.....	58
Figure 4.18 : Measured and simulated gain of the CPSSA.....	58
Figure 4.19 : Distribution of the surface current on the feed and ground of the CPSS antenna at 5GHz	58
Figure 4.20 : Geometry of the proposed CP monopole antenna	60
Figure 4.21 : Measured return losses and CP axial ratios of Ant. I, II, III and simulated data of Ant.III.....	62
Figure 4.22 : (a) radiation pattern of the Ant.III in Phi=90 at (a) 1.8GHz, (b) 4.8G.....	62
Figure 4.23 : Measured and simulated gain of the proposed CP Ant.III (a) radiation pattern of the Ant.III in Phi=90 at (a) 1.8GHz, (b) 4.8GHz.....	63
Figure 4.24 : Geometry configuration of proposed CPSSA antenna	64
Figure 4.25 : Improved prototypes of the presented CPSSA in design procedure ...	65
Figure 4.26 : Simulated (a) S_{11} and (b) axial ratio curves of the four improved prototypes of the CP antenna	67
Figure 4.27 : Current surfaces of the antenna with and without defected substrate at sample frequencies of (a) 4GHz (b) 5GHz.....	68
Figure 4.28 : Current distributions of 0° , 90° , 180° and 270° at sample CP frequency of 5GHz	68
Figure 4.29 : Simulated (a) S_{11} and (b) axial ratio variations for different values of L_h	69
Figure 4.30 : Simulated (a) S_{11} and (b) axial ratio variations for different values of L_{h2}	70
Figure 4.31 : Simulated (a) S_{11} and (b) axial ratio variations for different values of L_{h3}	71
Figure 4.32 : Photograph of the optimized antenna (Ant.4)	73
Figure 4.33 : Measured and simulated (a) impedance matching (b) 3dB ARBW of the optimized antenna (Ant. 4) and (c) measured axial ratio of the antenna at different phi values at sample frequency of 5.2GHz	74
Figure 4.34 : Measured and simulated gain of Ant. 4.....	75
Figure 4.35 : Measured radiation patterns: 4.5GHz (a) $\varphi=0$, (b) $\varphi=90$ and 5.5GHz (c) $\varphi=0$, (d) $\varphi=90$	77
Figure 4.36 : Geometry details of the proposed CPSS antenna (Unit:mm)	78
Figure 4.37 : Four improved prototypes of the proposed CPSSA	79
Figure 4.38 : Simulated S_{11} and AR for antennas 0-III (for CPSS antennas with optimized values of the design parameters summarized in Table 4.8).....	80
Figure 4.39 : Simulated and measured S_{11} and AR for Ant III	82
Figure 4.40 : Current distribution of the antenna at 0, 90,180 and 270 degrees	83
Figure 4.41 : Measured radiation patterns at 3.5 and 5.05GHZ at $\varphi=0$ and at $\varphi=90$ and measured gain of Ant. III.....	83
Figure 4.42 : Measured and simulated gain of the antenna.....	84

STUDY AND DESIGN OF CIRCULARLY POLARIZED ANTENNAS

SUMMARY

Due to the increasing usage of wireless communication applications, the performance improvement studies of such systems has found a growing investigation area in recent years. Antennas as one of the most important parts of these systems have gained a great attention. Among the various types of antennas, circularly polarized (CP) antennas are the most desired ones, owing to their inevitable merits like reducing polarization mismatch and multipath fading. To benefit from broadband and low profiles, various shapes and designs of broadband circularly polarized slot antennas have been developed by applying different techniques on patch and ground structures. Patch, microstrip and slot antennas due to their compatibility with integrated circuit systems are widely being used in circularly polarized structures. Recently different methods are presented for creating circularly polarized operation band. Embedding two inverted-L grounded strips around two opposite corners of the slot, embedding spiral slots in the slot, utilizing a shorted square-ring slot, annular-ring slots, the corrugated slot and meander line are of the most popular and recently presented techniques. But most of the presented antennas in the current literature have either large sizes as $80\text{mm} \times 80\text{mm}$, $60\text{mm} \times 60\text{mm}$ or narrow impedance matching as well as small axial ratio bandwidths. This thesis presents new techniques both in slot structures and feeding structures of circularly polarized antennas. Using these new techniques important results regarding the impedance matching and axial ratio bandwidth of the designed antennas are achieved. Antennas presented in this thesis work are designed in two different categories. The first category are the antennas based on optimizing the size and axial ratio and impedance matching bandwidths of the previously reported antennas. The second category are the novel designs and new techniques that are obtained during the studies done for this work. Through extensive simulation and measurements done, the designed antennas are all

optimized and presented. All the designed antennas are simulated using Ansoft High Frequency Structure Simulator (HFSS) and measured in the anechoic chamber of Istanbul Technical University.

KABLOSUZ DAİRESEL POLARİZE ANTENLER TASARIMI VE ARAŞTIRMASI

ÖZET

Son yıllarda kablosuz haberleşme uygulamalarında gerçekleşen artış nedeniyle, söz konusu sistemlerin performanslarının iyileştirilmesine yönelik araştırmalar önemli bir çalışma alanı oluşturmaktadır. Bu sistemlerin en önemli parçalarından birisini oluşturan antenler konusunda yoğun çalışmalar sürdürülmektedir. Anten, Elektronikte, boşlukta yayılan elektromanyetik dalgaları toplayarak bu dalgaların iletim hatları içerisinde yayılmasını sağlayan (alıcı anten) veya iletim hatlarından gelen sinyalleri boşluğa dalga olarak yayan (verici anten) cihazlardır. Elektromanyetik dalga, ışımının dalga teorisine göre, uzayda ya da maddesel bir ortamda yayılan ve salınım yapan bir elektrik alan vemanjetik alanın birlikte oluşturduğu kabul edilen dalgalara verilen addır. Antenler dalga boylarına göre boyutlanıp şekillenir ve genellikle dalga boylarına göre adlandırılırlar. GSM, wireless, radio ve tv yayınları, kablosuz anons sistemleri, telsizler, radarlar, bluetooth cihazları gibi uzun ya da kısa mesafe erişimli tüm sistemler birer anten sistemine sahiptir. Fiziki olarak anten, bir ya da birkaç kondüktörden oluşan düzenektir. Üzerine uygulanan enerjiyi manyetik alan enerjisi olarak ortama yayan anten aynı zamanda bunun tam tersi biçimde çalışır. İlk anten örneklerinin Heinrich Hertz tarafından 1888 yılında James Clerk Maxwell'in teorisini olan elektromanyetik dalgaların varlığını kanılamak amacıyla yapıldığı bilinmektedir. Hertz ilgili çalışma ve çizimlerini Annalen der Physik und Chemie (vol. 36, 1889) eserinde yayınlamıştır. Antenler Omni-directional yani her yöne ve Directional yani belirli bir yöne doğru alma ya da gönderme yapan antenler olarak ana gruplara ayrılırlar. Çeşitli amaçlara göre yön, kazanç ve ebat gibi konular dikkate alınarak en uygun anten sistemi kullanılır. Antenlerin boyları kilometrelerden milimetrelere kadar geniş bir yelpazeye sahiptir. Bir çok anten türü arasından dairesel polarize (DP) antenler, polarizasyon uyumsuzluğu ve çok yönlü sönümlenme etkilerini azaltmak gibi vazgeçilmez

özellikleri nedeniyle en çok tercih edilen antenlerdir. Polarizasyon dalganın hareket yönüne dik gelen düzlemdeki salınımların yönünü tanımlayan yansıyan dalgaların bir özelliğidir. Bu kavram dalga yayılımı ile ilgilenen optik, sismoloji ve uziletişim gibi bilim ve teknoloji sahalarında kullanılmaktadır. Elektrodinamikte polarizasyon, ışık gibi elektromanyetik dalgaların elektrik alanının yönünü belirten özelliğini ifade eder. Sıvılarda ve gazlarda ses dalgaları gibi boyuna dalgalar polarizasyon özelliği göstermez çünkü bu dalgaların salınım yönü uzunlamasına yani yönü dalganın hareketinin yönü tarafından belirlenmektedir. Tersine elektromanyetik dalgalarda (elektrik sahaya ait) salınımın yönü sadece yayılımın yönü ile belirlenmemektedir. Benzer şekilde katı bir maddede yansıyan ses dalgasında paralel stres yayılım yönüne dik gelen bir düzlemde her türlü yönlendirmeye tabi olabilir. Polarizasyon terimi dolayısıyla yansıyan dalga yoluna dik gelen düzlemdeki salınım işleminin olası yönlendirmelerini ifade eder. Bu antenler gezgin haberleşme sistemlerinden, erken uyarı sistemlerine, yeraltı görüntüleme radarlarından, yön bulma sistemlerine kadar bir çok alanda kullanılmaktadır. Anten çizgesi, bir antenden yayınlanan enerjinin göreceli yoğunluğu, veya elektrik ya da manyetik alan kuvvetlerini yöne bağlı olarak gösterir. Bir radaranteninin yönsel karakteristiklerini gösterir. Anten çizgesinde bir radar anteninin yöne bağlı olarak yayın kuvveti çizgesel (graphical) olarak gösterilir ve böylece o yöndeki yayın gücü için bir kestirim yapılabilir. Bu çizgeler, ölçü yöntemleri veya bilgisayarda benzetim (simulation) programları ile çizilir. Bir düzlem içinde her yönde eşit miktarda yayın yapabilen bir yön bağımsız (omni-directional) antene karşılık, yön bağımlı anten ile yayın bir yönde yoğunlaşır ve bu sayede daha az bir gönderim gücü ile daha uzun menzillere ulaşmak mümkün olabilir. Bir antene ait gönderim- ve alım çizgesinin karşılıklılık (reciprocity) özelliği nedeniyle, hem gönderilen yayının belirli bir yöndeki kuvvetini, hem de antenin bu yöndeki alım duyarlılığı tayin etmek mümkün olur. Yatay anten çizgesi hem kartezyen hem de kutupsal (polar) koordinat sisteminde çizilebilir. Kartezyen koordinat sistemi ile anten verileri daha iyi gösterilebilir. Bu veriler keza bir çizelge ile listelenebilir. Daha anlaşılabilir gösterim için kartezyen koordinat sisteminin aksine, yayın yönü açısının doğrudan gösterildiği kutupsal koordinat sistemi genellikle yeğlenir. Yayın gücü kutupsal koordinat sisteminde lokal eğrilerle belirtilir. Bu çizgede merkezinde antenin bulunduğu antene ait elektromanyetik alanının iki boyutlu düzlemde ki havadan görünüşü verilir. Diğer antenler kadar mikroşerit üzerinde tasarlanan antenlerde de dairesel polarize söz konusu. Geniş

banttan ve düşük profilden faydalanmak için, yama antenler ve anten toprağı yapıları üzerinde farklı teknikler uygulanarak farklı şekil ve tasarımlarda geniş bantlı dairesel polarize yarık antenler geliştirilmiştir. Yama, mikroşerit ve mikroşerit yarık antenler, entegre devre sistemlerine uyumlulukları nedeniyle, dairesel polarize yapılarda sıklıkla kullanılmaktadır. Son zamanlarda, dairesel polarize çalışma bantları oluşturmak amacıyla farklı yöntemler geliştirilmektedir. Bu yöntemlerin bazıları, yarığın iki zıt köşesine iki adet ters L topraklanmış şerit yerleştirilmesi, yarığa spiral yarıklar yerleştirilmesi, kısa devre edilmiş kare ve annular halka yarıklarının kullanılması, kıvrımlı yarıklar ve kıvrık hat kullanılmasıdır. Ancak, literatürde bulunan antenlerin büyük kısmı 80mm × 80mm, 60mm × 60mm gibi büyük boyutlara, dar empedans uyumuna veya küçük eksensel oran bant genişliğine sahiptirler. Bu tez, dairesel polarize antenlerin hem besleme hem de yarık yapıları için yeni teknikler önermektedir. Bu tez çalışmasında sunulan antenler iki farklı kategoride tasarlanmıştır. İlk kategori daha önce sunulan antenlerin band uyumluluğu ve aksenal optimizasyonu üzerine yapılmıştır. İkinci kategori tamamen yeni tasarımlardan oluşmuştur. Kapsamlı simülasyon ve yapılan ölçümler sayesinde, tüm tasarlanmış antenler optimize edilmiştir. Günümüzde geniş bantlı antenler ya da anten dizileri haberleşme sistemlerinin test ve ölçülerinin vazgeçilmezleri arasında. Anten test ve ölçüleri, ister emisyon ölçüleri olsun isterse bağışıklık testleri, her ürün için hazırlanan standartlarda belirtilen geniş bir band içinde yapılmak zorunda. Örneğin, radyo, TV cihazı, bilgisayar, telsiz telefon benzeri evsel gereçlerin DC'den yaklaşık 1 GHz'e kadar ölçü ve testleri yapılmak zorunda. Benzer şekilde dizüstü ya da avuç içi bilgisayarlarla haberleşme sistemlerinde, ofis içi, kısa mesafe (bluetooth) uygulamalarında, 900-1800-1900 MHz 3-bandlı GSM haberleşmesinde ve GSM cihazlarının bilgisayarlarla haberleşmesinde amaç tek bir anten sistemi ile bütün bu frekansları kapsayacak haberleşmeyi sağlayabilmek yönünde. Bugün kullanıcı dizüstü bilgisayarından ya da cep telefonundan FM radyo dinlemekten tutun, internet uygulamalarına, konuşmadan mesaj göndermeye hemen her şeyi tek bir cihaz üzerinden yapmak istemekte. Üretici de tüm bu servisleri verecek anten sisteminin peşinde. Tüm isterleri karşılayacak anten sistemleri kaçınılmaz olarak geniş bantlı olmak zorunda. Tüm tasarlanmış antenler Ansoft Yüksek Frekans Yapı Simülatörüyle (HFSS) simule edilmiş ve İstanbul Teknik Üniversitesi anekoik yansız odasında ölçülmüştür. Bu odadan alınan datalar network analyzerde islenip ve antenlerin karakteristigi elde edilmiştir.

1. INTRODUCTION

Through extensive demand for high rate communications nowadays, telecommunication systems are seeking for the most efficient ways of data transmission. Antennas as one of the key elements of the communication systems play an important part in transmissions of data. In a typical wireless communication system, increasing the gain of antennas used for transmission increases the wireless coverage range, decreases errors, increases achievable bit rates and decreases the battery consumption of wireless communication devices. One of the main sources of the losses in communication systems is the polarization mismatch in transceiver systems. To achieve this polarization matching the transmitter and the receiver should have the same axial ratio, spatial orientation and the same sense of polarization. To overcome this problem circularly polarized antennas are designed and investigated during years. Circularly polarized antennas owing to their inevitable merits like reducing polarization mismatch and multipath fading are among the most desired ones. To benefit from broadband and low profiles, various shapes and designs of broadband circularly polarized slot antennas have been developed to overcome both the narrow impedance and axial-ratio bandwidths (ARBW) by applying different techniques on patch and ground structures [15]-[44]. Array structures presented in [15], [18] and [21] use the same but duplicated structure in different special or phase positions to obtain circular polarization. Patch, microstrip and slot antennas due to their compatibility with integrated circuit systems are also widely used in CP structures [15-16], [20], [22], [26-27]. The antennas proposed in [28] and [31] have investigated upon embedding two inverted-L grounded strips around two opposite corners of the slot, each of which using different feedline shapes. Embedding two spiral slots is also presented in [29], in which current circulation in the spiral slots are employed to achieve the CP operation. Utilizing a shorted square-ring slot is another way of creating CP antennas which is presented in [30]. Recently some annular-ring slots [32], [34] are employed to achieve the CP characteristic. In these antennas the circular polarization is attained through a double-

bent microstrip line that feeds the antenna at two different positions. In [33], C-like monopole with one sleeve is used in order to excite the CP and improve the impedance bandwidth of the antenna. Asymmetric square slot presented in [35] and [36] provides a CP bandwidth which is larger than 10% simply by using an inverted-L tuning stub protruded from the signal line of the coplanar waveguide (CPW). In the stair-shaped slot presented in [37], CP operation is obtained by etching a longitudinal slot at a middle point of a stair-shaped slot. In [38], by introducing the corrugated slot and meander line, both the impedance bandwidth and CP bandwidth could be improved. Finally ring slot antenna, reported in [39], achieves CP radiation by introducing proper asymmetry in the ring slot structure and feeding the ring slot using a microstrip line at 45° from the introduced asymmetry. All of the discussed antennas have large dimensions which are not appropriate to be used in wireless communication systems. Also most of them have either small ARBWs or narrow impedance matching bandwidth. Starting with this motivation, in this letter, a new triple band, compact CPW-fed, circularly polarized square slot antenna with dual monopole feed and crooked F and T-strips is presented. The antenna has three functional bands operating from 1.96GHz to 3.26GHz, 3.61GHz to 6.98GHz and 7.87GHz to 11.24GHz. This design (for the optimized values) supports the three bandwidths in terms of impedance matching but for the 3dB ARBW, it supports only the second band. Employing dual monopole structure enhances the antenna with large bandwidth and small size. Also the proposed antennas in this work has the capability of showing CP characteristics in the important standards such as IEEE 802.11b/g (2.4–2.484 GHz), IEEE 802.11a (5.15–5.35 GHz and an additional band of 5.725–5.825 GHz), and HiperLAN2 (5.47–5.725 GHz) [28]-[29].

1.1 Purpose of Thesis

Circularly polarized antennas have been object of a considerable interest in the last years and a growing number of communication-navigation services are already working or are planning to use these kinds of antennas. The antennas presented in most of the previously reported works, cannot cover all of the standardized bands or cover just part of these bands like WLAN operating band. In addition, most of the antennas presented in the literature have big sizes, narrow impedance matching bandwidth, narrow axial ratio bandwidth or complicated structures. Motivating

through these drawbacks a study covering all these problems, and suggesting solutions for these drawbacks is presented in this work. Four novel types of such antennas have been designed, realized and measured in the anechoic chamber room of Istanbul Technical University. Through these four antennas four different techniques are used to excite the circular polarization. This special kind of polarization is excited when the E vector has the same amplitude and 90 degrees phase difference. In the first design a pair of crooked F-shape and a T-shape strip is used to enhance the antenna with wide 3dB axial ratio. In this design to gain a broadband a dual monopole technique is used in the feeding structure. Dual monopole structure also helps the enhancement of the 3dB axial ratio. The presented circularly polarized square slot antenna (CPSSA) design has the compact dimensions of $40 \times 40 \times 0.8$ mm³, total impedance matching bandwidth of 8.04GHz and exhibiting a 28.03% (4.6–6.1 GHz) 3dB axial ratio bandwidth. In this work a new, yet structurally simple, microstrip fed CP antenna is presented for GPS and WLAN applications. By inserting orthogonally located slots on the circular patch and extending the slot number, the designed antenna is found to possess a 3dB axial ratio bandwidth (ARBW) larger than 40%. The 3dB AR band is also found completely enclosed by the $VSWR < 2$ impedance match. In the third design a compact asymmetric coplanar waveguide CPW-fed circularly polarized antenna with defected substrate for broadband applications. The antenna is designed to have a U-shaped feedline in conjunction with an inverted L-strip and a 45° bent strip to cover a broad band of more than 103% in the frequency range of 2.69 to 8.83 GHz and 3dB axial ratio bandwidth (ARBW) of 58.93% in 2.92 to 5.36 GHz. Triangle shaped pieces are removed from top corners of the antenna to have better current surface circulation compared to the square structure and to excite circular polarization (CP). The antenna is manufactured and its parameters are measured. It has been shown that there is a good agreement between simulated and experimental results. The last design proposes an impressive design of a circular polarized square slot antenna (CPSSA). The proposed single layer antenna composed of a square ground plane embedded with three unequal sized inverted-L strips around corners, which are capable of generating a resonant mode for exciting two orthogonal E vectors. Compared to the previous similar CPSSA designs, the axial ratio bandwidth of the antenna is increased, more than 2 times. The designed CPSS antenna with its compact $40 \times 40 \times 0.8$ mm³ size operates over the frequency band between 2.63 and

6.38 GHz for $VSWR < 2$ exhibiting a 71.11% (3-6.1GHz) circular polarization (CP) bandwidth. Throughout this letter, the improvement process of the axial ratio (AR) and S_{11} properties are presented and discussed in detailed.

2. ANTENNA THEORY AND BASIC PARAMETERS OF AN ANTENNA

2.1 Antenna

An antenna (or aerial) is an electrical device, which converts electric currents into radio waves, and vice versa. It is usually used with a radio transmitter or radio receiver. In transmission, a radio transmitter applies an oscillating radio frequency electric current to the antenna's terminals, and the antenna radiates the energy from the current as electromagnetic waves (radio waves). In reception, an antenna intercepts some of the power of an electromagnetic wave in order to produce a tiny voltage at its terminals, that is applied to a receiver to be amplified. An antenna can be used for both transmitting and receiving [1]. Antennas are classified into six types: wire, aperture, microstrip, array, reflector, and lens antennas [2]. All antennas generate their radiation from surface currents. These currents set up electromagnetic resonances, which create near field electromagnetic fields. These fields leave the near field and generate propagating electromagnetic fields into the far field. These fields, both near and far field can be described accurately by using Maxwell's equations, shown in Equations (1.1)-(1.4) presented in [2].

$$\nabla \times \bar{\varepsilon} = \frac{-\partial \bar{B}}{\partial t} - \bar{M} \quad (1.1)$$

$$\nabla \times \bar{H} = \frac{\partial \bar{D}}{\partial t} + \bar{J} \quad (1.2)$$

$$\nabla \cdot \bar{D} = \rho \quad (1.3)$$

$$\nabla \cdot \bar{B} = 0 \quad (1.4)$$

where : $\bar{\varepsilon}$ = Electric field intensity in V/m
 \bar{H} = Magnetic field intensity in A/m
 \bar{D} = Electric flux density in Coul/m²
 \bar{B} = Magnetic flux density in Wb/m²
 \bar{M} = Magnetic current density in A/m²
 \bar{J} = Electric current density in A/m²
 ρ = Electric charge density in Coul/m³

2.2 Field Regions Of Antenna

2.2.1 Far field region

The far field region is the most important, as this determines the antenna's radiation pattern. Also, antennas are used to communicate wirelessly from long distances, so this is the region of operation for most antennas. We will start with this region. The far field is the region far from the antenna, as you might suspect. In this region, the radiation pattern does not change shape with distance (although the fields still die off as $1/R$, so the power dies off as $1/R^2$). Also, this region is dominated by radiated fields, with the E- and H-fields orthogonal to each other and the direction of propagation as with plane waves. If the maximum linear dimension of an antenna is D , then the following 3 conditions must all be satisfied to be in the far field region:

$$R > \frac{2D^2}{\lambda} \quad (1.5)$$

$$R \gg D \quad (1.6)$$

$$R \gg \lambda \quad (1.7)$$

The first and second equation above ensure that the power radiated in a given direction from distinct parts of the antenna are approximately parallel (see Figure 2.1). This helps ensure the fields in the far-field region behave like plane waves. Note that \gg means "much much greater than" and is typically assumed satisfied if the left side is 10 times larger than the right side.

2.2.2 Reactive near field region

In the immediate vicinity of the antenna, we have the reactive near field. In this region, the fields are predominately reactive fields, which mean the E- and H- fields are out of phase by 90 degrees to each other (recall that for propagating or radiating fields, the fields are orthogonal (perpendicular) but are in phase). The boundary of this region is commonly given as:

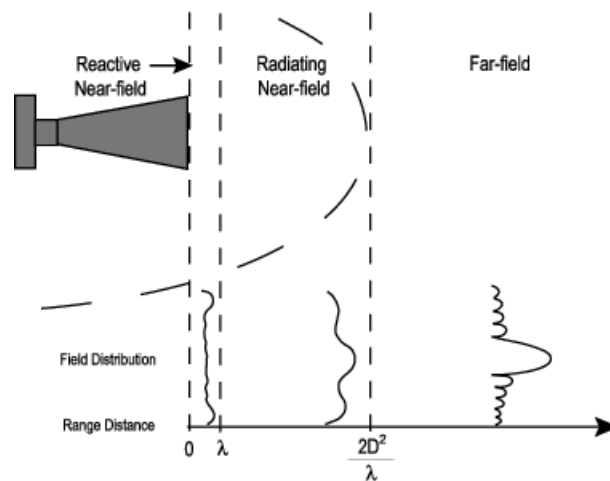
$$R < 0.62 \sqrt{\frac{D^3}{\lambda}}$$

2.2.3 Near field (Fresnel) region

The radiating near field or Fresnel region is the region between the near and far fields. In this region, the reactive fields are not dominant; the radiating fields begin to emerge. However, unlike the Far Field region, here the shape of the radiation pattern may vary appreciably with distance. The region is commonly given by:

$$0.62 \sqrt{\frac{D^3}{\lambda}} < R < \frac{2D^2}{\lambda}$$

Note that depending on the values of R and the wavelength, this field may or may not exist.



exist.

Figure 2.1 : Reactive near field, Near field and far field of an antenna

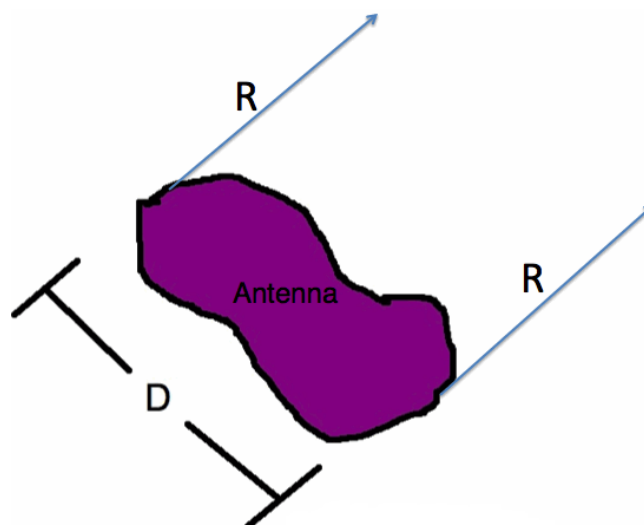


Figure 2.2 : The Rays from any Point on the Antenna

2.3 Radiation Pattern

The radiation pattern is a graphical depiction of the relative field strength transmitted from or received by the antenna. Antenna radiation patterns are taken at one frequency, one polarization, and one plane cut. The patterns are usually presented in polar or rectilinear form with a dB strength scale. Radiation pattern of a typical dipole is presented in Figure 2.3.

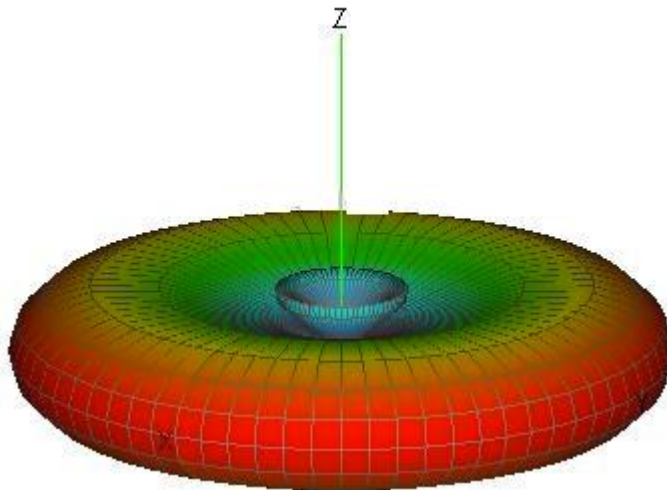


Figure 2.3 : Radiation pattern of a typical dipole

2.4 Polarization Of An Antenna

The polarization of an electromagnetic wave is defined as the orientation of the electric field vector. Recall that the electric field vector is perpendicular to both the direction of travel and the magnetic field vector. The polarization is described by the geometric figure traced by the electric field vector upon a stationary plane perpendicular to the direction of propagation, as the wave travels through that plane. An electromagnetic wave is frequently composed of (or can be broken down into) two orthogonal components as shown in Figure 2.4. The geometric figure traced by the sum of the electric field vectors over time is, in general, an ellipse as shown in Figure 2.5. Under certain conditions the ellipse may collapse into a straight line, in which case the polarization is called linear. In the other extreme, when the two components are of equal magnitude and 90° out of phase, the ellipse will become circular as shown in Figure 2.6. Thus linear and circular polarization are the two

special cases of elliptical polarization. Linear polarization may be further classified as being vertical, horizontal, or slant.

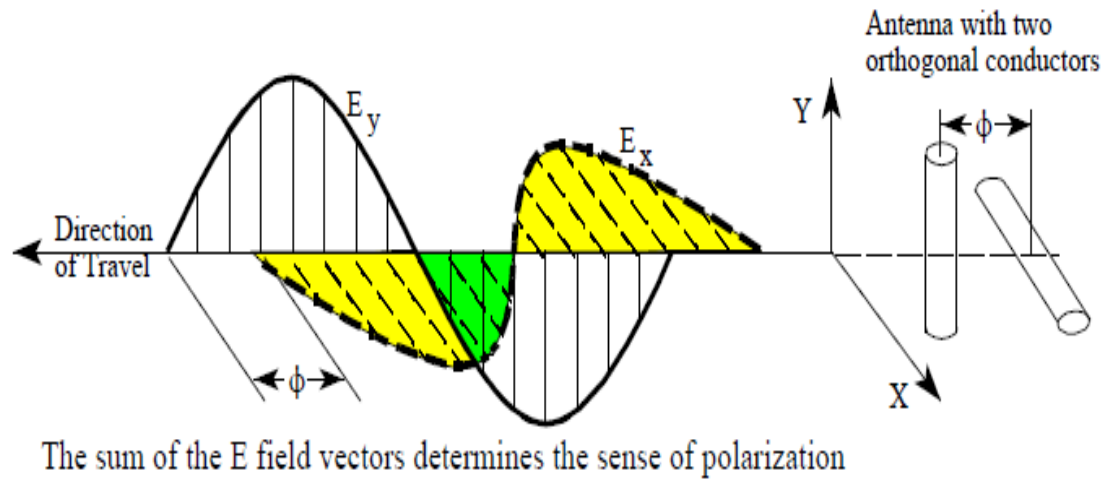


Figure 2.4 : Polarization Coordinates

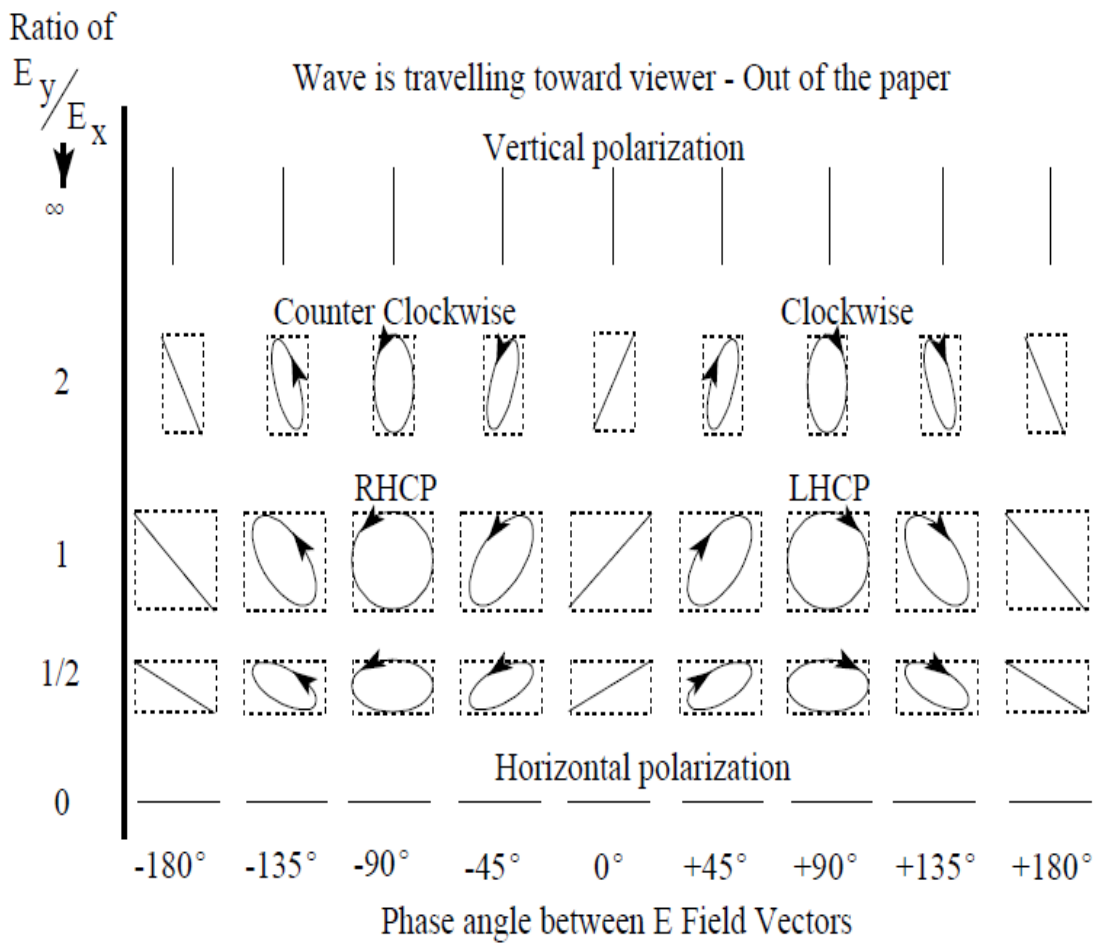


Figure 2.5 : Polarization as a Function of E_y/E_x and Phase angle

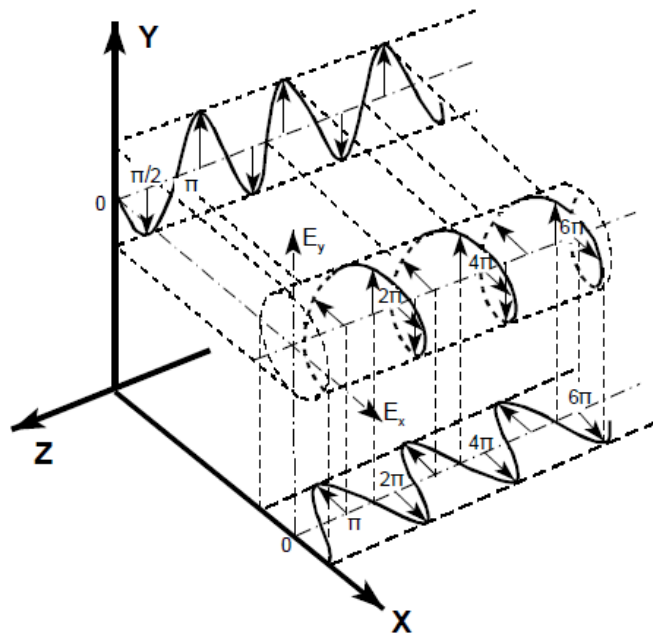


Figure 2.6 : Circular Polarization - E Field

3. OVERVIEW OF CIRCULARLY POLARIZED ANTENNAS

3.1 Advantages Of Circularly Polarized Antennas

3.1.1 Reflectivity

Radio signals are reflected or absorbed depending on the material they come in contact with. Because linear polarized antennas are able to “attack” the problem in only one plane, if the reflecting surface does not reflect the signal precisely in the same plane, that signal strength will be lost. Since circular polarized antennas send and receive in all planes, the signal strength is not lost, but is transferred to a different plane and are still utilized.

3.1.2 Absorption

As stated above, radio signal can be absorbed depending on the material they come in contact with. Different materials absorb the signal from different planes. As a result, circular polarized antennas give you a higher probability of a successful link because it is transmitting on all planes.

3.1.3 Phasing issues

High-frequency systems (i.e. 2.4 GHz and higher) that use linear polarization typically require a clear line-of-sight path between the two points in order to operate effectively. Such systems have difficulty penetrating obstructions due to reflected signals, which weaken the propagating signal. Reflected linear signals return to the propagating antenna in the opposite phase, thereby weakening the propagating signal. Conversely, circularly polarized systems also incur reflected signals, but the reflected signal is returned in the opposite orientation, largely avoiding conflict with the propagating signal. The result is that circularly polarized signals are much better at penetrating and bending around obstructions.

3.1.4 Multi-path

Multi-path is caused when the primary signal and the reflected signal reach a receiver at nearly the same time. This creates an "out of phase" problem. The receiving radio must spend its resources to distinguish, sort out, and process the proper signal, thus degrading performance and speed. Linear Polarized antennas are more susceptible to multi-path due to increased possibility of reflection. Out of phase radios can cause dead-spots, decreased throughput, distance issues and reduce overall performance in a 2.4 GHz system.

3.1.5 Inclement weather

Rain and snow cause a microcosm of conditions explained above (i.e. reflectivity, absorption, phasing, multi-path and line of sight) Circular polarization is more resistant to signal degradation due to inclement weather conditions for all the reason stated above.

3.1.6 Line-of-sight

When a line-of-sight path is impaired by light obstructions (i.e. foliage or small buildings), circular polarization is much more effective than linear polarization for establishing and maintaining communication links.

3.1.7 Power loss

For a linearly polarized antenna, the radiation pattern is taken both for a co-polarized and cross-polarized response. The polarization quality is expressed by the ratio of these two responses. In all practicality, perfect circular polarization is not achievable. The parameter, which is used to measure the quality of the circular polarization, is called axial ratio (AR). Axial ratio is the ratio of the major to the minor axis, which is mathematically described in Equations (3.1), (3.2), and (3.3) with reference to Figure 3.1. Typically, in antenna measurement and evaluation, this ratio is expressed in dB, where perfect circular polarization equates to 0 dB. For most applications, 3 dB is the criteria for achieving circular polarization.

$$AR = \frac{\text{major axis}}{\text{minor axis}} = \frac{OA}{OB} \quad (3.1)$$

$$OA = \left[\frac{1}{2} \left\{ E_{x0}^2 + E_{y0}^2 + [E_{x0}^4 + E_{y0}^4 + 2E_{x0}^2 E_{y0}^2 \cos(2\Delta\phi)]^{\frac{1}{2}} \right\} \right]^{\frac{1}{2}} \quad (3.2)$$

$$OB = \left[\frac{1}{2} \left\{ E_{x0}^2 + E_{y0}^2 - [E_{x0}^4 + E_{y0}^4 + 2E_{x0}^2 E_{y0}^2 \cos(2\Delta\phi)]^{\frac{1}{2}} \right\} \right]^{\frac{1}{2}} \quad (3.3)$$

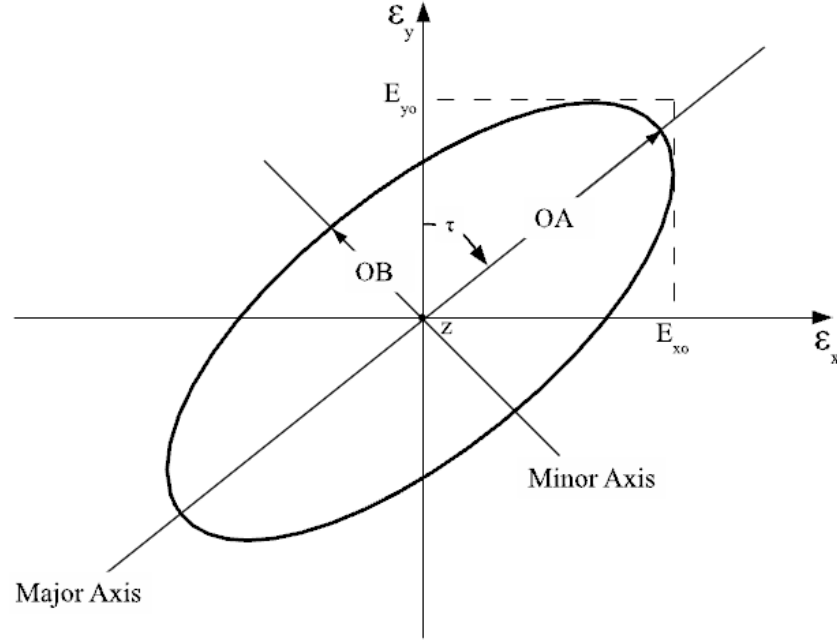


Figure 3.1 : Polarization ellipse illustrating the parameters associated with polarized electromagnetic wave propagation

3.2 Circularly Polarized Square Slot Antennas

Low profile circularly polarized broadband antennas have found its application extensively in communications for satellites, radars and global positioning systems (GPS). These applications require broadband characteristics both in impedance matching and axial ratio characteristics. Circularly polarized (CP) radio propagation links in satellite communications, satellite positioning and radio frequency identification (RFID) systems are preferred to linear polarization schemes, which are subject to losses when arbitrary polarization misalignment occurs between the transmitter and receiver. With CP antennas at both radios, the enhanced gain and cross-polar discrimination improve the resilience of the system to multipath propagating effects. To create circular polarization, the antenna must radiate from

modes of equal magnitude that are orthogonal in space and in phase quadrature. Several techniques have been used in various types of circularly polarized antennas that have been reported in recent decades. Printed circular or square patch geometries with perturbing narrow slots or truncated stubs achieve CP by introducing degenerate modes with 90° phase difference [3]. A typical square slot is presented in Figure 3.2. Different excitation techniques can be adopted depending on the structure and application of the antenna. Practically microstrip or coplanar waveguide (CPW) excitation modes are adopted for these types of antennas. As it can be seen it consists of a square substrate, a conductor plate with slot area of $L \times L$, feeding line of W_f width and length of L_f .

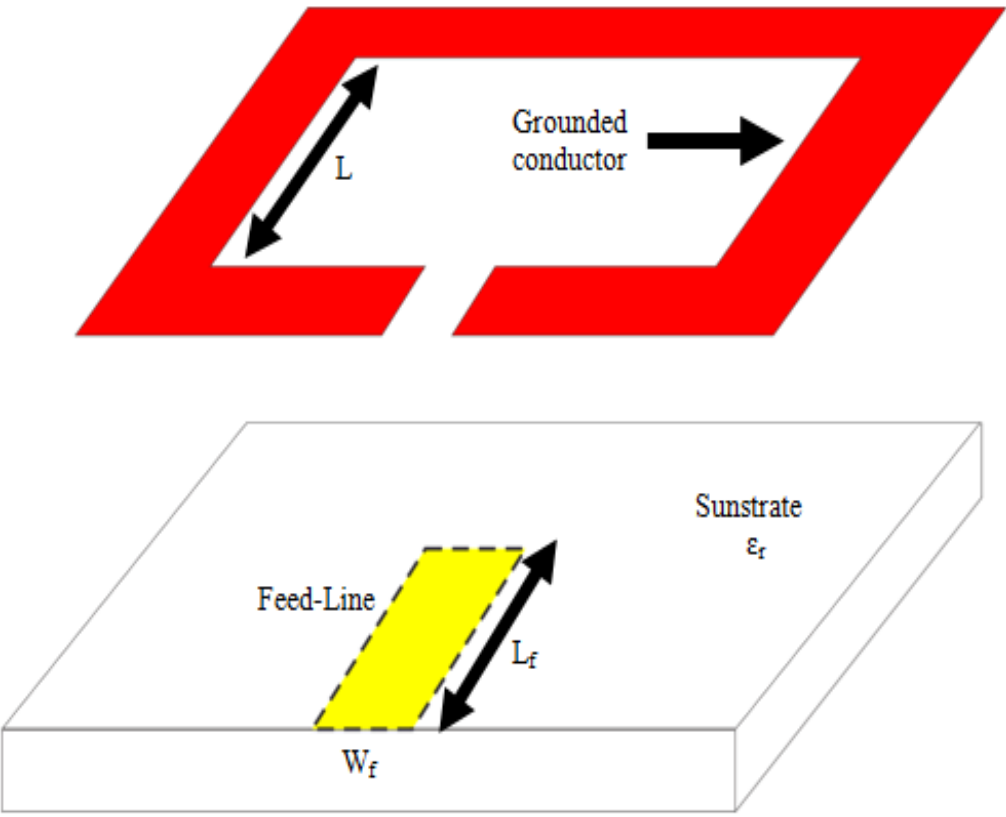


Figure 3.2 : Typical square slot antenna structure

Various types of square slot antennas are presented during recent years. Square slot antennas have adopted different structures both in grounded plane and in the feeding line to create wide impedance matching and 3dB axial ratio bandwidths. Of the most popular and referenced antennas are the works done by Dr. Sze et.al in [4-6]. Antenna presented in [4] is depicted in Figure 3.3. As it can be seen a square slot is has been adopted as the grounded plane. The antenna has feedline, which had become narrow

in its lower part. The new technique used in this work is adding a crooked T-shape strip to the upper right corner of the slot to excite two E vectors with the same magnitude and 90° phase difference. Due to their attractive features such as wide impedance bandwidth, single metallic layer, low profile, and easy integration with active devices or MMICs, printed wide slot antennas (PWSA) with a CPW feed have received increasing attention in circular polarization applications.

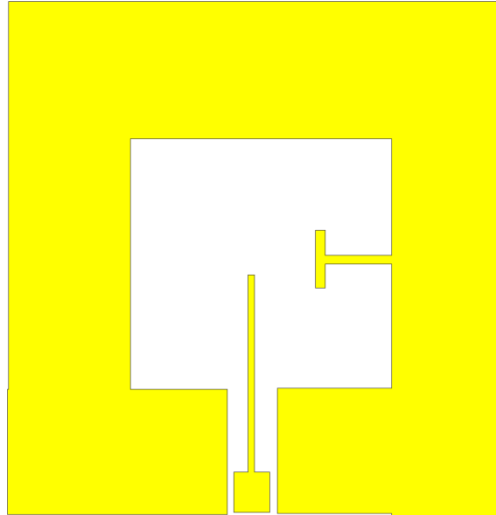


Figure 3.3 : Antenna presented in [4]

Among those CP PWSAs, the ones having a simple slot shape and a 3-dB axial-ratio (AR) bandwidth of more than 15% have been designed by embedding into the square slots appropriate perturbation structures. These perturbation structures can redistribute the magnetic currents in the slots so that two orthogonal resonant modes with equal amplitude and a 90° phase difference can be excited. The perturbation structure can be constructed by loading in the square slot a crisscross patch (Figure 3.4 (a)) or inverted-L conducting strip connected to the signal strip of the CPW (Figure 3.4 (b)), or a grounded T-shaped metallic strip that is perpendicular to the axial direction of the feeding CPW (Figure 3.3)

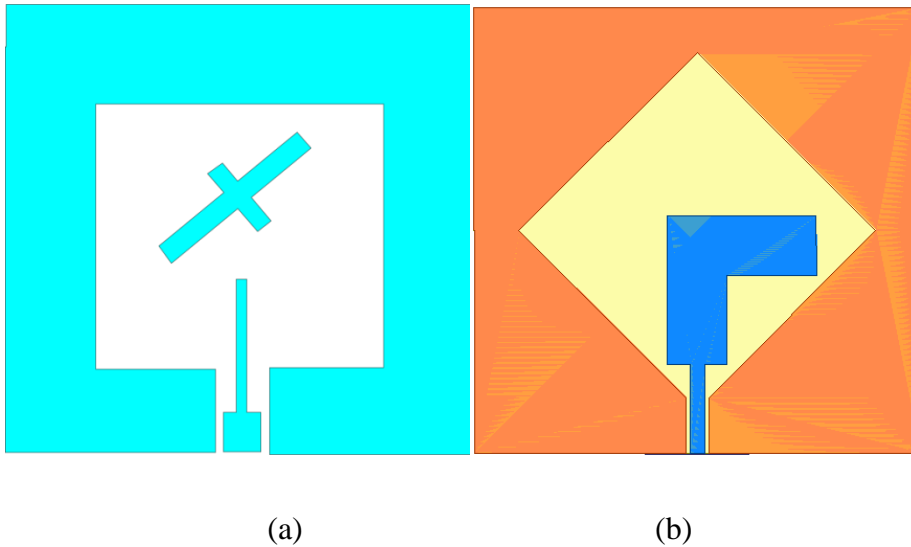


Figure 3.4 : (a) square slot with crisscross patch, (b) inverted-L conducting strip slot

3.3 Anular Ring Slot Antennas

These antennas are mainly achieved through changing the feedline shape and location. Different types of them are designed and reported during recent years. These antennas can be fed using microstrip line, CPW line or slot line as presented in Figure 3.5. Axial ratio bandwidths achieved by annular ring slots are relatively low. But recently in the work done in [7] it was shown that an annular ring slot antenna can achieve more than 60% of 3dB axial ratio bandwidth relative to the center frequency of CP band.

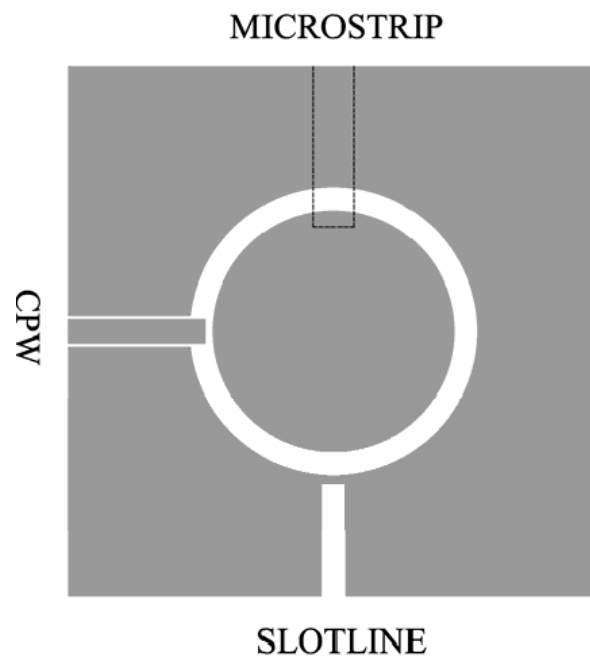


Figure 3.5 : Different feeds for annular ring antennas

3.4 Overview Of Microstrip Antennas

A microstrip antenna consists of conducting patch on a ground plane separated by dielectric substrate. This concept was undeveloped until the revolution in electronic circuit miniaturization and large-scale integration in 1970. After that, many authors have described the radiation from the ground plane by a dielectric substrate for different configurations. The early work of Munson on micro strip antennas for use as low profile flush-mounted antennas on rockets and missiles showed that this was a practical concept for use in many antenna system problems. Various mathematical models were developed for this antenna and its applications were extended to many other fields. The number of papers, articles published in the journals for the last ten years, on these antennas shows the importance gained by them[8-14] . The micro strip antennas are the present day antenna designer's choice. Low dielectric constant substrates are generally preferred for maximum radiation. The conducting patch can take any shape but rectangular and circular configurations are the most commonly used configuration. Other configurations are complex to analyze and require heavy numerical computations. A microstrip antenna is characterized by its Length, Width, Input impedance, and Gain and radiation patterns. Various parameters of the microstrip antenna and its design considerations were discussed in the subsequent chapters. The length of the antenna is nearly half wavelength in the dielectric; it is a very critical parameter, which governs the resonant frequency of the antenna. There are no hard and fast rules to find the width of the patch. In microstrip feed, the patch is fed by a microstrip line that is located on the same plane as the patch. In this case both the feeding and the patch form one structure. Microstrip feeding is simple to model, easy to match and easy to fabricate. It is also a good choice for use in antenna-array feeding networks. However microstrip feed has the disadvantage of narrow bandwidth and the introduction of coupling between the feeding line and the patch which leads to spurious radiation and the required matching between the microstrip patch and the 50Ω feeding line. Microstrip feed can be classified into 3 categories:

3.4.1 Direct feed

where the feeding point is on one edge of the patch. As shown in Figure 2-4. Direct feed needs a matching network between the feed line and the patch (such as quarter

wavelength transformer). The Quarter wave length transformer compensates the impedance differences between the patch and the 50Ω feed line.

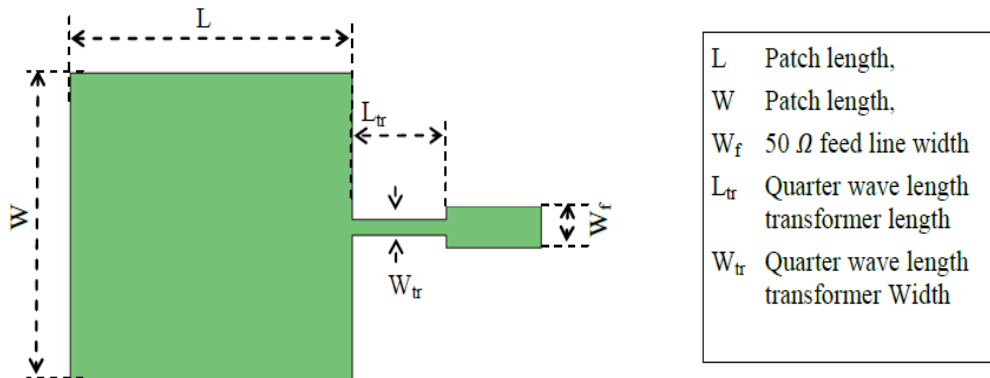


Figure 3.6 : Direct microstrip feed line

3.4.2 Inset feed

where the feeding point is inside the patch. The location of the feed is the same that will be used for coaxial feed. The 50Ω feed line is surrounded with an air gap till the feeding point as shown in Figure 3.7 . The inset microstrip feeding technique is more suitable for arrays feeding networks.

3.4.3 Gap-coupled

The feeding line does not contact the patch; there is an air gap between the 50Ω line and the patch as shown in Figure 3.8 .The antenna is fed by coupling between the 50Ω feed line and the patch.

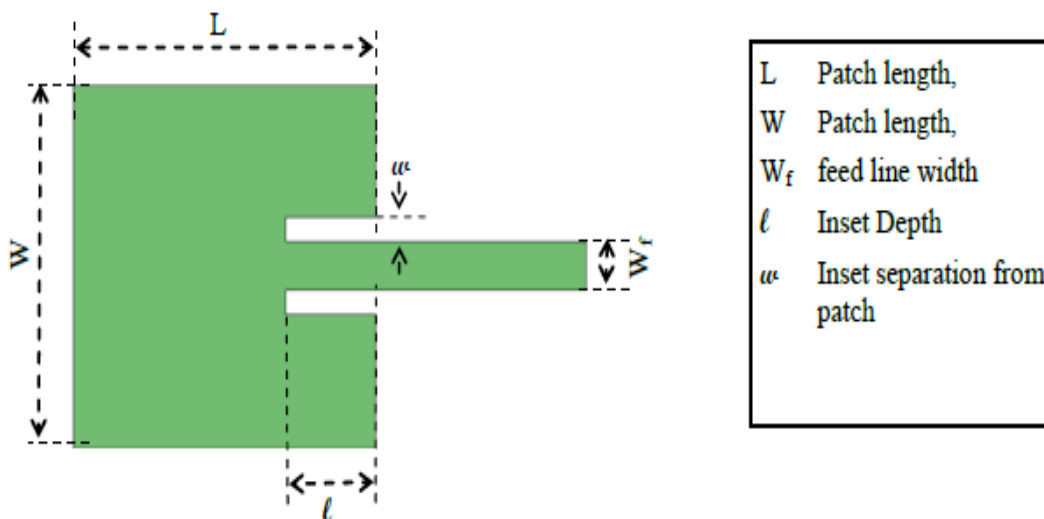


Figure 3.7 : Gap-coupled microstrip feed line

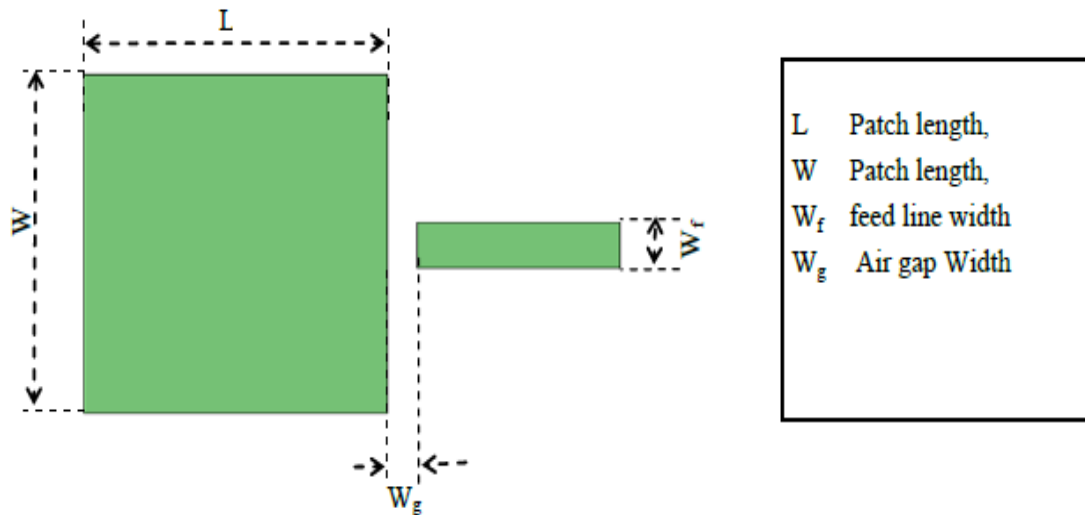


Figure 3.8 : Inset microstrip feed line

3.4.4 Proximity coupled feeding

Proximity coupled feeding consists of two dielectric substrate layers. The microstrip patch antenna is located on the top of the upper substrate & the microstrip feeding line is located on the top of the lower substrate as shown in Figure 3.9. It is a non contacting feed where the feeding is conducted through electromagnetic coupling that takes place between the patch and the microstrip line. The two substrates parameters can be chosen different than each other to enhance antenna performance. The proximity coupled feeding reduces spurious radiation and increase bandwidth. However it needs precise alignment between the 2 layers in multilayer fabrication.

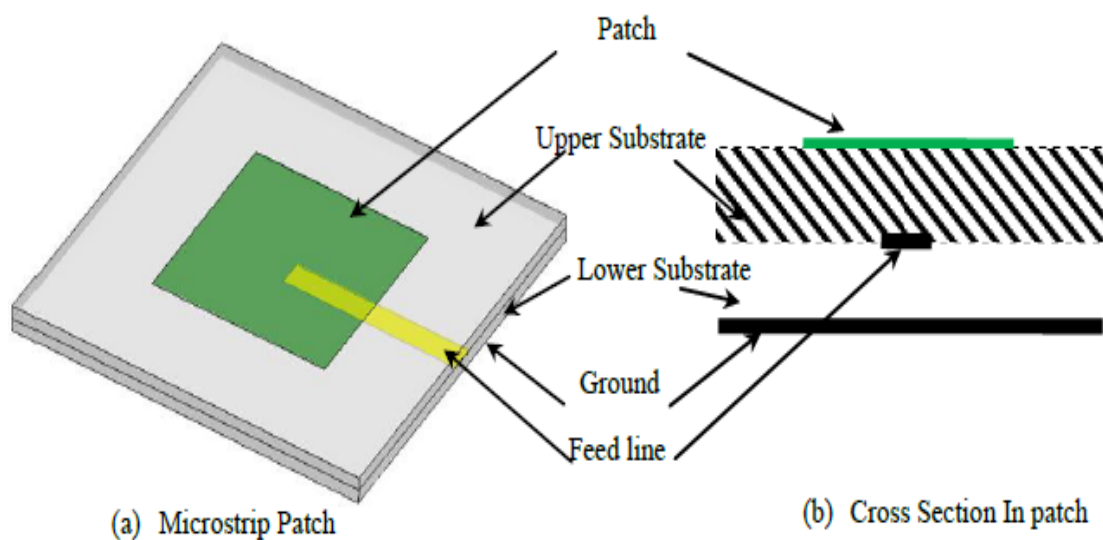


Figure 3.9 : Proximity coupled microstrip feeding

3.4.5 Microstrip circularly polarized

Circular polarization is produced by adding two orthogonal linearly polarized fields with the same magnitude and a 90° phase difference. Several single-feed, single-radiator configurations of microstrip patch antennas can provide such dual orthogonal field components without the need of an external polarizer, by appropriate excitation of the patch cavity. The conventional single feed circularly polarized microstrip antenna typically has a relatively narrow AR bandwidth of about 1%-2%. But recently designs with higher axial ratios are also presented. Figure 3.10 presents some of the conventional circularly polarized microstrip antennas.

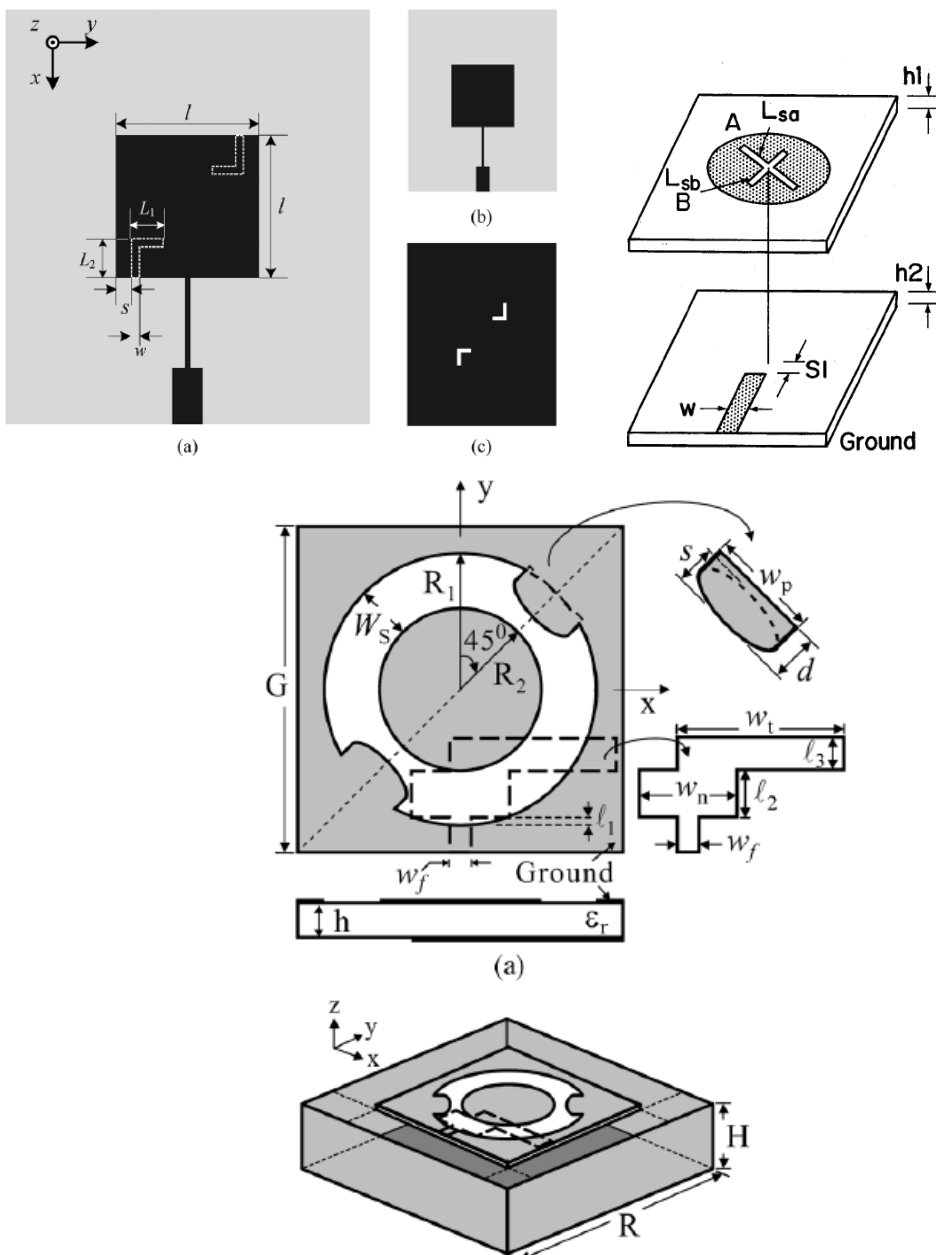


Figure 3.10 : Different microstrip circularly polarized antenna configurations

4. DESIGN OF CIRCULARLY POLARIZED ANTENNAS

Considering the previous works done in the field of circularly polarized antenna, in this thesis four such antennas were designed and tested.

4.1 A New Triple Band Circularly Polarized Square Slot Antenna Design with Crooked T and F-Shape Strips for Wireless Applications

4.1.1 Introduction

Due to the increasing usage of wireless communication applications, the performance improvement studies of such systems has found a growing investigation area in recent years. Antennas as one of the most important parts of these systems have gained a great attention. Among the various types of antennas, circularly polarized (CP) antennas are the most desired ones, owing to their inevitable merits like reducing polarization mismatch and multipath fading. To benefit from broadband and low profiles, various shapes and designs of broadband circularly polarized slot antennas have been developed to overcome both the narrow impedance and axial-ratio bandwidths (ARBWs) by applying different techniques on patch and ground structures [15]-[44]. Array structures presented in [15], [18] and [21] use the same but duplicated structure in different special or phase positions to obtain circular polarization. Patch, microstrip and slot antennas due to their compatibility with integrated circuit systems are also widely used in CP structures [15-16], [20], [22], [26-27]. The antennas proposed in [28] and [31] have investigated upon embedding two inverted-L grounded strips around two opposite corners of the slot, each of which using different feedline shapes. Embedding two spiral slots is also presented in [29], in which current circulation in the spiral slots are employed to achieve the CP operation. Utilizing a shorted square-ring slot is another way of creating CP antennas which is presented in [30]. Recently some annular-ring slots [32], [34] are employed to achieve the CP characteristic. In these antennas the circular polarization is attained

through a double-bent microstrip line that feeds the antenna at two different positions. In [33], C-like monopole with one sleeve is used in order to excite the CP and improve the impedance bandwidth of the antenna. Asymmetric square slot presented in [35] and [36] provides a CP bandwidth which is larger than 10% simply by using an inverted-L tuning stub protruded from the signal line of the coplanar waveguide (CPW). In the stair-shaped slot presented in [37], CP operation is obtained by etching a longitudinal slot at a middle point of a stair-shaped slot. In [38], by introducing the corrugated slot and meander line, both the impedance bandwidth and CP bandwidth could be improved. Finally ring slot antenna, reported in [39], achieves CP radiation by introducing proper asymmetry in the ring slot structure and feeding the ring slot using a microstrip line at 45° from the introduced asymmetry. All of the discussed antennas have large dimensions which are not appropriate to be used in wireless communication systems. Also most of them have either small ARBWs or narrow impedance matching bandwidth. Starting with this motivation, in this letter, a new triple band, compact CPW-fed, circularly polarized square slot antenna with dual monopole feed and crooked F and T-strips is presented. The antenna has three functional bands operating from 1.96GHz to 3.26GHz, 3.61GHz to 6.98GHz and 7.87GHz to 11.24GHz. This design (for the optimized values) supports the three bandwidths in terms of impedance matching but for the 3dB ARBW, it supports only the second band. Employing dual monopole structure enhances the antenna with large bandwidth and small size. Also the proposed antennas in this work has the capability of showing CP characteristics in the important standards such as IEEE 802.11b/g (2.4–2.484 GHz), IEEE 802.11a (5.15–5.35 GHz and an additional band of 5.725–5.825 GHz), and HiperLAN2 (5.47–5.725 GHz) [28]-[29].

4.1.2 Antenna design

The proposed circularly polarized square slot (CPSS) antenna geometry and its dimensions are presented in figure 4.1. The configuration of the antenna is combination of the dual-monopole antenna [40] and the square slot CP antenna [41]. As a result, the proposed antenna inherits a wide CP bandwidth. The antenna is printed on a FR4 dielectric substrate with a thickness of 0.8 mm, $\epsilon_r=4.4$ and loss tangent of $\tan\delta=0.02$. Total dimension of the antenna is as compact as $40 \times 40 \times 0.8$

mm3. The antenna is fed by a 50Ω CPW with a signal strip of 3mm width and two identical gaps of 0.5mm width. The feed line is terminated with a standard SMA connector. Two main features incorporated into the design are enhancing the ARBW and enlarging the impedance bandwidth. For achieving efficient excitation and good impedance matching, the signal strip of the CPW should be protruded into the square slot. In general, the length of monopole antenna is usually about a quarter-wavelength. The approximate value for the length L16 of monopole radiating strip is then given by $L16 = \frac{\lambda_g}{4}$, and λ_g is

$$\lambda_g = \frac{\lambda_r}{\sqrt{\text{eff}}} = \frac{c}{\sqrt{\text{eff}}f_r} \quad (4.1)$$

$$\text{eff} = \frac{r+1}{2} \quad (4.2)$$

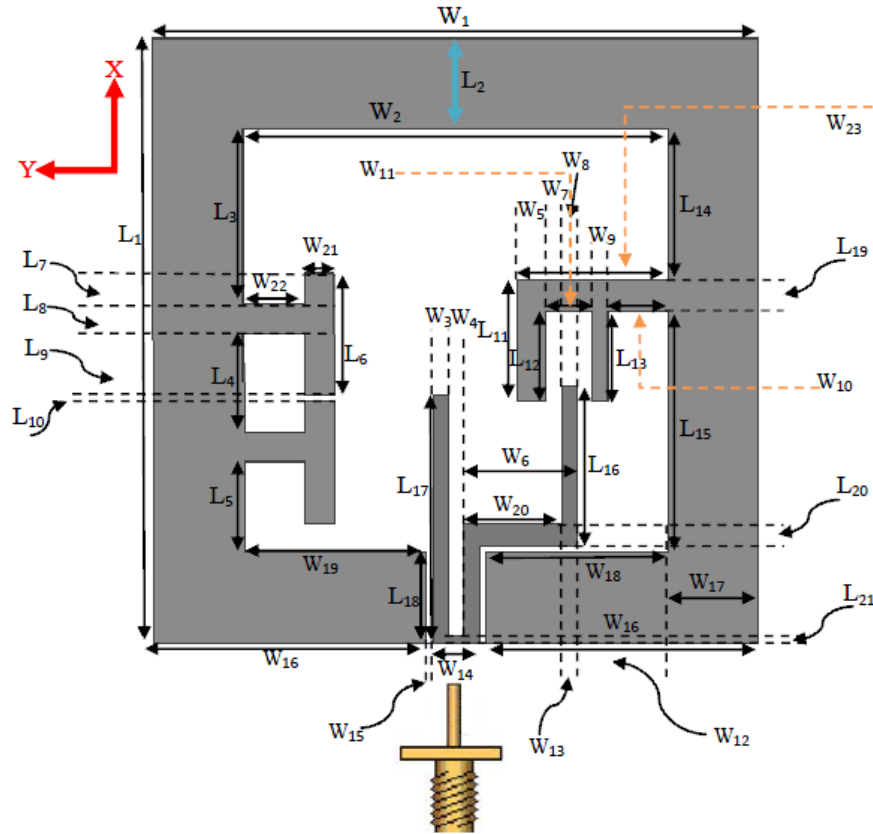


Figure 4.1 : Geometry of the proposed CP triple band antenna ($L_1=40$, $L_2=6$, $L_3=11.5$, $L_4=6.5$, $L_5=6$, $L_6=8$, $L_7=2$, $L_8=2$, $L_9=4$, $L_{10}=0.5$, $L_{11}=8$, $L_{12}=6$, $L_{13}=6$, $L_{14}=10$, $L_{15}=16$, $L_{16}=10.5$, $L_{17}=16.5$, $L_{18}=6$, $L_{19}=2$, $L_{20}=2$, $L_{21}=0.5$ $W_1=40$, $W_2=28$, $W_3=1$, $W_4=1$, $W_5=2$, $W_6=7.5$, $W_7=1$, $W_8=1$, $W_9=1$, $W_{10}=4$, $W_{11}=3$, $W_{12}=6$, $W_{13}=1$, $W_{14}=3$, $W_{15}=0.5$, $W_{16}=18$, $W_{17}=6$, $W_{18}=12$, $W_{19}=12$, $W_{20}=6.5$, $W_{21}=2$, $W_{22}=4$, $W_{23}=10$) (Unit : mm)

where in (4.1), c is the speed of light, λ_r is the free-space wavelength of the monopole resonant frequency f_r , and in (4.2) ϵ_{eff} is the approximated effective dielectric constant [44]. There are two deformed parallel monopoles in the feeding line. Their lengths are selected as $L_{17}=0.58L_s$ and $L_{16}=0.37L_s$ where $L_s=L_3+2L_8+L_4+L_5$. The width of the monopole on the right side is selected as $W_{20}=0.16W_2$. Due to the presence of different lengths of the two monopoles, the first resonant frequency of the proposed antenna is expected to be controlled mainly by the length of the longer monopole, and the second resonant frequency is greatly dependent on the length of the shorter monopole. The gap between these two monopoles is adjusted to be 1 mm. Unlike the T-shaped strips used in most of the conventional CPW-fed CP antennas a cactus shaped strip is adopted in the presented design. Dual monopole antenna is used to enhance the antenna with wider bandwidth, since the dual monopole structure creates two resonant frequencies and by carefully adjusting the elements of the dual monopole, antenna can support a wider operating frequency band. To generate an asymmetrical feeding stub and thus excite the new resonance modes for improving the CP and impedance bandwidth, a strip with dimensions of $1\text{mm} \times 7.5\text{mm}$ is cut and removed from the feedline; a further study is done on the effect of this strip on the impedance matching and 3dB ARBWs of the antenna in Section III. The simulation results show that embedding the arms (L_{16} and L_{17}) to the feedline and adjusting their lengths increases the impedance matching bandwidth. In the CPSS design, a crooked F-shape strip and two equal sized crooked T-shape strips are embedded as shown in Fig. 1. The CP operation of the proposed antenna is mainly attributed to the two grounded crooked-T and a crooked-F metallic strip placed at the center of the square slot to excite two orthogonal radiation fields with equal amplitudes. The combination of the feedline and the crooked F and T- strips, which lead to a large ARBW, may not guarantee a satisfying impedance matching, and tuning the distance between the crooked F and T-strips on the grounded patch is required. In the antenna structure presented in Fig. 1, during several tests and simulations, it could be understood that the circular polarization operation of the antenna is principally interrelated to the grounded F and T strips placed around two bottom corners of the square slot.

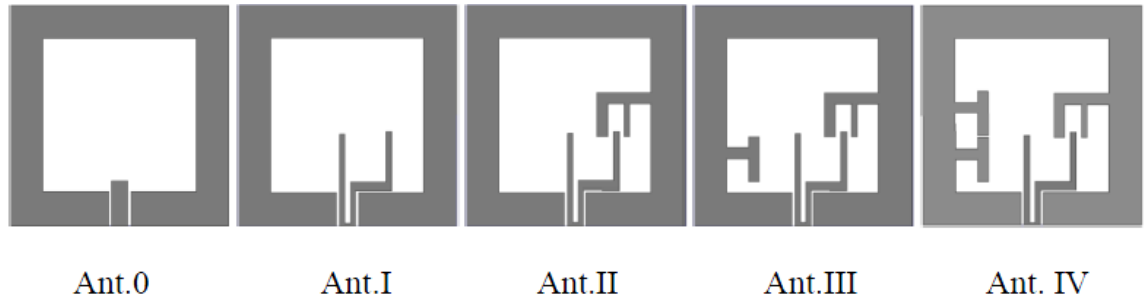


Figure 4.2 : Four improved prototypes of the antenna

4.1.3 Parametric study of the antenna

Through figure 4.2 four improved designs of the proposed CPSS antenna are presented. The antenna design is started by applying a simple strip feedline (Ant. 0) and then improved through adding arms (L_{16} and L_{17}) to the feedline to form a cactus shape. A further improvement is achieved by etching a tuning slit on the feedline to obtain a wide impedance matching bandwidth (Ant. I). -10dB impedance matching curves of the antenna are presented in figure 4.3. As it is observed from figure 4.3, by employing a simple strip as the feedline, a great impedance mismatch is experienced (black curve) and consequently any bandwidth of the antenna under -10dB is available. By adding arms to the simple strip feedline, antenna operates between $2.9\text{GHz}\sim 3.5\text{GHz}$ and $4.8\text{GHz}\sim 10.5\text{GHz}$ (blue curve). The optimized feed line structure (Ant I) is created through cutting a strip from the feedline (red curve). The simulation results show that embedding the arms to the feedline (Ant 0-Ant IV) and adjusting the parameters, an improvement on the impedance bandwidth as well as CP characteristic can be accomplished for the proposed antenna.

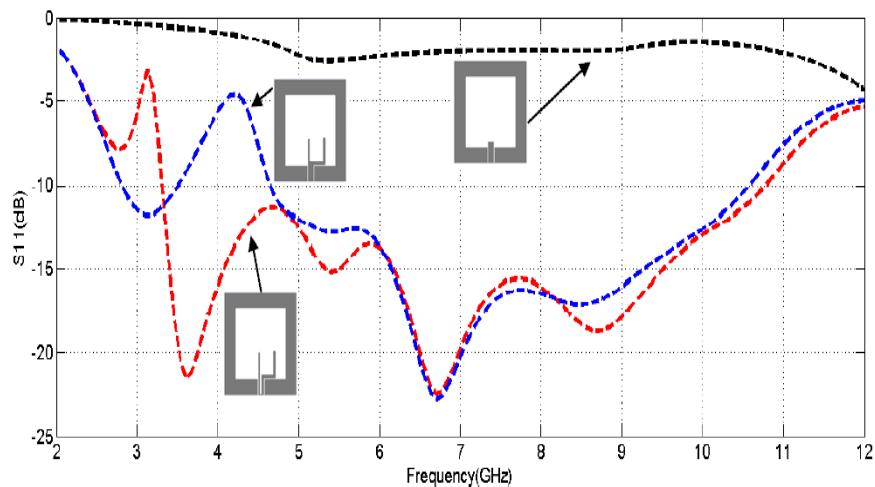


Figure 4.3 : Improved S_{11} of the antenna

As Jou et al. presented in [44], the general behavior of a monopole antenna is either vertical or horizontal linearly polarized. To obtain CP operation by exciting two orthogonal polarizations, the design is improved by adding a crooked F-shape strip to the right bottom corner of the structure. This structure is presented as Ant. II in figure 4.2 Return loss variations of Ant. I-Ant. IV are presented in figure 4.4 Considering the CP characteristic of the antenna, the changing regulation of the right hand side monopole is similar to that of left hand side one. Through figure 4.5 it can be observed that by adding a crooked F-shape to the antenna structure, a small improvement in the axial ratio of the antenna is created, and antenna operates CP about 3.2% (5.72~5.91GHz). To further improve the CP characteristic of the antenna, two crooked T-shape strips are sequentially added to the structure. As it is seen from figure 4.4, adding strips to Ant. I make the antenna operate triple band, and in the final design (Ant. IV), 404MHz (26.9%) extra bandwidth is obtained compared to the Ant. I. It can be seen in figure 4.5 that the ARBW of the antenna increased to 4.7~4.95GHz and 5.78~5.95GHz for Ant. III and 4.6~6.1GHz for the final structure (Ant. IV) respectively. In order to investigate the effects of various parameters on the antenna performance, parametric study has been carried out by the Ansoft High Frequency Structure Simulator (HFSS). Except the studied parameters, all the other parameters are fixed to the values as in figure 4.1.

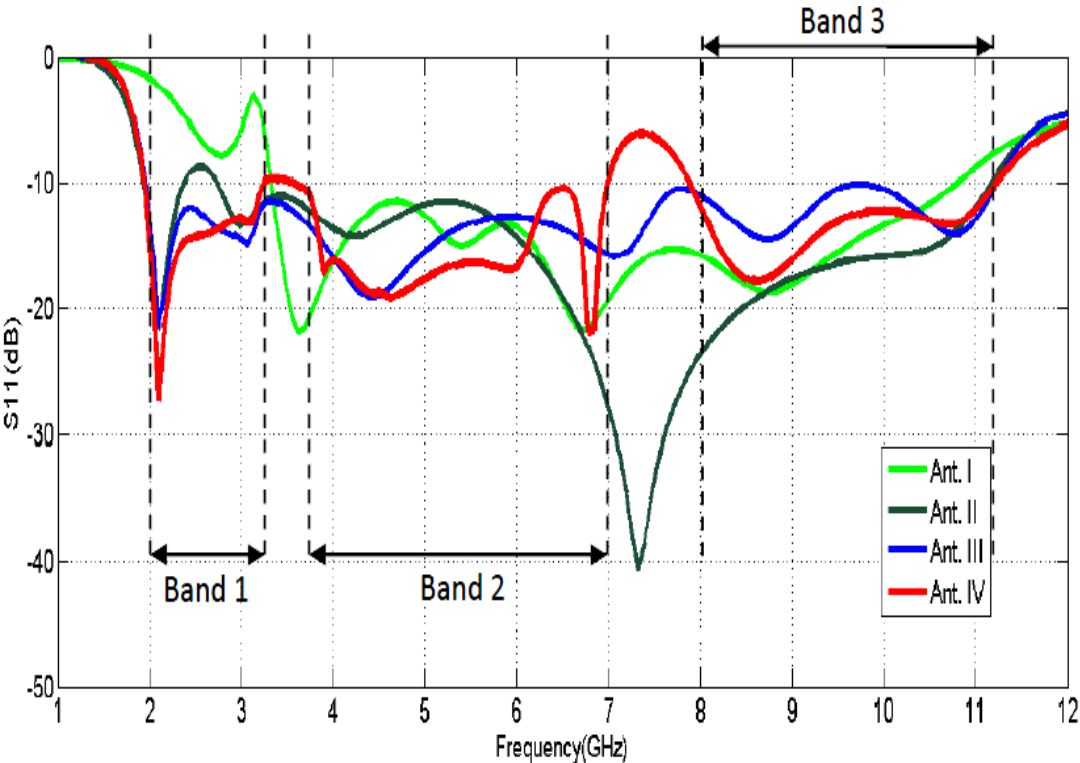


Figure 4.4 : S_{11} of the proposed antennas in figure 4.2

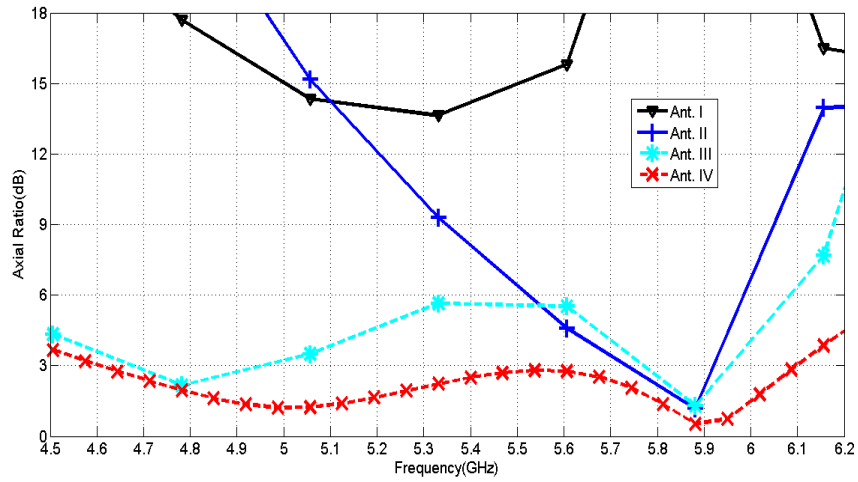


Figure 4.5 : Axial ratio of the proposed antennas in figure 4.2

4.1.3.1 Studying effects of L_{16}

The simulated 10dB return loss and axial ratio bandwidths for different lengths of the L_{16} parameter of the dual monopole antenna is presented in figures 4.6 and 4.7 respectively. The optimized value of the L_{16} is given in Section II. It can be observed that increasing the length of L_{16} , causes a decrease on the center frequencies of all three impedance bands. But the change of the first band is more noticeable. The impedance matching bandwidths of the first and third bands become much smaller when the length of L_{16} increases, while the second band becomes much wider. On the other hand increasing the length of L_{16} , creates the CP at the first band, between 2.38~2.78GHz, but through figure 4.6, it could be understood that the CP bandwidth does not guarantee the impedance matching bandwidth for the same frequency band.

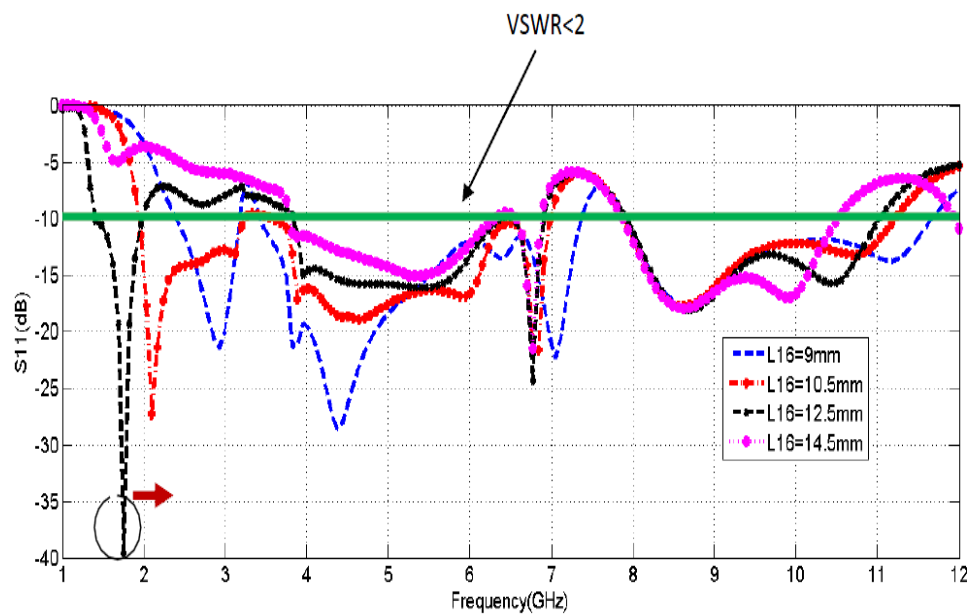


Figure 4.6 : S_{11} for different iterations of L_{16}

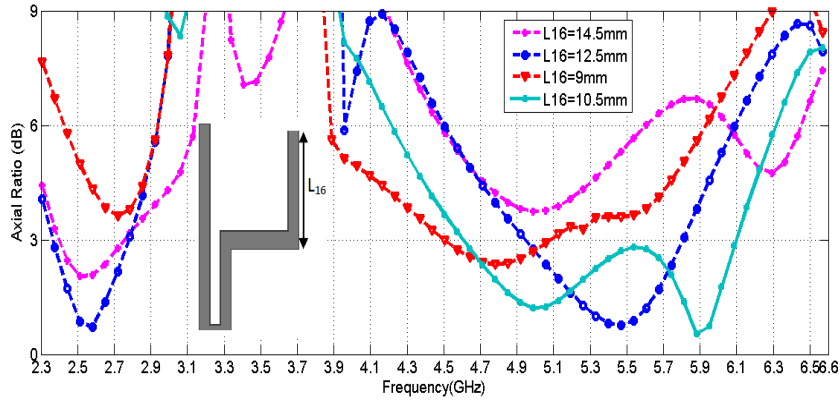


Figure 4.7 : Axial Ratio for different iterations of L_{16}

4.1.3.2 Studying effects of W_7

Picking $W_7=1\text{mm}$ (optimized value), enhances the antenna with maximum axial ratio of 28.03% for the final design (Ant. IV). Even small changes in this parameter (W_7) leads to considerable variations in both impedance matching and 3dB axial ratio bandwidths of the antenna. To highlight these variations, different values of W_7 are studied. As presented in figures 4.8 and 4.9, by increasing W_7 , center frequencies of all three operating bands move to lower frequencies and a decrease in impedance matching bandwidth is experienced. Considering the ARBW, for $W_7=3\text{mm}$, a new lower band CP characteristic, between 2.4GHz and 2.9GHz is created which covers the IEEE 802.11b/g standard for wireless local area network (WLAN), but the second band ARBW degrades about 600MHz. Although there is no change in the overall ARBW of the antenna, the antenna covers all IEEE 802.11a, a band of 5.15–5.35 GHz and HiperLAN2, a band of 5.47–5.725 GHz besides the band of 5.15–5.35 GHz which is very desirable.

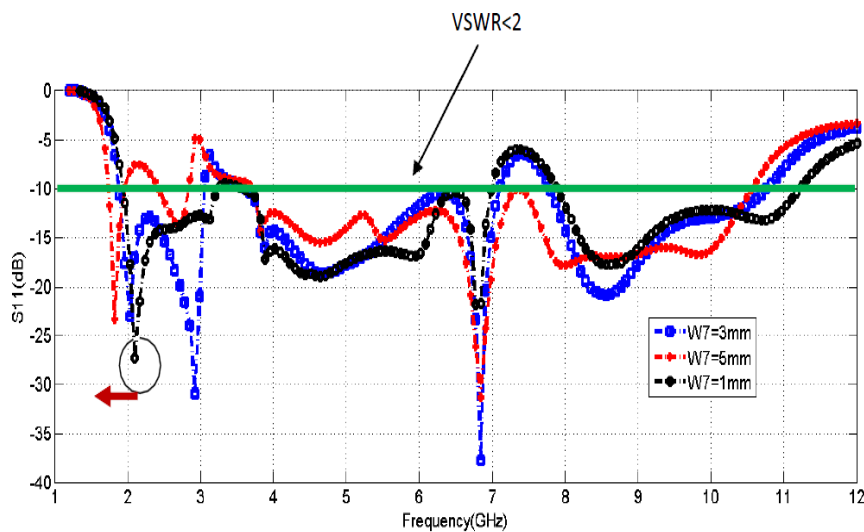


Figure 4.8 : S_{11} for different iterations of W_7

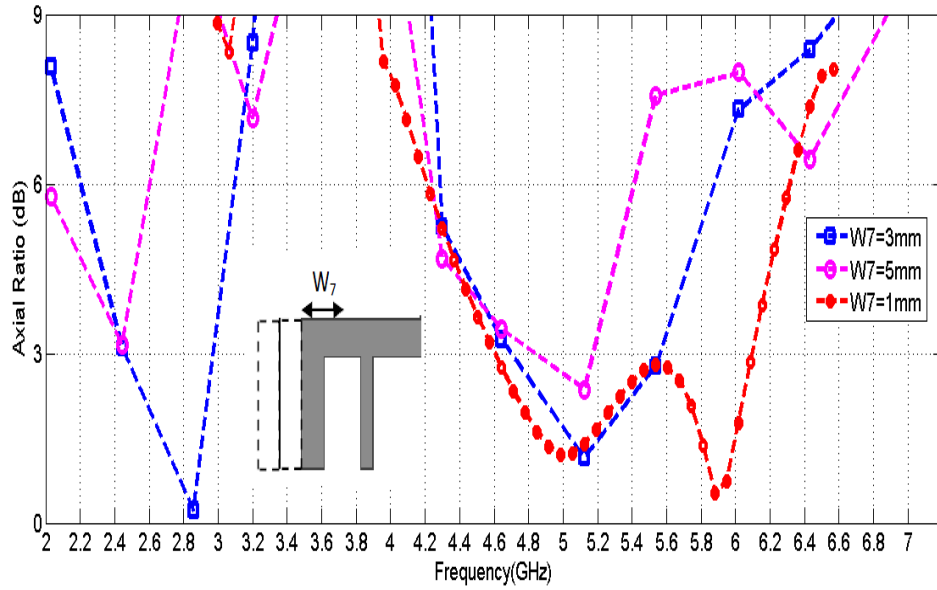


Figure 4.9 : Axial Ratio for different iterations of W_7

4.1.3.3 Studying effects of L_6 and L_{10}

Through extensive simulations and experiments, it was found that length of the crooked T-shape strips should be selected as $0.28L_s$, and the distance between them should be $0.23L_s$, to attain the 28.03% ARBW. Changing the length or distance between these strips will degrade the axial ratio and subsequently CP characteristic of the antenna seriously. Considering figures 4.10 and 4.11, it is understood that changing the size of L_6 to $0.21L_s$ and $0.14L_s$, will cause a slight shift to the left in the first resonance frequency of the antenna in the first band and a slight shift to the right in the third band. Adjusting $L_6=0.21L_s$, an UWB CPSS antenna will be obtained which its ARBW is 13.33% and covers more than 141% of frequency band. By setting $L_6=0.14L_s$, again an UWB antenna is obtained which has the same frequency characteristics as previous one ($L_6=0.21L_s$), but ARBW of the antenna degrades as much as 1.3GHz compared to the optimized antenna. The optimized antenna structure (Ant. IV) is also sensitive to the distance between the crooked T-strips, which is presented by L_{10} . Through extensive simulations and empirical experiences, the distance between the crooked T-shaped strips was optimized as 0.5mm. The effect of L_{10} variations on the ARBW of the antenna is studied and results are presented in figure 4.12. Setting $L_{10}=1.5\text{mm}$ will degrade the 3dB axial ratio bandwidth seriously as 1.1GHz. Increasing the L_{10} will also cause poverties in the ARBW which are not presented.

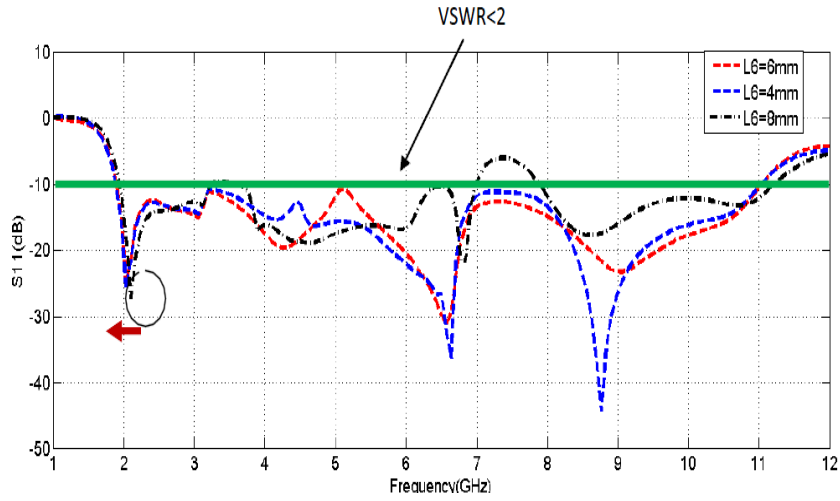


Figure 4.10 : S_{11} for different iterations of L_6

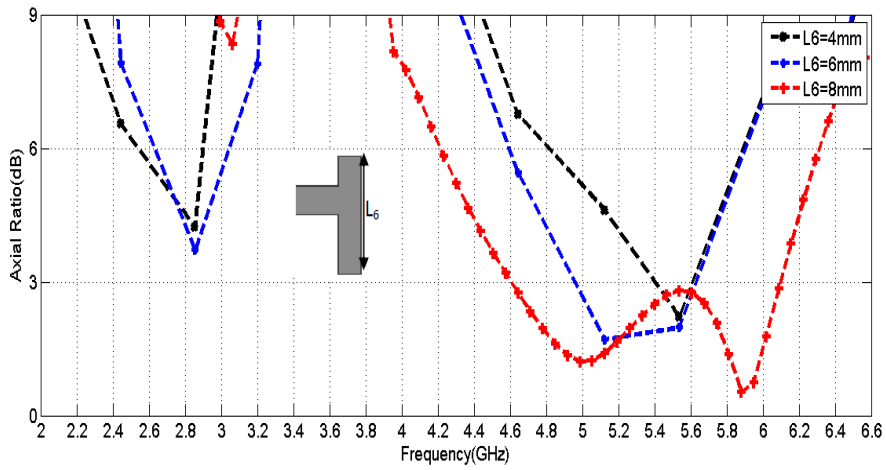


Figure 4.11 : Axial Ratio for different iterations of L_6

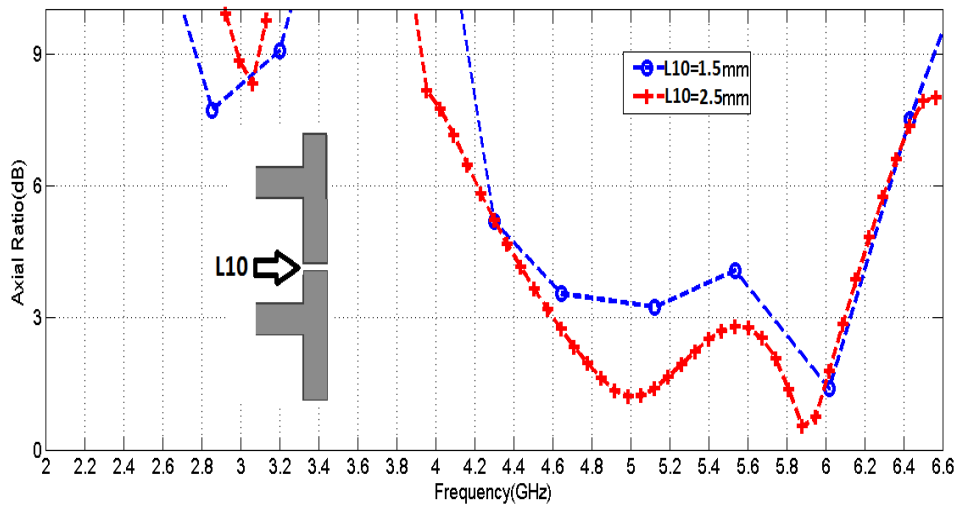


Figure 4.12 : Axial Ratio for different iterations of L_{10}

To illustrate the circular polarization mechanism, which requires modes of equal magnitude that are in opposite phase, the simulated surface current distributions

viewed from the microstrip side are illustrated in figure 4.13. The direction of the surface currents on the dipole arms and the microstrip feed network is presented at 5.4 GHz as the phase changes from 0 through 270 degree. It is observed that the surface current distribution in 90 and 270 degrees are equal in magnitude and opposite in phase as in 0 and 180 degrees. Antenna shows mainly RHCP at $z > 0$ and LHCP at $z < 0$. Measured RHCP and LHCP radiation patterns and directivity of the antenna at typical frequencies of 4.8GHz and 5.3GHz are presented at figure 4.14. Finally prototypes of the optimized antennas (Ant. I-Ant. IV) are fabricated and measured. Photographs of the antennas are shown in figure 4.15. Measured and simulated return loss and 3dB axial ratio bandwidth of the optimized antenna (Ant. IV) are presented in figure 4.16 and in addition, return loss and 3dB ARBW of the Ant. I-Ant. IV are presented in Table 4.1. A good agreement is observed between the measured and simulated data. One can observe a small difference between measured and simulated data at center frequencies. This might be due to other unknown parasitic effects which are not considered in the simulation. Since the soldering is not done with a machine on the PCB, positional errors might give rise to the discrepancy. The face to face and side to side group delay of the optimized antenna is also measured and presented in figure 4.17. As it is obvious, the measured group delay of the antenna is under 0.5ns which is very desirable for a low delay communication. Measured and simulated gains of the antenna are shown in figure 4.18. Antenna can attain a measured peak gain of 3.3dBi. The current surface of the antenna at sample frequency of 5GHz is also presented in figure 4.19. It can be seen from the plots, the current concentration of the antenna after adding the strips is at the lower center of the patch.

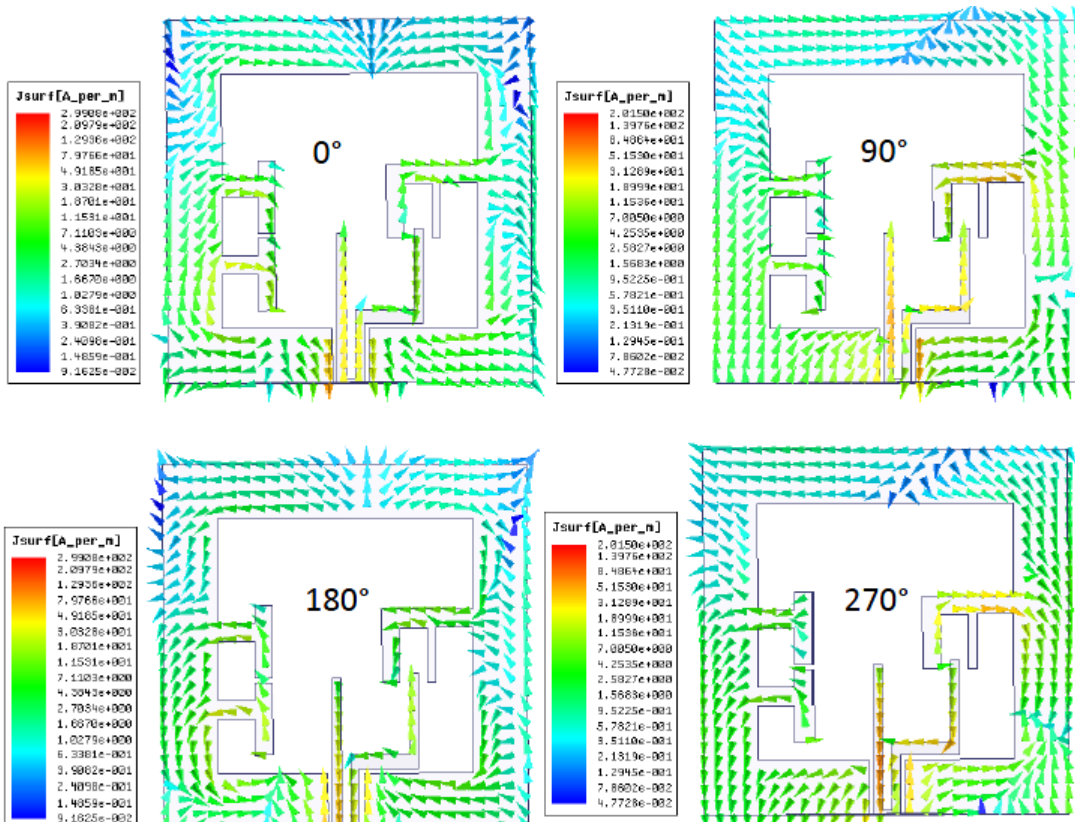


Figure 4.13 : Distribution of the surface current on the feed and ground of the CPSS antenna at 5.4 GHz in 0° , 90° , 180° , and 270° phase.

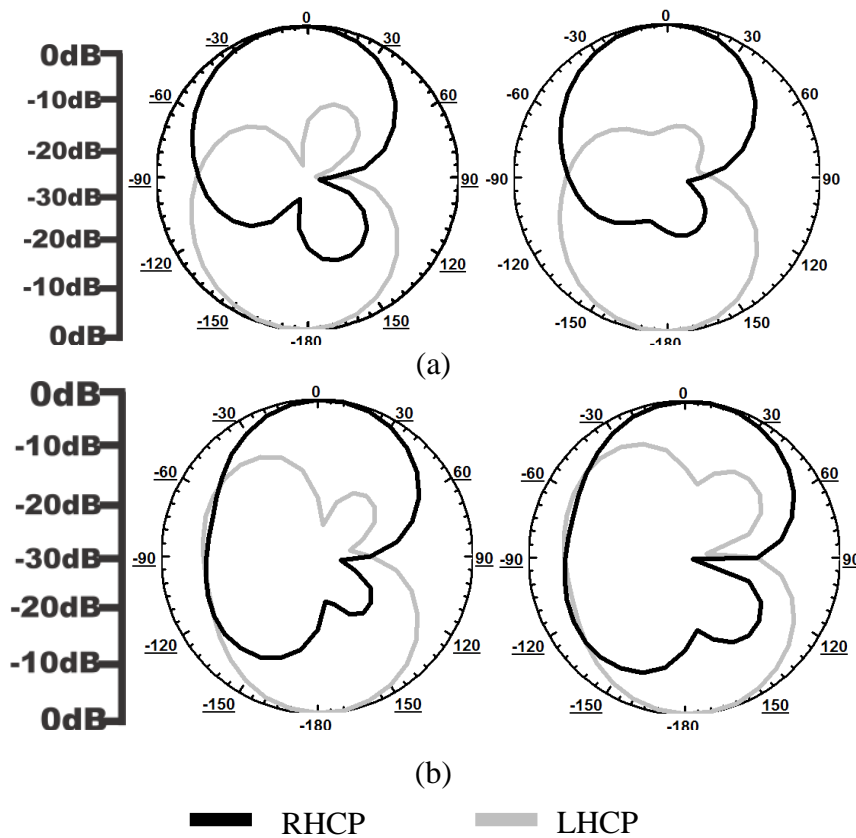


Figure 4.14 : Measured radiation patterns of the antenna at 4.8GHz (Left) and 5.3GHz (Right) at (a) $\phi=0^\circ$, (b) $\phi=90^\circ$

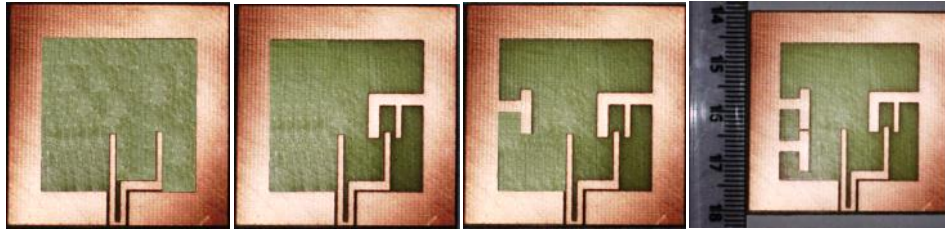


Figure 4.15 : Photograph of the four prototypes of CPSS antennas

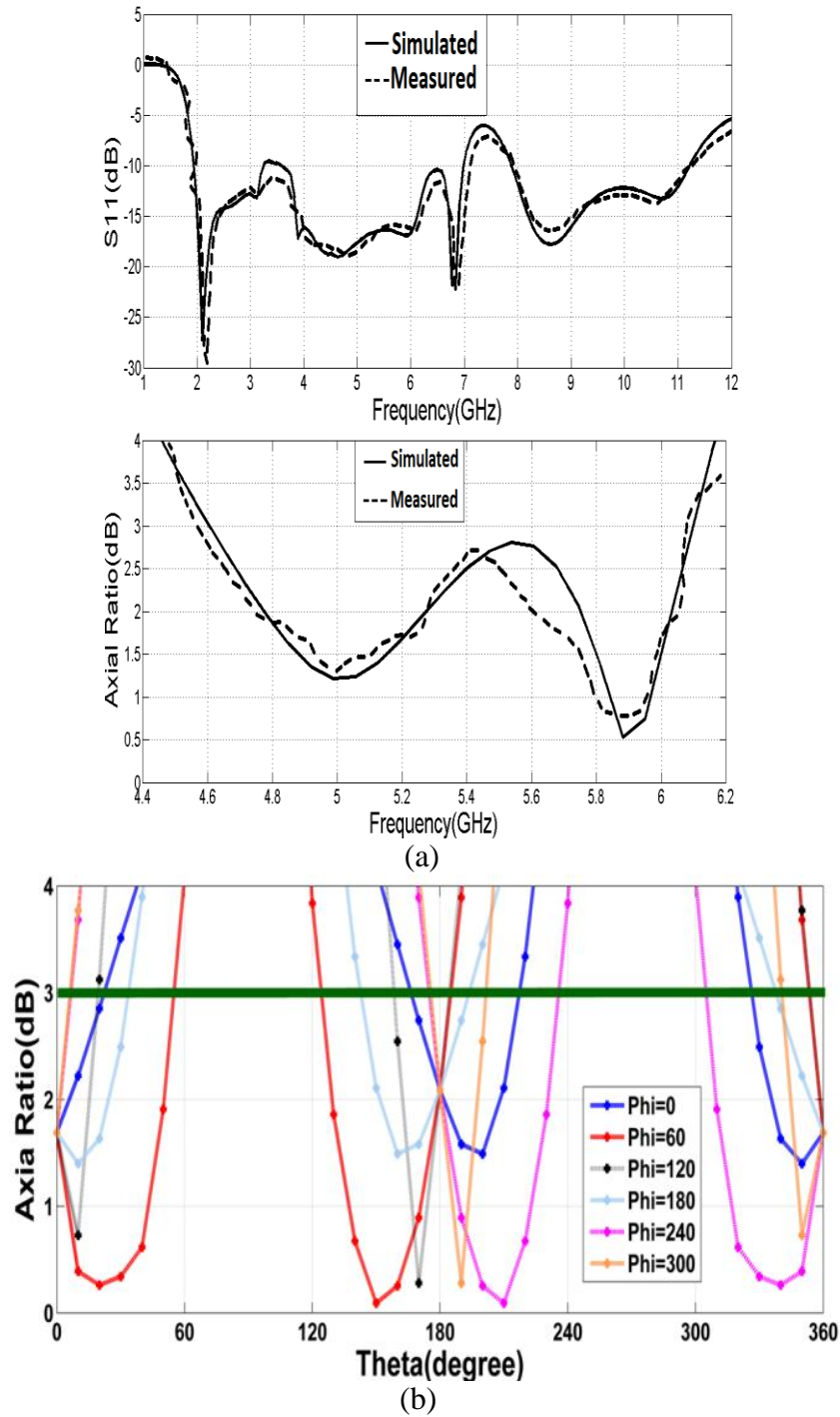


Figure 4.16 : Measured and simulated (a) impedance matching and 3dB axial ratio bandwidths of the proposed CPSSA with frequency and (b) different ϕ angles at sample frequency of 5GHz.

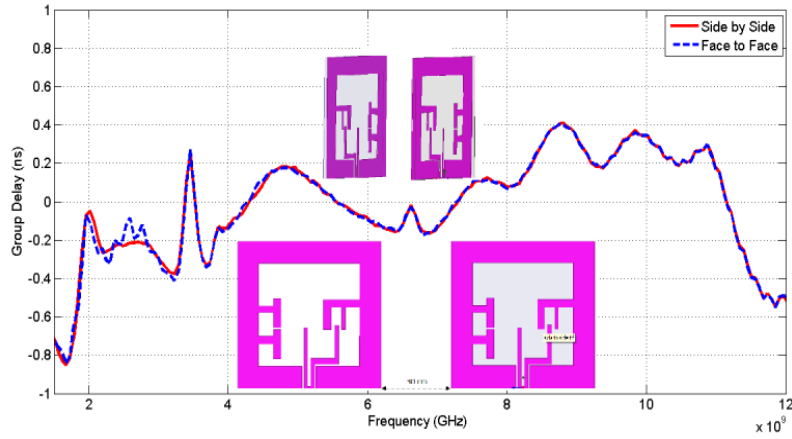


Figure 4.17 : Measured group delay of the antenna

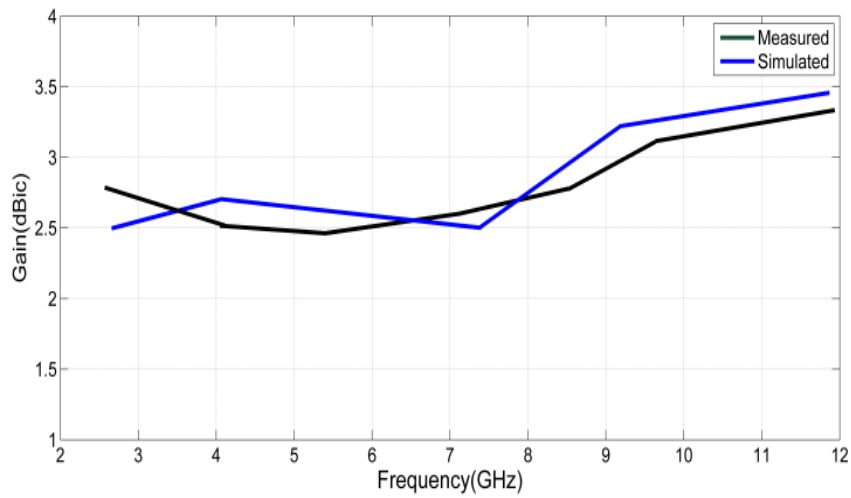


Figure 4.18 : Measured and simulated gain of the CPSSA

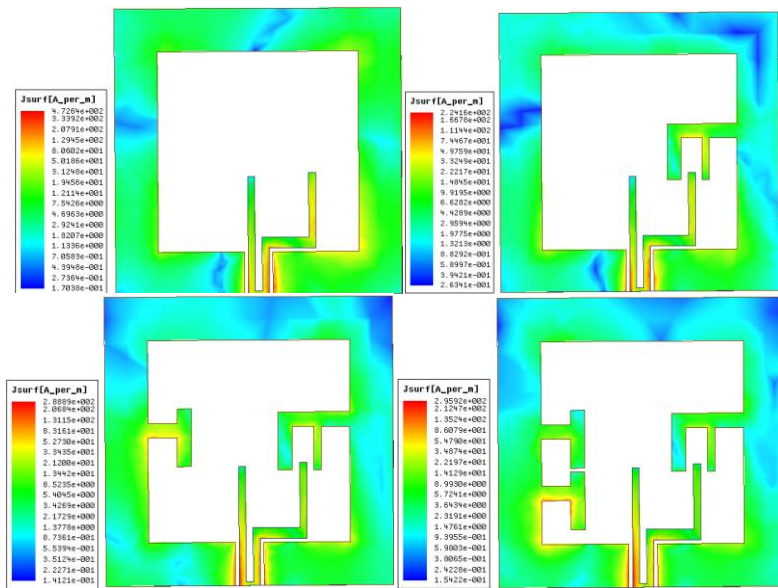


Figure 4.19 : Distribution of the surface current on the feed and ground of the CPSS antenna at 5GHz

Table 4.1 : Measured S11 and 3dB ARBWs of CPSS antennas.

	BW(VSWR<2) MHz	3dB ARBW (%)
Ant. I	3423-1091	0
Ant. II	1823-2283	3.76%
	2821-11131	
Ant. III	1795-9621	2.05%
	9821-10096	
Ant. IV	1871-3321	28.03%
	3731-7012	
	7887-11196	

4.2 Dual Band Dual Sense Circularly Polarized Monopole Antenna for GPS and WLAN Applications

4.2.1 Antenna design

The geometry of the proposed circularly polarized monopole antenna is presented in figure 4.20, in which the radiating patch and grounded conductor are on the top and bottom layers of a cheap FR4 square substrate with a side length of $L=30\text{mm}$, thickness of $h=1\text{mm}$, a dielectric constant of $\epsilon_r=4.4$, and a loss tangent of $\tan \delta=0.02$ respectively. The antenna is fed by a 50Ω microstrip feed line, where the signal strip is fixed at $W=1.875$, and gap between the radiating patch and grounded conductor is fixed at $g=0.2\text{mm}$. The radiating patch is a simple circle of radius 10mm ($0.33L$), connected to the microstrip feed line with length of 2mm . At first 4 slots with lengths of L_1 , L_2 , L_3 and L_4 are created on the circular radiating patch to excite the CP operation of the antenna. As the aim of the presented work is to design the antenna for GPS and WLAN operating bands and enclose CP in both these operating frequencies, two bigger and smaller vertically and horizontally slots with L_5 , L_6 , L_7 and L_8 lengths are created on the circle radiating patch respectively. Note that the antenna presented in figure 4.20 can provide left and right hand circular (LHCP and RHCP) waves in the $z<0$ and $z>0$ respectively. To better understand the effect of the stubs three improved prototypes of the proposed CP monopole are designed and presented in Table 4.2.

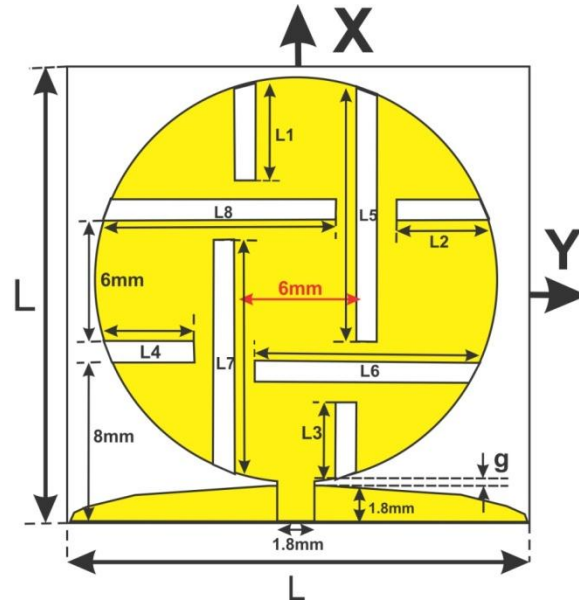


Figure 4.20 : Geometry of the proposed CP monopole antenna

Table 4.2 : Parameters and performance of three antennas under investigation

	L1	L2	L3	L4	L5	L6	L7	L8	BW (VSWR< 2) (MHz)	fc (MHz)	3 dB ARBW MHz, (%)
	mm	mm	mm	mm	mm	mm	mm	mm			
Ant. I	4.79	4.53	3.79	4.16	0	0	0	0	6700 (1900-8600)	5250	0,0
Ant. II	4.79	4.53	3.79	4.16	12.5 3	0	11.5 3	0	1524 (2133-3657) 1863 (4568-6431)	2895 5499.5	1179&1050,40&1 9 (1538-2717) (5690-6740)
Ant.III	4.79	4.53	3.79	4.16	12.5 3	11.1 6	11.5 3	11.5 3	1000 (1500-2500) 1143 (4700-5843)	1797.5 5271.5	595&624,33.1& 11.83 (1500-2095) (4711-5335)

4.2.2 Parametric study of the antenna

Ant. I has just four slots (L_1 , L_2 , L_3 and L_4) created on the circular radiating patch. Figure 4.21, shows its frequency responses (including the return loss and AR), whereas Table 4.2 lists the structural parameters and summarizes the bandwidth data. Notice that these slots cannot create 3dB ARBW for the Ant. I. This ARBW cannot improved by increasing or decreasing the length of the L_1 , L_2 , L_3 and L_4 . To demonstrate that the additional pair of bigger vertical slots implanted in the radiating patch can greatly improve the CP performance of the proposed monopole antenna, we keep the L_1 , L_2 , L_3 and L_4 unchanged. The width of all the slots is fixed at 1mm. Ant. II with $L_5=12.53\text{mm}$, and $L_7=11.53\text{mm}$ was measured to exhibit an ARBW of 40% and 19% for lower and upper band respectively. Note that the lower impedance

matching band ($VSWR < 2$), does not entirely enclose the ARBW. Ant. II encloses WLAN (specified by IEEE 802.11a/b/g), WiMax band at 2500 (specified by IEEE 802.16m) with CP characteristic. By adding L_8 and L_9 the discussed desired design is obtained. As presented in figure 4.21, antenna operates in 1500-2500MHz for lower band and 4700-5843MHz for upper band which covers the GPS and 3G, WLAN (IEEE 802.11b/g) frequencies in lower band and WLAN (specified by IEEE 802.11a), upper WiMax, and HiperLAN (specified by IEEE 802.11) operational frequencies for upper band respectively. CP operation of the antenna encloses GPS, DCS (1710-1880MHz), and PCS (1850-1990MHz) bands in lower and WLAN (5150-5350MHz) in upper band respectively. It can be seen from figure 4.21 that by addition of two bigger vertical slots antennas ARBW is in its maximum value. In figure 4.21 the simulated and measured data for Ant.III by Ansoft HFSS and Agilent N5320A network analyzer are presented, respectively. There is a reasonable agreement between the simulated and measured data. Note that in terms of antenna size, the presented design is smaller than previously proposed antennas . Furthermore the construction of the antenna is simpler than most the reported antennas. Nevertheless the achieved 3dB axial ratio is larger than that of antennas presented previously. Figure 4.22 shows the measured radiation pattern of Ant.III at 1800MHz and 4800MHz. The measured (simulated) gain of the Ant.III shown in figure 4.23 was found to have a maximum value of 3.1dBic with a variation of less than 1 dB.

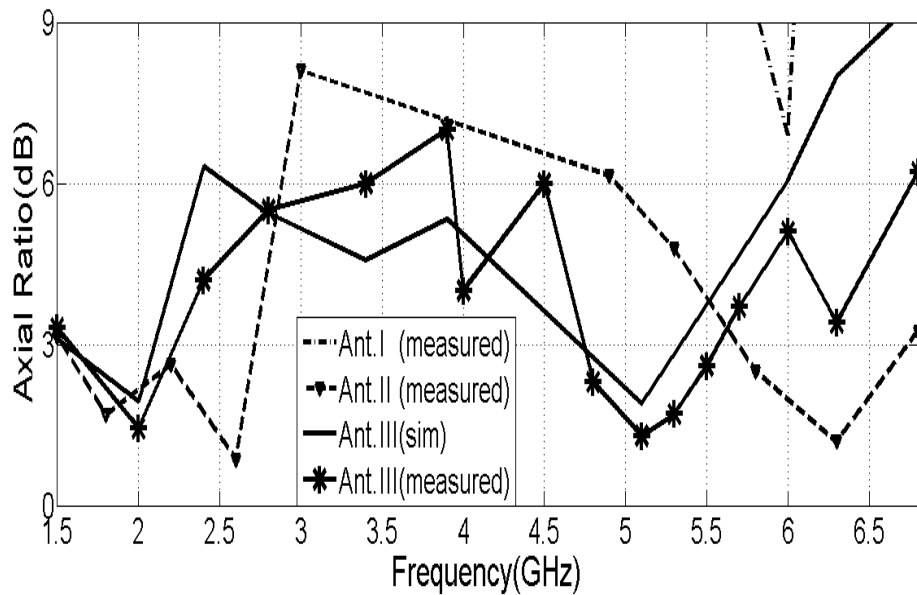
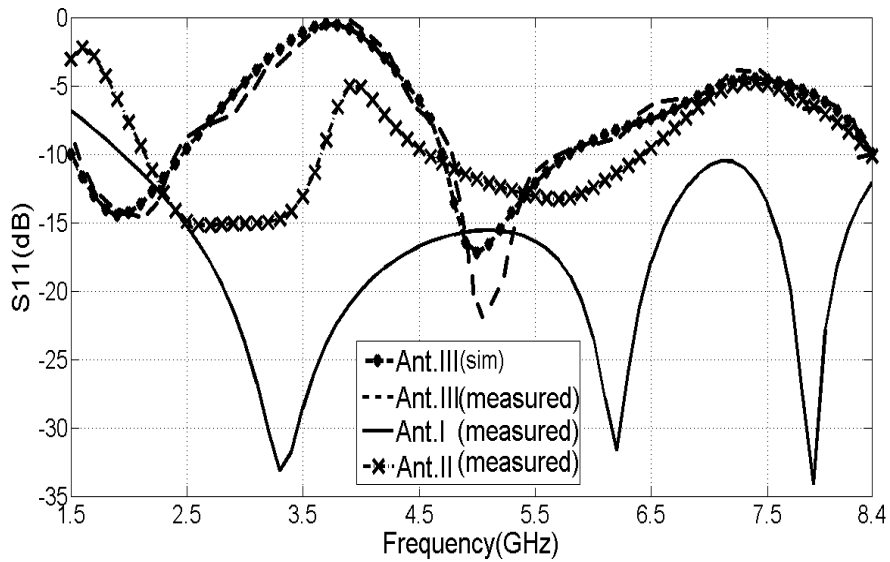


Figure 4.21 : Measured return losses and CP axial ratios of Ant. I, II, III and simulated data of Ant.III

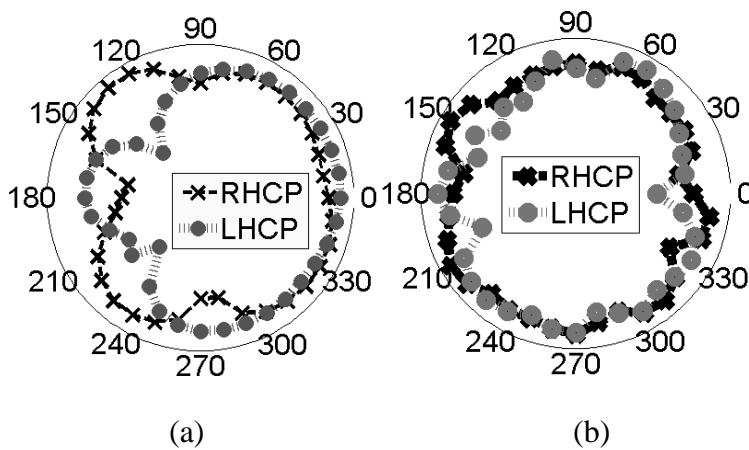


Figure 4.22 : (a) radiation pattern of the Ant.III in $\Phi=90$ at (a) 1.8GHz, (b)4.8GHz

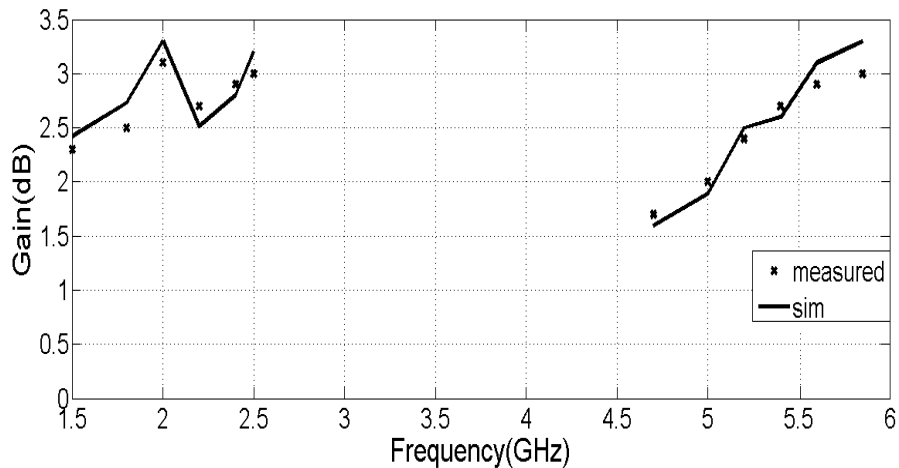


Figure 4.23 : Measured and simulated gain of the proposed CP Ant.III (a) radiation pattern of the Ant.III in $\Phi=90$ at (a) 1.8GHz, (b) 4.8GHz

4.3 A Broadband Asymmetric-CPW-fed Circularly Polarized Antenna with Defected Substrate

4.3.1 Introduction

Most of the CP antennas have large sizes, small 3dB axial ratio bandwidths, narrow operating bands or layered and stacked structures which are both costly and not appropriate for the PCBs. For partial improvement of these drawbacks a novel, compact, coplanar and low profile circularly polarized antenna for mobile and wireless applications is designed and experimented. The presented antenna in this work uses a U-shape asymmetric CPW feedline in conjunction with an inverted L-strip on the lower left and a 45° bent strip on the upper left corner of the antenna respectively. These strips in coincidence with the defected structure of the substrate and patch on the upper right and left corners of the antenna are employed to enhance the antenna with a relatively wide circular polarization bandwidth. Cutting the substrate has a significant effect on the improvement of surface current distribution and consequently establishment of circular polarization. Using this configuration, the circularly polarized antenna (CPSSA) can achieve impedance matching bandwidth between 2.69 to 8.83 GHz. The designed CPSSA has a circular polarization in the frequency band of 2.92 to 5.36GHz which covers wireless local area network (WLAN) for IEEE 802.11.a (operating in 5.15–5.35 GHz) and WiMax systems. Rest of the material is arranged as follows; in 4.3.2 the geometry and configuration of the optimized CPSSA is given. In 4.3.3 the design procedure and effects of each design

element on antenna improvement are described step by step. In 4.3.31 parametric study of the antenna and effects of changing each part of the optimized design are discussed and accomplished results are presented.

4.3.2 Antenna design

The configuration of the proposed broadband circularly polarized asymmetric CPW-fed antenna is illustrated in figure 4.24. The antenna is fabricated on a defected FR4 substrate of thickness 0.8mm and permittivity 4.4 with an overall dimension of $G \times G$.

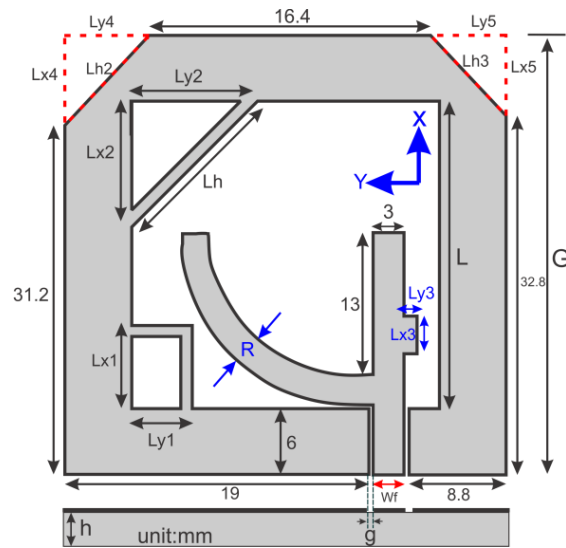


Figure 4.24 : Geometry configuration of proposed CPSSA antenna

The antenna is fed by a 50Ω CPW feedline with a signal strip of width $W_f=3\text{mm}$ and two identical gaps of width $g=0.3\text{mm}$. Antenna uses a U-shape feed line coincides with an inverted L-strip and a 45° bent strip facilitate enhancing the ARBW of the antenna. The U-shaped feedline is formed by extending the signal strip of the asymmetric CPW feedline in the $+y$ direction to the upper left corner of the slot (the horizontal feed section) and protruded into the slot. The structure in possession of a branch stub (with width Ly_3 and length Lx_3) at the center of the signal strip is used to obtain a better impedance matching. A square slot with a side length of L is located at the centre of the ground plane. Two additional triangle slots cut and removed from two upper corners of the square slot. Each of them consists of a pair of triangle slots with different sizes. These slots will help better surface current circulation and excite the CP operation. The left triangle slot has lengths Ly_4 and Lx_4 in $+y$ and $+x$ directions respectively and hypotenuse of length L_{h2} and the right one has lengths Lx_5 and Ly_5 in $+x$ and $+y$ directions respectively and hypotenuse of length L_{h3} . By adjusting the dimensions of Lx_4 , and Ly_4 and as a result adjusting L_{h2} , circular

polarization can be controlled in lower frequencies and adjusting L_{h3} can control circular polarization in upper frequencies. To induce two orthogonal resonant modes with a 90 degree phase difference and equal amplitude, a conventional inverted L-strip with L_{x1} and L_{y1} dimensions and a 45° bent strip with L_{x2} and L_{y2} dimensions, both with identical widths of 1mm are added to the left lower and upper sides of the patch respectively. Adjusting the dimensions of L_{x1} , L_{x2} , L_{y1} and L_{y2} , facilitate creating the circular polarization characteristic. The structure shown in Fig.1 can generate LHCP and RHCP radiations in the $+z$ and $-z$ directions respectively.

4.3.3 Design procedure

Success of a CP antenna mainly depends on whether the entire 3dB AR band is entirely enclosed by the 10dB return loss band. For that reason the first step in the design procedure focuses on how U-shape feed and branch strip affect both the 3dB axial ratio (AR) bandwidth and the impedance matching. Along this line, it is first considered the antenna structure Ant.0 given in figure 4.25, where it includes only a square slot and a rectangular patch located at the lower right corner. It has been observed that such an antenna configuration has no 10dB impedance matching.

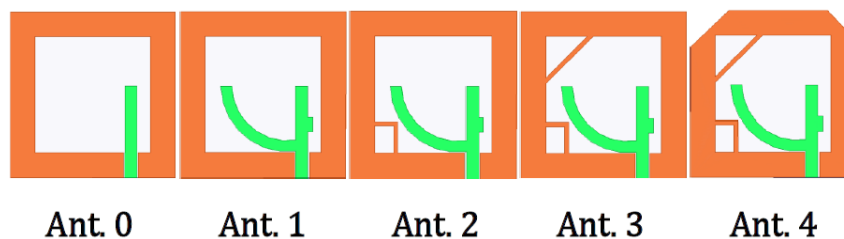
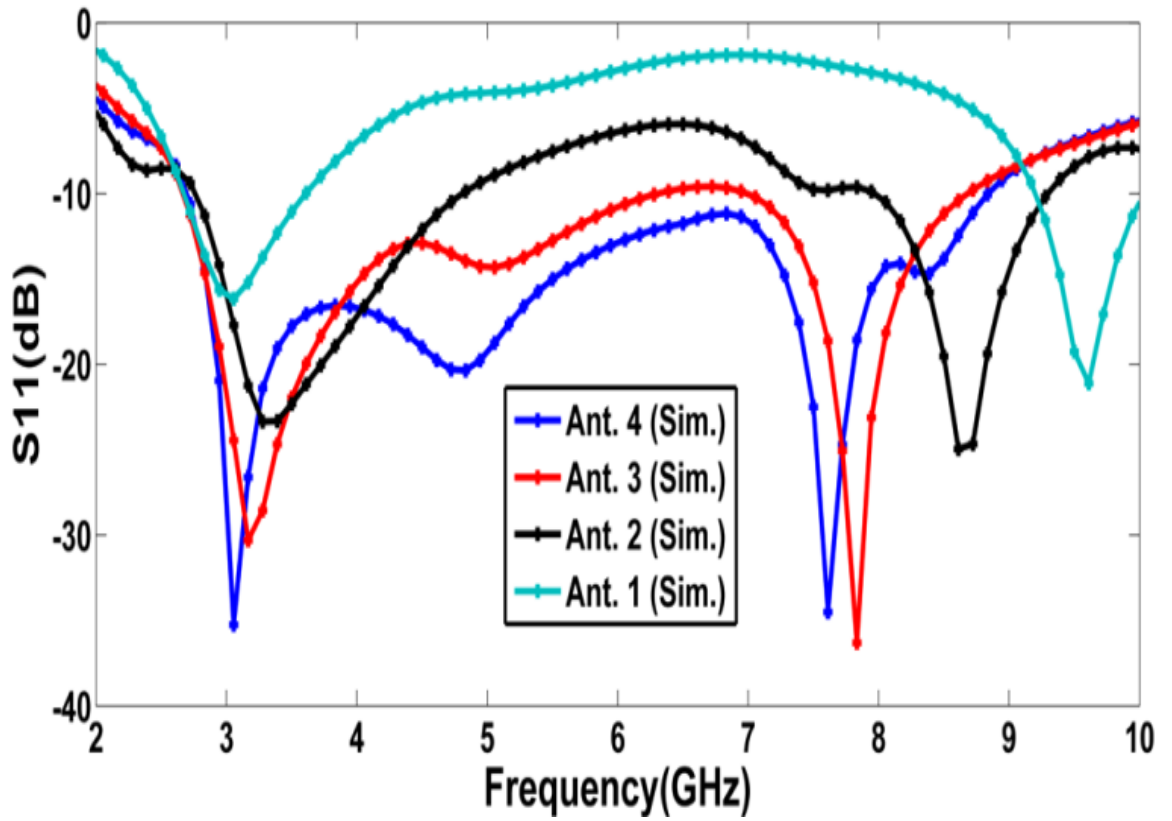


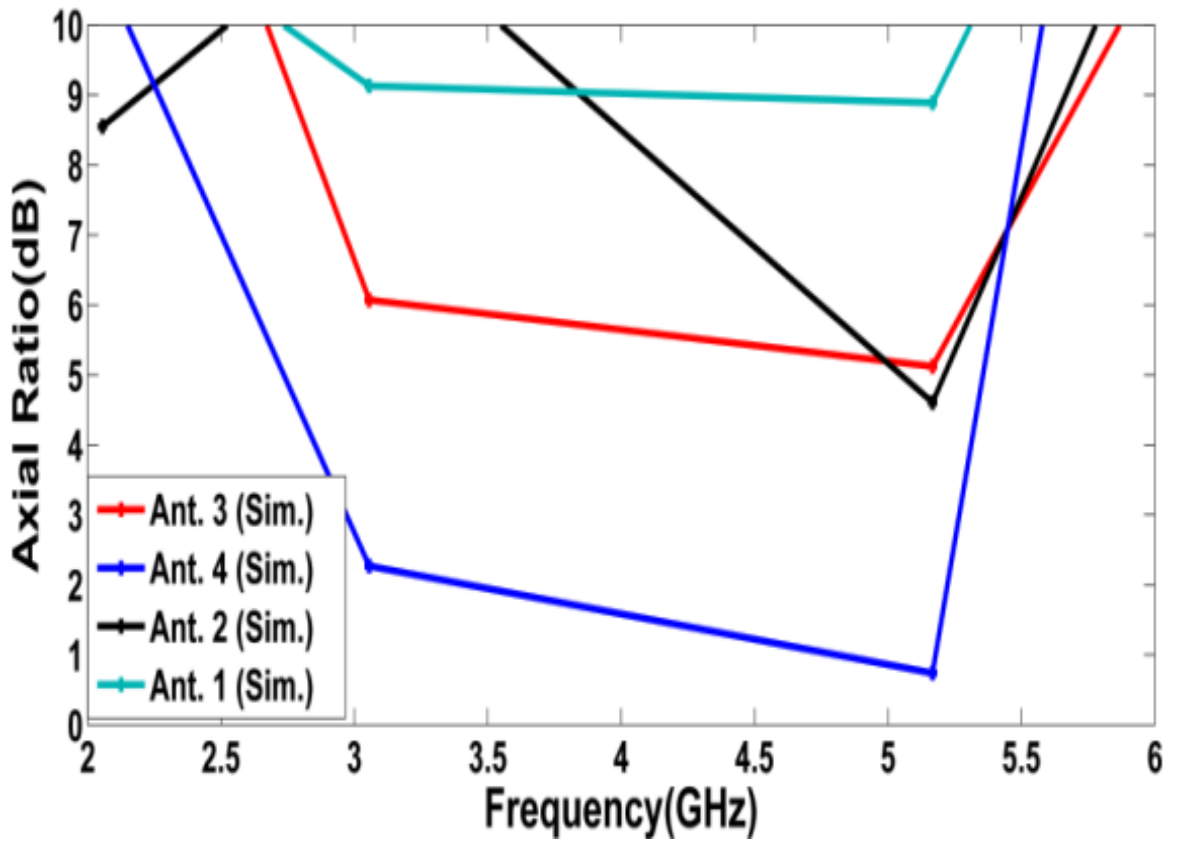
Figure 4.25 : Improved prototypes of the presented CPSSA in design procedure

In order to improve the impedance matching bandwidths of the antenna a U-shape branch is added to the feeding structure. Also to generate an asymmetrical feeding branch and thus excite the new resonance modes for improving the CP and impedance bandwidth, a stub with dimensions of $L_{x3} \times L_{y3}$ is further added to the feedline (See Ant.1 in figure 4.25). This will improve the impedance matching of the antenna mainly due to the coupling between the feedline and the grounded slot at the lower center and right center of the slot. The corresponding 10dB return loss and axial ratio variations versus frequency are demonstrated in figure 4.26a and figure 4.26b, respectively. As can easily be observed the new contributions bring an observable impact in the return loss. But there is still an impedance mismatch in frequencies between 4-9GHz. To improve the impedance matching property and also

3dB axial ratio bandwidth of the antenna a conventional inverted L-strip is added to the antenna structure, presented as Ant.2 in figure 4.25 This improves the impedance matching bandwidth of the antenna to a great extent (see figure 4.26a). For further improvement of the impedance matching of the antenna between 5-7.5GHz, another 45° bent strip is added to the upper left corner of the antenna (See Ant.3 in figure 4.25). The contribution of this structure to the impedance matching bandwidth can be observed in figure 4.26a. On the other hand, as seen in figure 4.26b, there is still no 3dB ARBW available. Ant. 4 has the same structure as Ant.3 but with triangle shape cuts removed from the upper left and right corners. In order to radiate circularly polarized, it is necessary to induce two orthogonal resonant modes with a 90 degree phase difference and equal amplitude. This can be accomplished by removing two triangular shaped pieces from top right and left corners of the antenna as depicted in Fig.2 (Ant.4). As depicted in figure 4.27 cutting two triangular slots with the optimized dimensions mentioned in Table 4.3 and properties discussed previously, improves the current circulation around the top corners of the slot and creates the circular polarization of the antenna. As it can be observed from figure 4.26b the simulated ARBW of the antenna is available from 3.08-5.23GHz. On the other hand, the current distributions on the defected grounded slot are stronger at the center frequencies. This can be equivalent to the case that the defected grounded slot area is used for the excitation of the proposed antenna in CP band. The antennas current distributions of 0, 90, 180 and 270 degrees at sample CP frequency of 5GHz are plotted in figure 4.28. It is observed that the surface current distribution in 180° and 270° are equal in magnitude and opposite in phase of 0° and 90°.

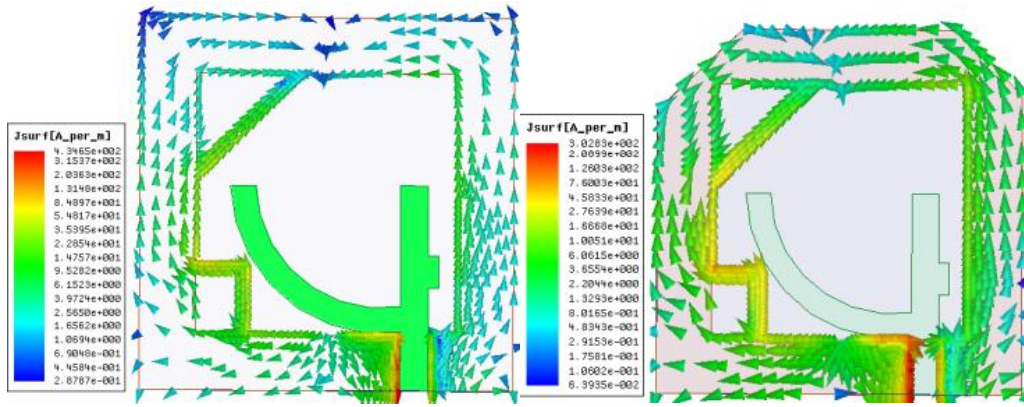


(a)

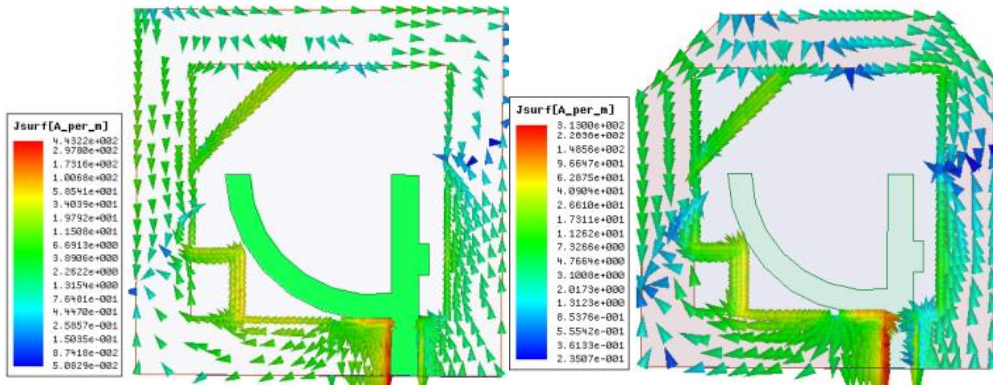


(b)

Figure 4.26 : Simulated (a) S_{11} and (b) axial ratio curves of the four improved prototypes of the CP antenna



(a)



(b)

Figure 4.27 : Current surfaces of the antenna with and without defected substrate at sample frequencies of (a) 4GHz (b) 5GHz

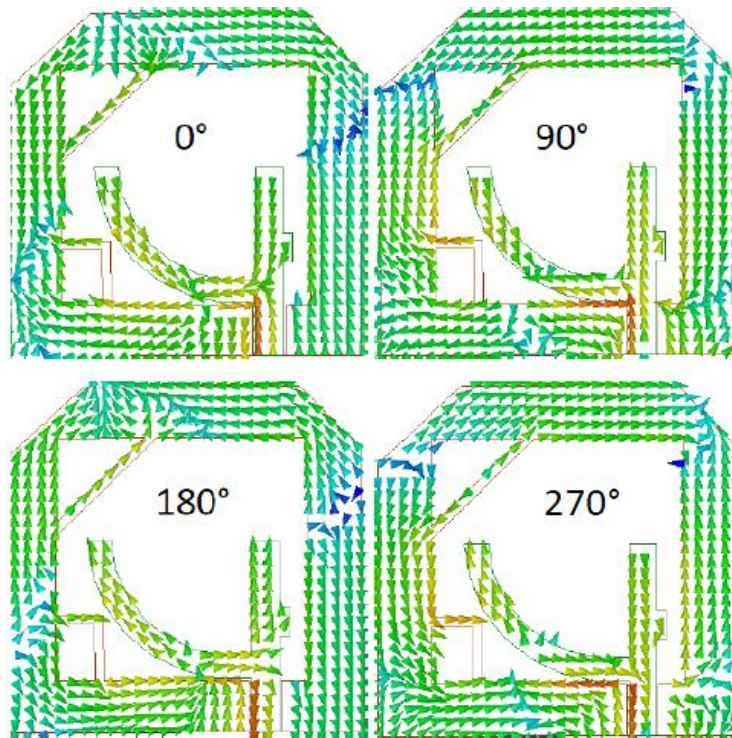


Figure 4.28 : Current distributions of 0° , 90° , 180° and 270° at sample CP frequency of 5GHz

4.3.3.1 Effect of L_h on CP

The 10dB return loss and 3dB axial ratio bandwidths for different values of L_h are given in figures 4.29a, b respectively. The optimized value of the L_h is found to be $0.35L$ in the optimized design (Ant.4). Notice that decreasing the size of L_h from $0.35L$ to $L_h=0.31L$ causes a decrease of 14.24% on the total 3dB ARBW of the antenna, especially in lower frequencies. On the other hand, decreasing the size of L_h has no significant effect on 10dB impedance matching. Increasing the length of L_h to $0.53L$ causes a noticeable decrease and dissipation of the total CP operating band of the antenna. Also by increasing the length of L_h an impedance mismatch occurs between 5-6GHz (See figure 4.29a).

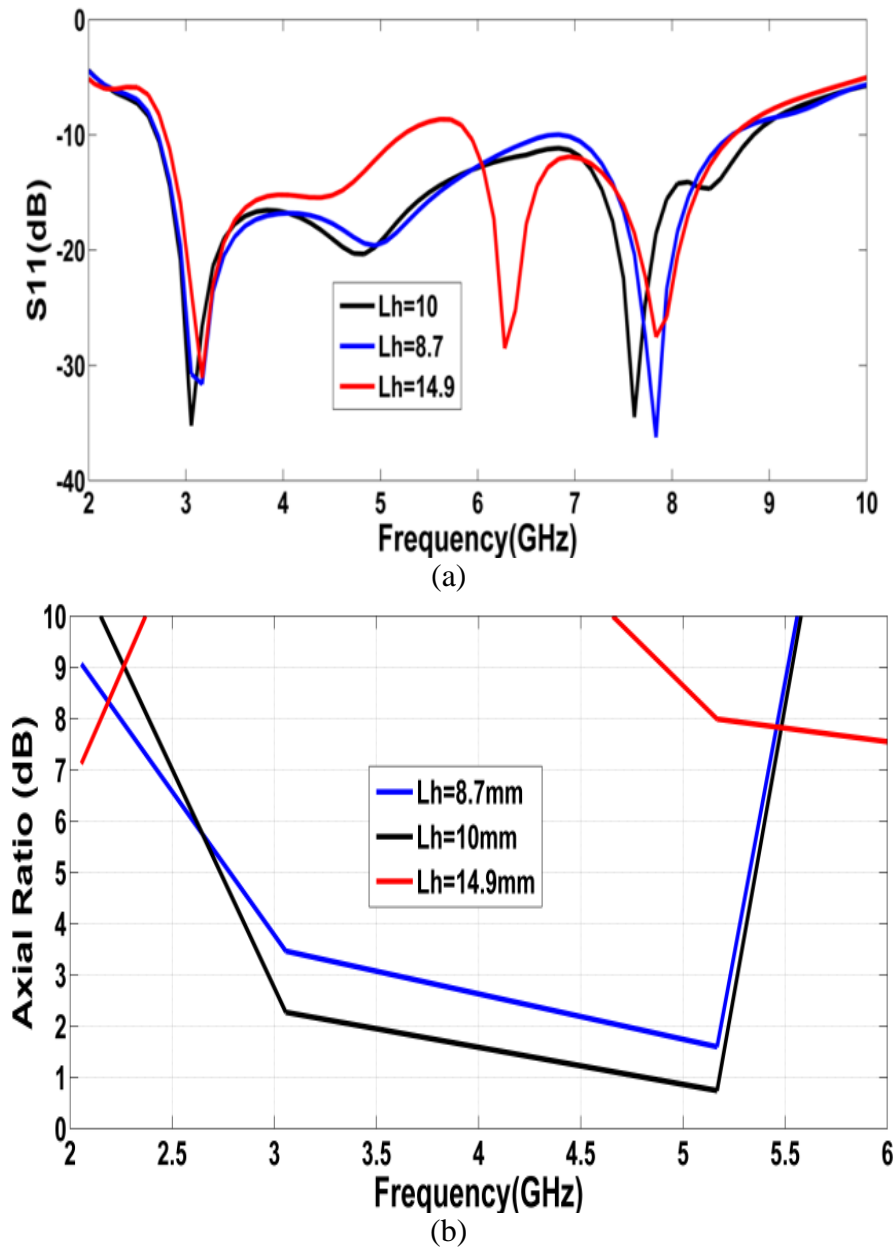


Figure 4.29 : Simulated (a) S_{11} and (b) axial ratio variations for different values of L_h

4.3.3.2 Effects of L_{h2} and L_{h3} on CP band

The effects of changing the lengths of L_{h2} and L_{h3} are also studied and the results are demonstrated in figures 4.30 and 4.31 respectively. As can clearly be seen from figure 4.30 a and figure 4.31a, they have no significant effect on the return loss variations while the 3dB ARBW changes by assigning different values for them. The optimum value for L_{h2} and L_{h3} are obtained as 0.33L and 0.35L respectively. When L_{h2}=0.27L the center frequency of the CP operating band moves to about 5.2GHz and the 3dB ARBW decreases to about 19% (considering the center frequency of 5.2GHz) as presented in figure 4.30b. Increasing L_{h2} to L_{h2}=0.56L and its proximity to the edge of the inner slot area (L×L), decreases the current distribution around the corner and consequently CP excitation. As a result a remarkable decrease in the 3dB ARBW for about 475MHz or 9.6% occurs (See figure 4.30b). The same cases are considered for the L_{h3} and the results are presented in figure 4.31.

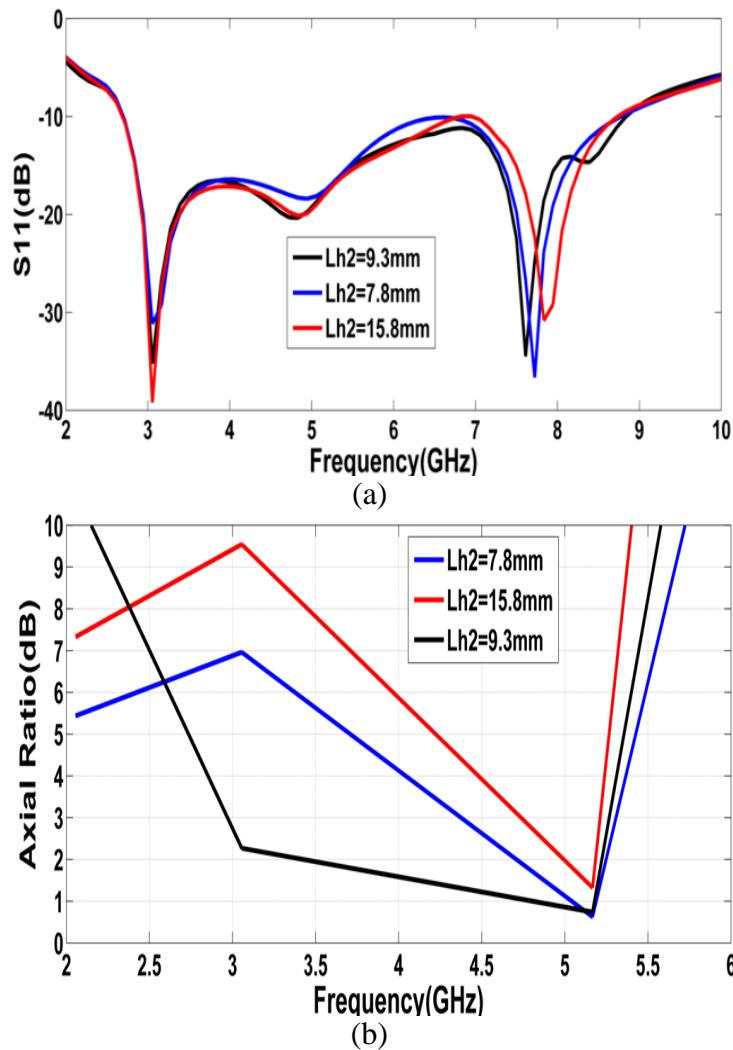
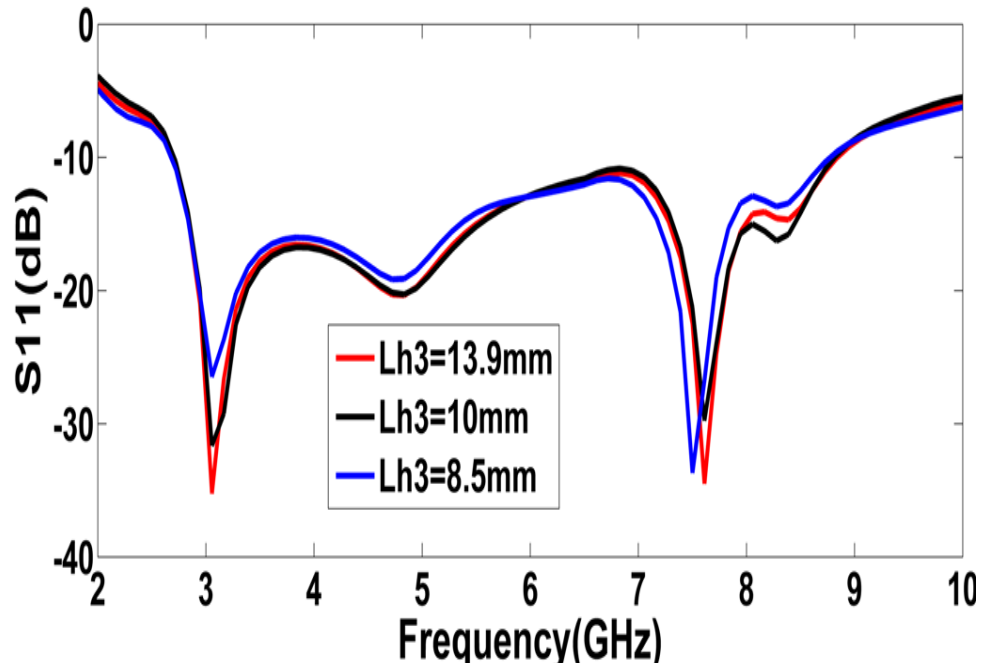
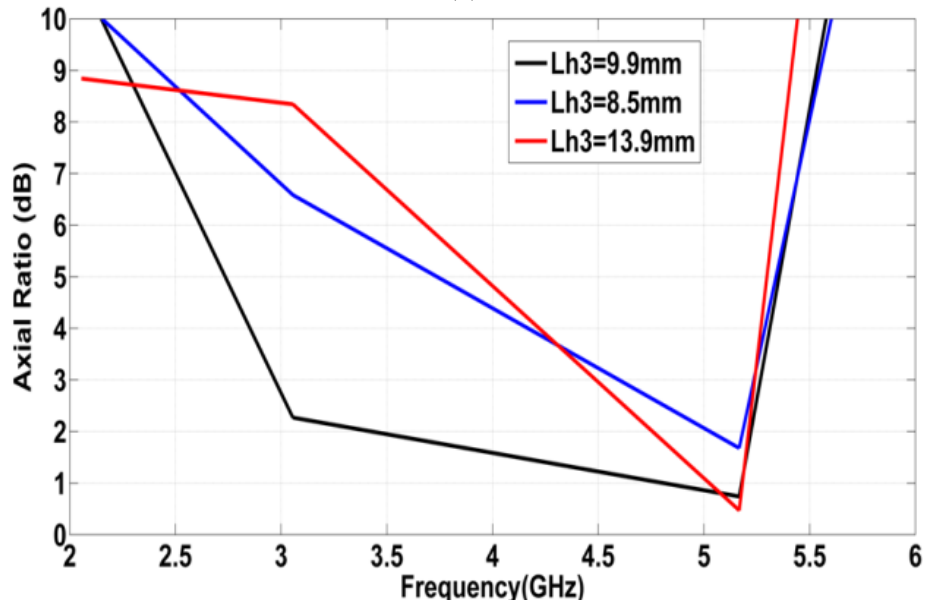


Figure 4.30 : Simulated (a) S₁₁ and (b) axial ratio variations for different values of L_{h2}



(a)



(b)

Figure 4.31 : Simulated (a) S_{11} and (b) axial ratio variations for different values of L_{h3}

4.3.3.3 Effects of L_{x1} and R on CP

To enhance the 3dB ARBW of the antenna, at first an inverted L-strip was employed as suggested in . Its variations and effects of them are also studied. With the extensive simulations the optimum value of L_{x1} found to be $0.26L$. Decreasing and increasing L_{x1} from the optimum value is going to cause a decrease in impedance matching and 3dB ARBW of the antenna. This is mainly caused due to the coupling between the inverted L-strip and the U-shape feedline and decrease in the current

distribution intensity at the lower left corner of the antenna. The radius of the U-shape strip was also studied, and optimum value of the R was found to be 2.7mm. It is observed that changes around the optimum radius of the U-shape strip causes to occur at dual band in the return loss variation while CP is dissipated. This is due to the fact that such variations change the current intensity on the feedline.

4.3.3.4 Further design verifications

To verify the presented design, the optimized antenna (Ant. 4) is studied on different substrate materials, i.e.: RT5880 substrate (h=0.8mm), Taconic Cer.10 substrate (h=0.8mm), Isola Gigaver210 substrate (h=0.8mm) and FR4 (h=0.8, 1 and 1.6 mm). The 3dB ARBWs are all above 10% and completely enclosed by their impedance bands, signifying that the presented design procedure can be applied to antennas using substrates with a broad range of substrate thickness and with dielectric constants of as low as 2.2 and as high as 10 and with 3dB ARBW between 10 and 57%.

4.3.4 Measured results

Through the design procedure and the parametric study given in the previous sections, the optimized dimensions of the antenna are obtained as in Table II (Ant.4). The prototypes of the proposed antenna (figure 4.25) are constructed and the photograph of the optimized one is revealed in figure 4.32. All the prototypes discussed in the previous sessions were constructed and measured using Agilent N5230A network analyzer in the anechoic chamber with dimensions 6X7X3.3m and working frequencies 80Mhz to 20GHz. For abbreviation only the photograph of the optimized design is presented. The measured results for four prototypes of the antenna depicted in figure 4.25 are also given in Table I. The comparison between simulated and measured S_{11} and axial ratio characteristics for Ant.4 (optimized design) is given in figures 4.33a and b, which provides sufficiently 10dB return loss impedance bandwidth of 103%, from 2691-8833MHz relative to the centre frequency of 5762MHz. Also measured axial ratio of the antenna at different Phi values at sample frequency of 5.2GHz is presented in figure 4.33c. Due to the effect of the SMA connector and the mismatching tolerance, the measured impedance bandwidth is in fairly accurate agreement with the simulated one. Despite of this discrepancy, the impedance match remains acceptable. The parametric studies of the antennas are

validated through measurement. The measured results are presented in Table 4.4 and Table 4.5 respectively. The simulated and measured maximum gain is shown in figure 4.34. It can be seen that simulated gain is between 2.8-3.8dBic within the 3dB axial ratio bandwidth from 2.92 – 5.36GHz. The measured peak gain is 3.6dBic at 8.12GHz while the simulated peak gain is 3.82dBic. The far-field radiation patterns of the fabricated optimized antenna (Ant. 4) using the 0.8-mm-thick FR4 substrate in both the $\phi=0^\circ$ and $\phi=90^\circ$ planes at 4.5 and 5.5 GHz were measured. As can be seen in figure 4.35, the CP antenna produces mainly LHCP radiations in $z>0$ and RHCP radiations in $z<0$. After testing all characteristics of the antenna, the present work was compared to the previously reported antennas. It can be seen that the antenna presented in Ref.[34] achieves broader 3dB axial ratio than the antenna in this work. However when the 3dB bandwidth of the antenna in [34] is considered, it is observed that it covers about 1.5GHz CP bandwidth. However the antenna presented in this work achieves about 2.3GHz of CP bandwidth. The second merit of the presented work is its broader impedance matching bandwidth compared to one of [34]. And as the last point the presented antenna in this work is smaller than previously reported antennas in the literature.

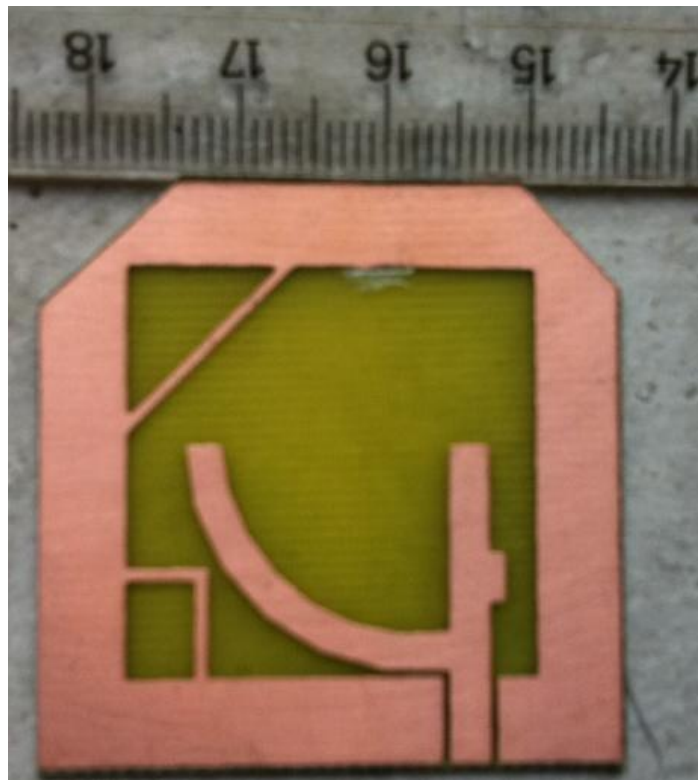


Figure 4.32 : Photograph of the optimized antenna (Ant.4)

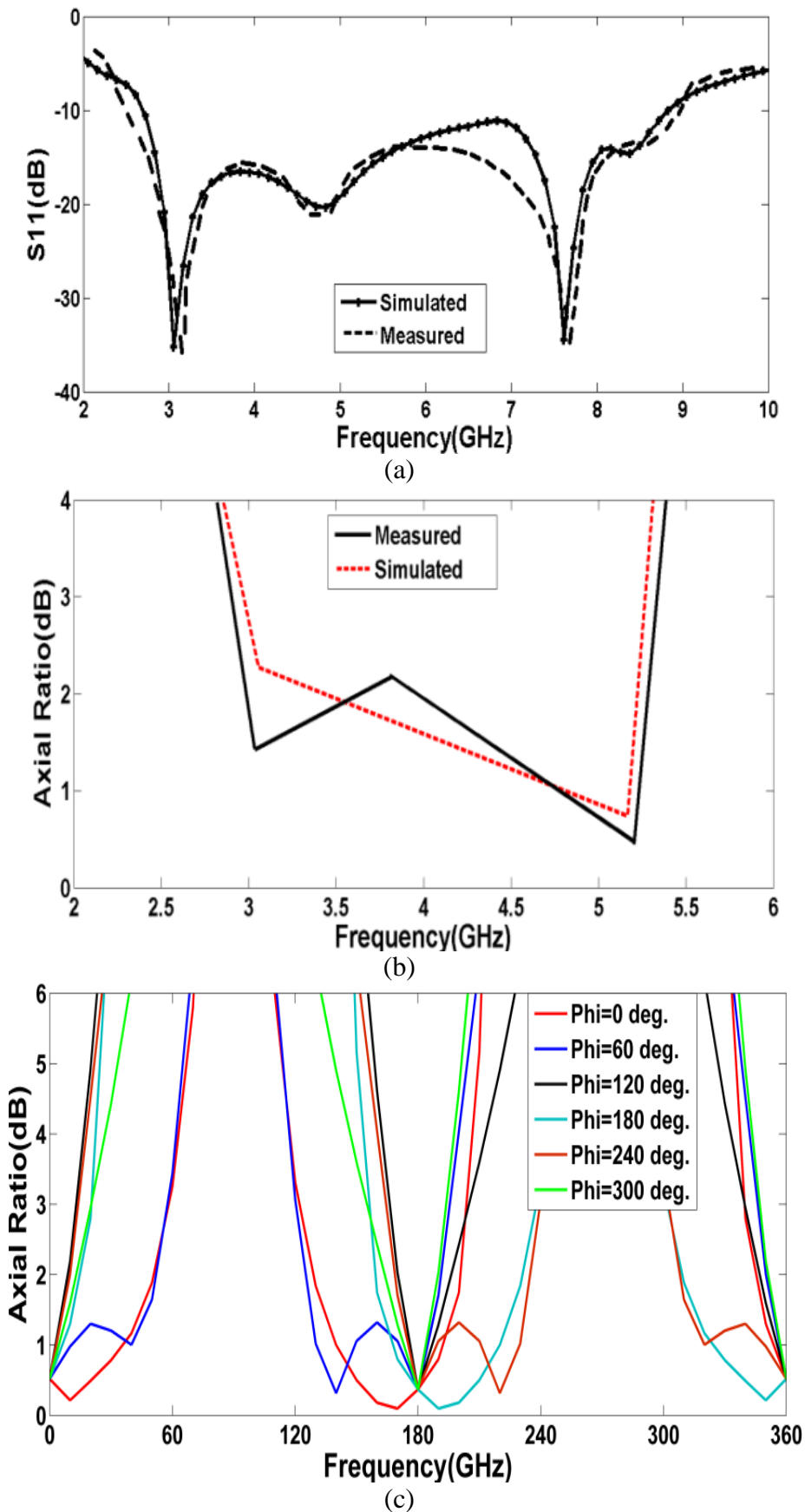


Figure 4.33 : Measured and simulated (a) impedance matching (b) 3dB ARBW of the optimized antenna (Ant. 4) and (c) measured axial ratio of the antenna at different phi values at sample frequency of 5.2GHz

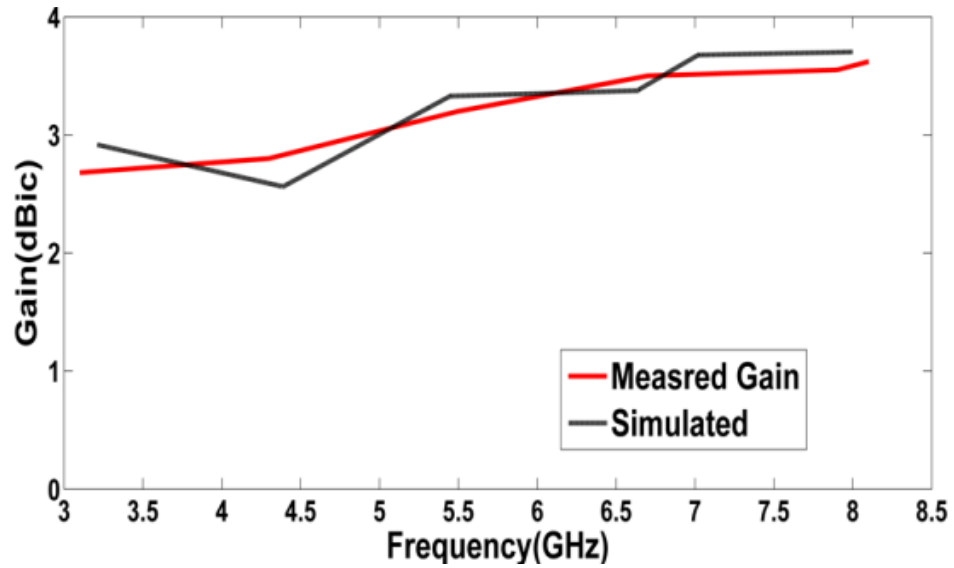


Figure 4.34 : Measured and simulated gain of Ant. 4

4.3.5 Conclusion

A compact, defected substrate structured, and circularly polarized antenna is designed, realized and measured. Circular polarization is excited mainly through removing triangular shaped pieces. Antenna shows a relatively broad band characteristic both in impedance matching and 3dB axial ratio bandwidths. The antenna presented in this work shows broader 3dB bandwidth and smaller size compared to the reported antennas in the literature.

Table 4.3 : Measured 3-Db Arbws, And Measured VSWR<2 Impedance Bandwidths Of Antennas 1–4 (f_c Is The Center Frequency Of VSWR<2) (Unit: mm)

Antennas	VSWR<2 (MHz)	f_c (MHz)	3dB ARBW MHz, %
Ant. 1	2766-3874	3320	0,0
	9232-10213	9722.5	
Ant. 2	2685-4852	3768.5	0,0
	7221-9943	8582	
Ant. 3	2731-6821	4776	0,0
	7351-8853	8102	
Ant. 4	2691-8833	5762	2440,58.93

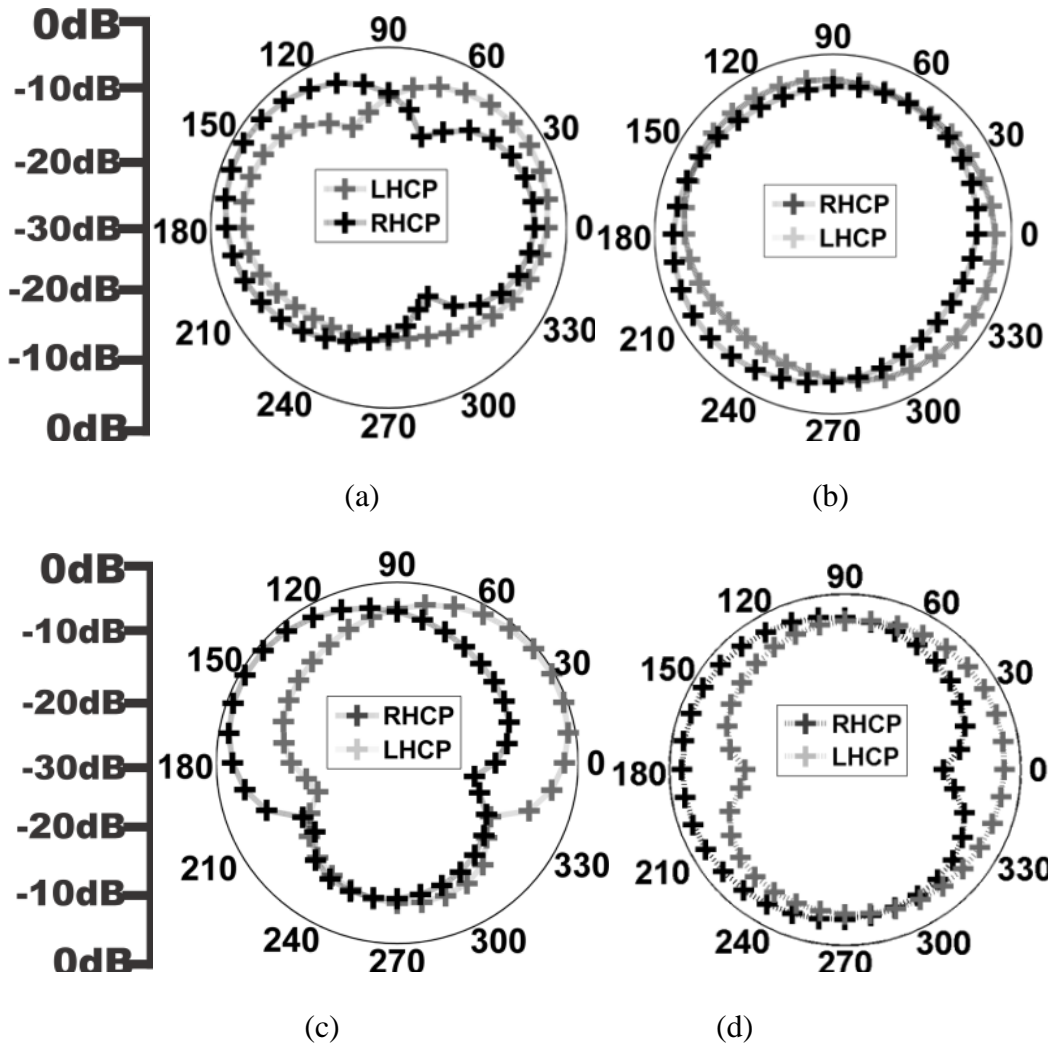


Figure 4.35 : Measured radiation patterns: 4.5GHz (a) $\phi=0$, (b) $\phi=90$ and 5.5GHz (c) $\phi=0$, (d) $\phi=90$

Table 4.4 : Measured Performances Of The Proposed Antenna In The Development Process; $\epsilon_r=4.4$, $\tan \delta=0.02$, $H=0.8$, $G=60$, $L=28$, $Wf=3$, $G=0.3$ (F_c Is The Center Frequency of $VS_{WR}<2$)(Unit: mm)

	Lx1	Ly1	Lx2	Ly2	Lx3	Ly3	Lx4	Ly4	Lx5	Ly5	Lh	Lh2	Lh3	R	VS _{WR} <2 (MHz)	f _c (MHz)	3dB ARBW MHz, %
Ant. 4	7.5	5.5	11.4	11.4	3.5	1.1	8.8	9.3	7.2	6.8	10	9.3	9.9	2.7	2691-8833	5762	2440,58.93
Ant. 5	7.5	5.5	11.4	11.4	0	0	8.8	9.3	7.2	6.8	10	9.3	9.9	2.7	2722-6500 7338- 10005	4611 8671.5	349,6.78
Ant. 6	7.5	5.5	11.4	11.4	3.5	1.1	8.8	9.3	7.2	6.8	8.7	9.3	9.9	2.7	2793-8743	5768	2354,46.53
Ant. 7	7.5	5.5	11.4	11.4	3.5	1.1	8.8	9.3	7.2	6.8	14.9	9.3	9.9	2.7	2785-5166 5944-8611	3975.5 7277.5	0,0
Ant. 8	7.5	5.5	11.4	11.4	3.5	1.1	5.3	5.6	7.2	6.8	10	7.8	9.9	2.7	2722-8722	5722	928,19.16
Ant. 9	7.5	5.5	11.4	11.4	3.5	1.1	10.9	11.5	7.2	6.8	10	15.8	9.9	2.7	2710-8721	5715.5	475,9.6
Ant. 10	7.5	5.5	11.4	11.4	3.5	1.1	8.8	9.3	6.2	6	10	9.3	8.5	2.7	2710-8721	5715.5	636,12.93
Ant. 11	7.5	5.5	11.4	11.4	3.5	1.1	8.8	9.3	7.2	6.8	10	9.3	13.9	2.7	2710-8721	5715.5	749,15.39
Ant. 12	6	5.5	11.4	11.4	3.5	1.1	8.8	9.3	7.2	6.8	10	9.3	9.9	2.7	2722-5944 6833-8944	4333 7888.5	615,12.34
Ant. 13	8.5	5.5	11.4	11.4	3.5	1.1	8.8	9.3	7.2	6.8	10	9.3	9.9	2.7	2693-6500 6944-8722	4596.5 7833	603,11.53
Ant. 14	7.5	5.5	11.4	11.4	3.5	1.1	8.8	9.3	6.2	6.8	10	9.3	8.5	2.1	2744-6166 7500- 10055	4455 8777.5	0,0
Ant. 15	7.5	5.5	11.4	11.4	3.5	1.1	8.8	9.3	7.2	6.8	10	9.3	13.9	3.5	2722-6611 7055-8277	4666.5 7666	0,0

Table 4.5 : Measured Performances Of The Proposed Antennas With Different Substrates And Substrate Thicknesses (F_c is The Center Frequency Of $VS_{WR}<2$)(Unit: mm)

Substrate	$\epsilon_r, \tan \delta$	VS _{WR} <2 (MHz)	f _c (MHz)	3dB ARBW MHz, %
Taconic CER-10(0.8)	10,0.0035	2182-3944 4833-5306 6500-6875	3063 5069.5 6678.5	643,11
Rogers 5880(0.8)	2.2,0.0009	3166- 11116	7141	757,16
Isola Gigaver210(0.8)	3.75,0.003	2793-9277	6035	712,13
FR4(0.8)	4.4,0.02	2691-8833	5762	2440,58.93
FR4(1)	4.4,0.02	2611-8500	5555.5	1522,32.25
FR4(1.6)	4.4,0.02	2611-8500	5555.5	834,17.43

4.4 Broadband CPW-Fed Circularly Polarized Square Slot Antenna with Inverted L-Strips for Wireless Applications

4.4.1 Antenna design

The geometry of the proposed single layer CPW-fed CPSS antenna is shown in figure 4.36. As it is indicated in the figure 4.36, the proposed antenna consists of two united h-shape main patches placed at distance of W_x from each other, embedded to the feed line (L_f). It has three inverted-L strips around corners. Two tuning slits of the size of $W_s \times L_s$ have been cut and removed from feed line. Two main properties, enhancing the impedance bandwidth and enlarging the ARBW have been included within the design. The feed line in conjunction with three inverted-L strips is used for the enhancement of the ARBW. The simulation results show that embedding united h-shape patch to fed mechanism (Ant. I-Ant. III) and increasing L_h parameter result in an increase on the impedance bandwidth. Two tuning stubs are carved and removed from the feeding structure to widen the 3dB ARBW. The proposed CPSS antenna is printed on a FR4 substrate with permittivity of $\epsilon = 4.4$, a loss tangent of 0.024, and compact dimension of $40 \times 40 \times 0.8 \text{ mm}^3$. The width of the CPW feed line is fixed at $W = 3 \text{ mm}$ to achieve $50\text{-}\Omega$ characteristic impedance. The feed section is separated from the grounded structure by a gap of $g = 0.3 \text{ mm}$. The feed line is terminated with a standard SMA connector. The circular polarization mechanism of the proposed CPSS antenna is principally related to the three unequal-size inverted-L strips placed around corners of the square slot with $l_{x1} \times l_{y1}$, $l_{x2} \times l_{y2}$ and $l_{x3} \times l_{y3}$ dimensions.

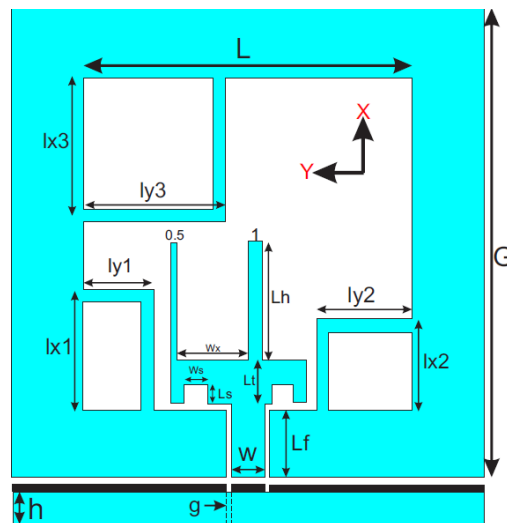


Figure 4.36 : Geometry details of the proposed CPSS antenna (Unit:mm)

4.4.2 Parametric study

The simulated CPSSA structures have been fabricated using conventional printed circuit board (PCB) techniques. The performances of the CPSS antenna in parametric studies have been investigated to find optimized parameters using Ansoft HFSS software. The impedance bandwidth and axial ratio of the CPSSA are measured using the Agilent N5230A vector analyzer.

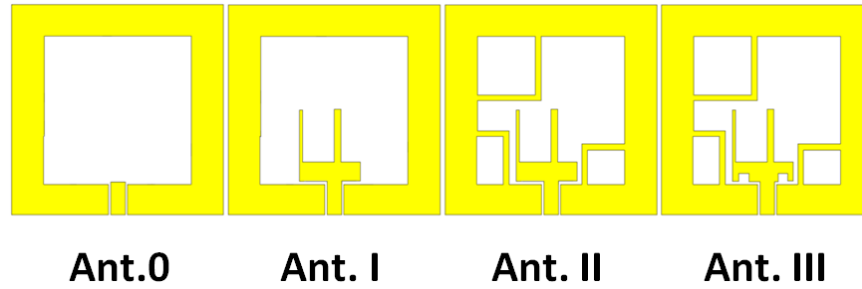


Figure 4.37 : Four improved prototypes of the proposed CPSSA

To simplify the comparison of the proposed antenna design to the antennas introduced in [1-4], the same parameters including $L=28$ mm, $G=40$ mm, and width of inverted-L strips equal to 1 mm have been selected. At first, for clarifying the improvement process, four prototypes of the CPSS antenna are defined as follows (figure 4.37): Ant 0 includes only a rectangular patch; Ant. I contains a 4-shape patch; Ant II has a 4-shape patch, three inverted-L grounded strips; and finally two rectangular tuning slits of the size of $W_s \times L_s$ are removed from the patch with optimized parameters to obtain the Ant.III. W_s and L_s parameters, based on the parametric analysis of the proposed CPSS antenna by HFSS, are optimized to achieve the maximum impedance bandwidth and a wide ARBW. The simulated results for S_{11} and 3dB ARBW of four CPSS antennas are plotted in figure 4.38. As shown in figure 4.38, embedding the inverted-L metal strips to the ground plane has a great effect on the ARBW of Ant I. The 3dB ARBW achieved for Ant II is about 45.80% (3.77–6.01 GHz). The simulation results in figure 4.38 show that if l_{x1} , l_{y1} , l_{x2} , l_{y2} , l_{x3} and l_{y3} of the inverted-L strips are set equal to 7 mm (0.25L), 3dB fractional ARBW will be reduced to 0%. This result indicates the sensitivity of the L-strips on the 3dB axial ratio performance of the antenna. Through extensive simulations and experiments, we have found that increasing l_{x1} , l_{x2} , l_{y2} , l_{x3} and l_{y3} decreasing l_{y1} , based on optimized results presented in Table II, not only increases the amount of ARBW to 45.80% (relative to the center frequency of 4.89GHz) , but also improves impedance bandwidth in higher frequencies between 4–6 GHz.

Furthermore, two equal sized tuning slits are cut and removed from the feeding structure to widen the 3dB axial ratio bandwidth (called Ant III). Simulation results show that if the tuning slits are adjusted in their optimized values (as in figure 4.36), impedance matching in the 3dB AR band can be greatly improved. The horizontal tuning slits are located on the right and left side of the feed section with 0.5 and 2mm distances (considering the x- axis) respectively. As revealed in figure 4.38 and 39, the axial-ratio curve of Ant II is very similar to that of Ant. III, where their S_{11} variations are quite different. The horizontal tuning slits are adjusted to $W_s=2\text{mm}$ and $L_s=1.5\text{mm}$ for the Ant. III, and an additional 3dB axial ratio band between 3–3.77GHz is obtained. In Ant. III the L_h value is adjusted as $L_h=10\text{mm}$ to provide the maximum impedance matching of 2.63-6.38GHz and axial ratio bandwidth of 71.11% (3-6.1GHz).

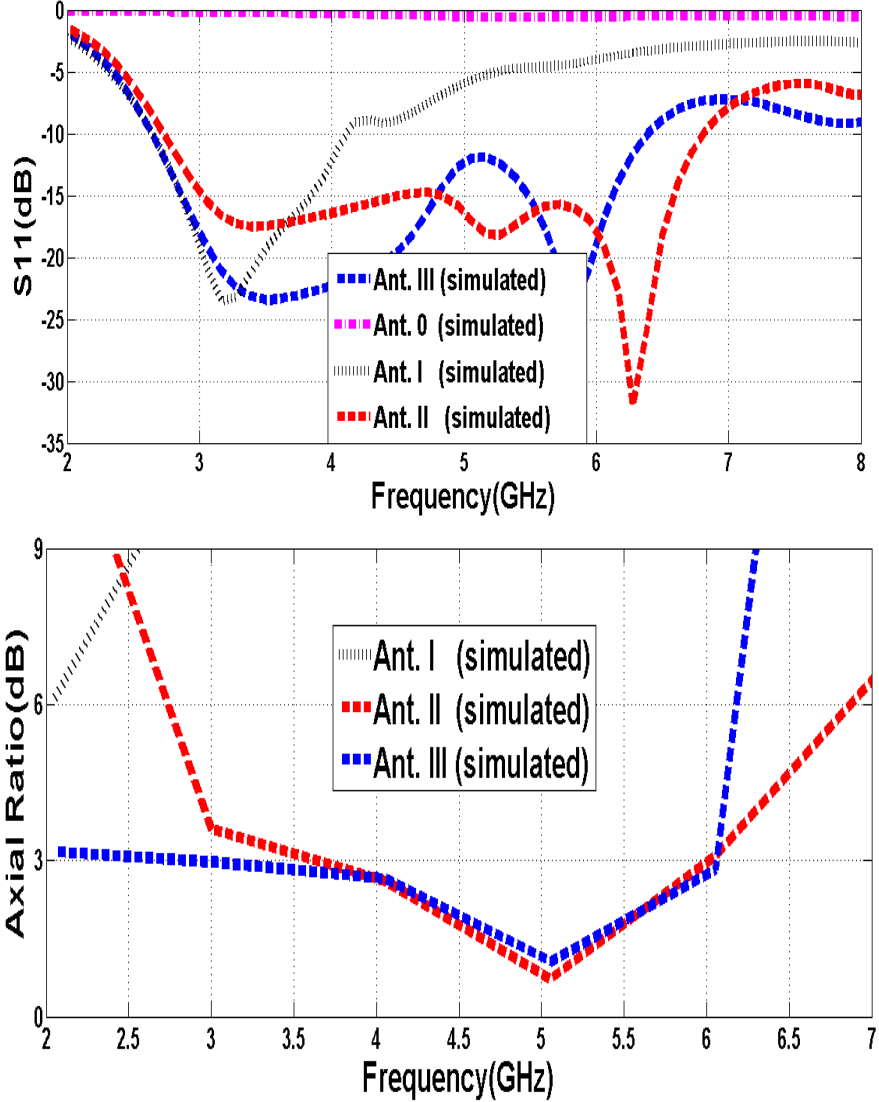


Figure 4.38 : Simulated S_{11} and AR for antennas 0-III

Figure 4.39 indicates the close correspondence between the measured and simulated curves for the Ant. III with optimized values presented in Table 4.8. Both the tuning horizontal slits, when properly adjusted, can not only enhance the coupling among the feed line and inverted-L strips (lower left and right corner), but also further perturb the current distribution in the square slot so that the 3dB axial-ratio bandwidth would be shifted to a lower frequency band as shown in figure 4.38, yet preserving the large 3dB ARBW. Time-varying surface current distribution on Ant.III at 5 GHz which is the center frequency of ARBW is simulated and the results are shown in figure 4.40. It is observed that the surface current distribution in 180° and 270° are equal in magnitude and opposite in phase of 0° and 90° . If the current rotates in the clockwise (CW) direction, the antenna can radiate the right-hand circular polarization (RHCP). The simulated and measured maximum gains are shown in figure 4.41. It can be seen that the both simulated and measured gain are between 3.8–5.8 dBi within the 3dB axial ratio bandwidth from 2.7 to 6.7 GHz. The measured peak gain is 5.8 dBi at 6.28 GHz, while the simulated peak gain is 5.91 dBi. The measured results of the normalized radiation patterns of the CPSS Ant III are also presented in figure 4.41. The radiation pattern is left-hand circular polarization (LHCP) for $Z < 0$ and RHCP for $Z > 0$, as can be deduced from surface current distributions in figure 4.40. It is also interesting to notice that the proposed CPSS antenna has 83.24% impedance bandwidth, which is three times and four times wider than the impedance bandwidth with similar CP technique, respectively. Moreover, the proposed CPSS antenna has a 71.11% fractional circular polarization bandwidth (FCPBW), which is more than two times of FCPBW in antenna with 60X60 substrate, FCPBW of 33% smaller than the same antenna. Its dimensions are also 42% smaller than the antenna presented in [34].

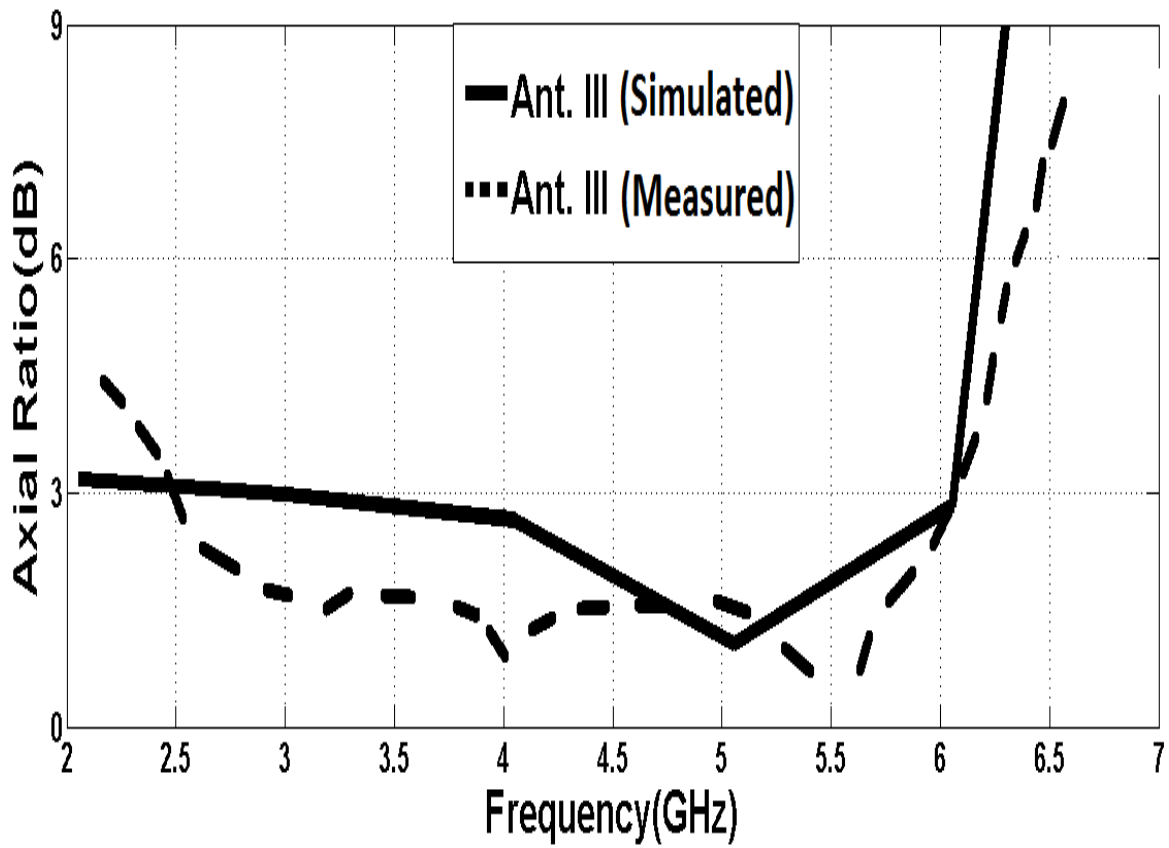
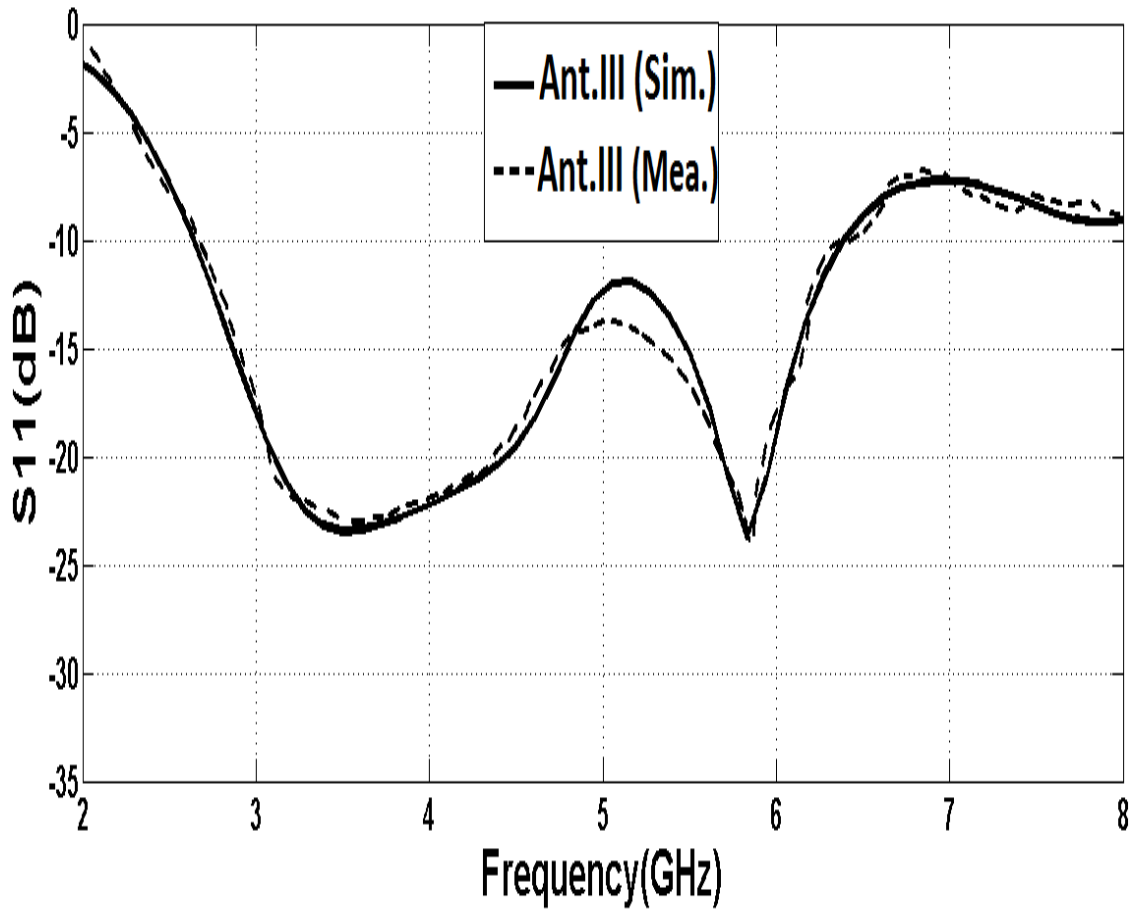


Figure 4.39 : Simulated and measured S_{11} and AR for Ant III

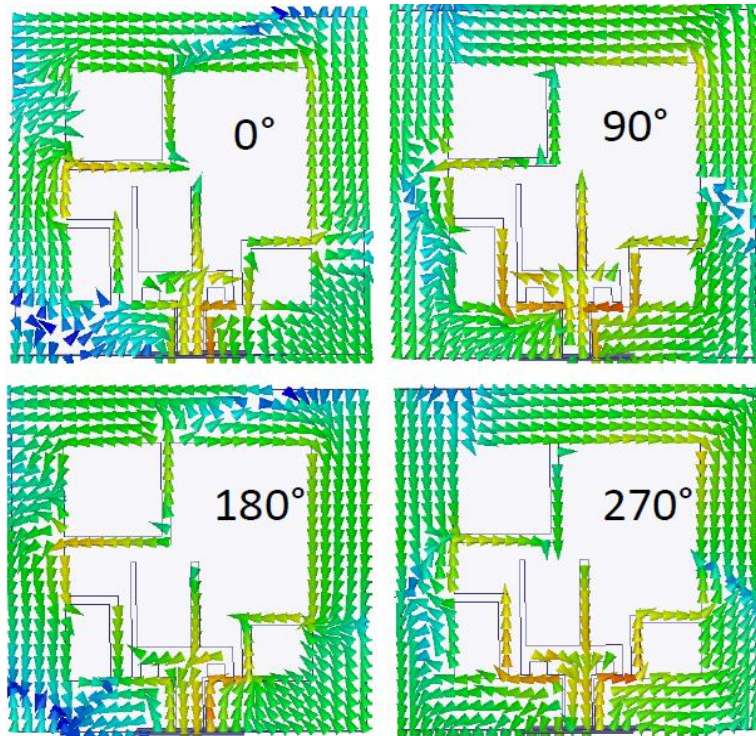


Figure 4.40 : Current distribution of the antenna at 0, 90,180 and 270 degrees

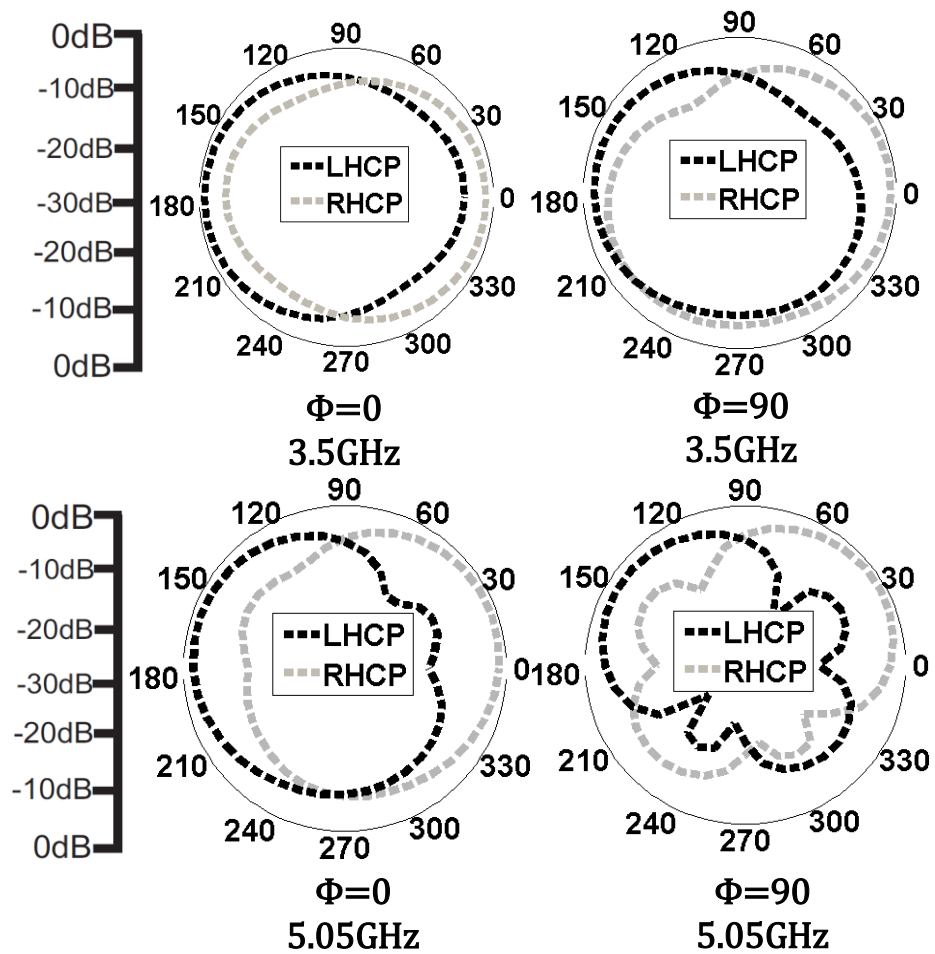


Figure 4.41 : Measured radiation patterns at 3.5 and 5.05GHz at $\phi=0$ and at $\phi=90$ and measured gain of Ant. III

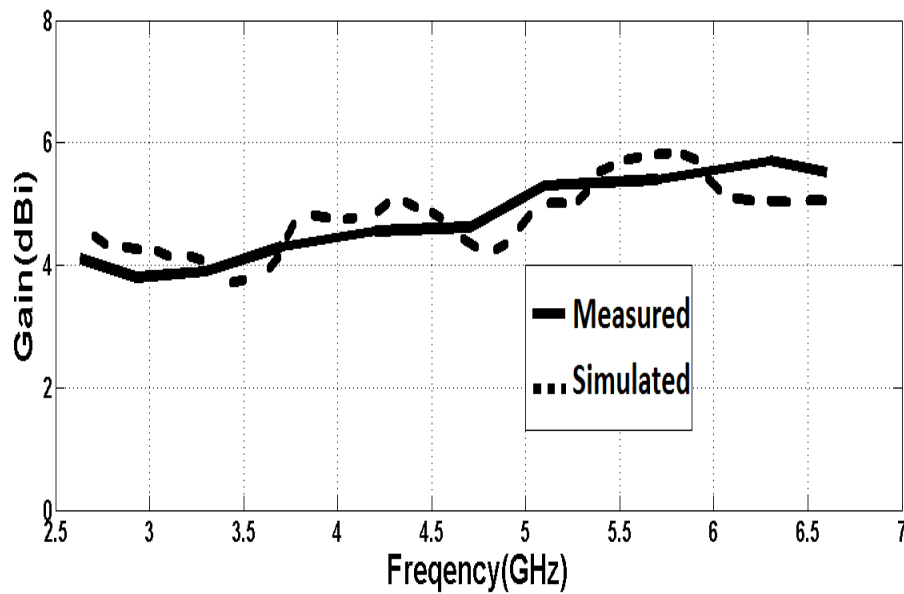


Figure 4.42 : Measured and simulated gain of the antenna

Table 4.6 : Comparison Of Characteristics Of Some Cpss Antennas Reported With The Proposed Antenna In This Work

	BW(VSWR<2) (MHz)	3dB axial ratio (%)	Dimensions (mm)
Ant. II	2772-6833	45.8%	40×40×0.8
Ant. III	2681-6381	71.11%	40×40×0.8
Ref.[28]	2671-1300	32.2%	60×60×0.8
Ref.[35]	1455	25%	60×60×0.8
Ref.[4]	865	18%	70×70×1.6
Ref.[5]	2023-3421	48.8%	60×60×0.8
Ref.[29]	1575-1600	8.4%	70×70×1.6
	1900-2200	19.24%	
Ref.[35]	1772–2591	30.6%	60×60×0.76
Ref.[37]	2240–3940	31.2%	40×60×0.8
Ref.[38]	1330–1580	12.4	70×70×1.6
Ref.[44]	2120 - 6580	23%	40× 39× 1.6
Ref.[32]	2021-3033	9.9%	60×60×1.6
Ref.[39]	1347-1533	4.3%	80×80×1.6
Ref.[30]	1830-2760	12.9%	64×60×1.6
Ref.[34]	1020-2679	65.6%	45×45×0.8

Table 4.7 : Summary Of Measured And Simulated Characteristics Of Some CPSS Antennas. The Impedance Bandwidth Is The Frequency Range where The VSWR Is Equal To Or Less Than 2. ($\epsilon=4.4$, $\tan \delta=0.024$, $H=0.8, G=40, L=28, G=0.3$, $W=3$, $L_f = 6$, $L_t = 3.5$, $W_x=6.25$, $L_h=10$) (Unit: mm)

	lx3	ly3	lx2	ly2	lx1	ly1	Ws	Ls	BW (VSWR<2)	3dB ARBW (%)
Ant. I	0	0	0	0	0	0	0	0	2631-3823	0
Ant. II	12	12	7.5	8	10	6	0	0	2772-6833	45.80%
Ant. III	12	12	7.5	8	10	6	2	1.5	2681-6381	71.11%

5. CONCLUSION

The work presented focused on designing new circularly polarized microstrip and CPW fed antennas operating at various standardized bands. The thesis presented four new designs based on various techniques discussed in CHAPTER 4. It could be seen that inserting inverted L-strips can improve the circular polarization characteristic of the antenna. Using crooked F and T structures was another new technique which was approached during the thesis work. Using defected ground is one of the new techniques which is used in designing CP antennas. To best of the author's knowledge covering a dual band operating antenna frequency band with circular polarization only by changing the feed shape is being achieved for the first time.

REFERENCES

- [1] **Hojoon Lee, Byungchil Han, Yoan Shin, Sungbin Im**, 2000 , Multipath characteristics of impulse radio channels, *Vehicular Technology Conference Proceedings, 2000. VTC 2000-Spring Tokyo. 2000 IEEE 51st* , vol.3, no., pp.2487-2491 vol.3
doi: 10.1109/VETECS.2000.851720
- [2] **CA Balanis** , 2008 . Wiley Online Library
- [3] **Xiu Long Bao, Ammann, M.J., McEvoy, P.**, 2010 ,Microstrip-Fed Wideband Circularly Polarized Printed Antenna," *Antennas and Propagation, IEEE Transactions on* , vol.58, no.10, pp.3150-3156, Oct.
doi: 10.1109/TAP.2010.2055776
- [4] **Jia-Yi Sze, Kin-Lu Wong, Chieh-Chin Huang**, 2003 , Coplanar waveguide-fed square slot antenna for broadband circularly polarized radiation, *Antennas and Propagation, IEEE Transactions on* , vol.51, no.8, pp. 2141- 2144, Aug.
doi: 10.1109/TAP.2003.815421
- [5] **Jia-Yi Sze, Hsu, C.-I.G., Zhi-Wei Chen, Chi-Chaan Chang**, 2010, Broadband CPW-Fed Circularly Polarized Square Slot Antenna With Lightning-Shaped Feedline and Inverted-L Grounded Strips, *Antennas and Propagation, IEEE Transactions on* , vol.58, no.3, pp.973-977, March
doi: 10.1109/TAP.2009.2039335.
- [6] **Jia-Yi Sze, Chi-Chaan Chang**, 2008 , Circularly Polarized Square Slot Antenna With a Pair of Inverted-L Grounded Strips, *Antennas and Wireless Propagation Letters, IEEE* , vol.7, no., pp.149-151
doi: 10.1109/LAWP.2008.921341.
- [7] **Jia-Yi Sze, Wei-Hung Chen**, 2011 , Axial-Ratio-Bandwidth Enhancement of a Microstrip-Line-Fed Circularly Polarized Annular-Ring Slot Antenna, *Antennas and Propagation, IEEE Transactions on* , vol.59, no.7, pp.2450-2456,July
doi: 10.1109/TAP.2011.2152314
- [8] **Pozar, D.M.**, 1985, Microstrip antenna aperture-coupled to a microstripline, *Electronics Letters* , vol.21, no.2, pp.49-50, January 17
doi: 10.1049/el:19850034
- [9] **Carver, K., Mink, J.**, 1981 , Microstrip antenna technology, *Antennas and Propagation, IEEE Transactions on* , vol.29, no.1, pp. 2- 24, Jan.
doi: 10.1109/TAP.1981.1142523

- [10] **G. Singh**, 2010, Design considerations for rectangular micro strip patch antenna on electromagnetic crystal substrate at terahertz frequency, *Infrared Physics& Technology*, Volume 53, Issue 1, January Pages 17-22, ISSN 1350-4495, 10.1016/j.infrared.2009.08.002
- [11] **A. A. Heidari, M. Heyrani, and M. Nakhkash**, 2009, A dual-band circularly polarized stub loaded microstrip patch antenna for GPS applications, *Progress In Electromagnetics Research*, Vol. 92, 195-208
- [12] **Palandoken, M.; Grede, A., Henke, H.**, 2010 , Broadband Microstrip Antenna With Left-Handed Metamaterials, *Antennas and Propagation, IEEE Transactions on* , vol.57, no.2, pp.331-338, Feb. doi: 10.1109/TAP.2008.2011230
- [13] **Dan Sun, Wenbin Dou, Lizhi You**, 2010 , A wideband aperture-coupled microstrip patch antenna with backed cavity of dielectric," *Antennas Propagation and EM Theory (ISAPE), 2010 9th International Symposium on* , vol., no., pp.226-228, Nov. 29 2010-Dec. doi: 10.1109/ISAPE.2010.5696439
- [14] **Moon, S.-M.; Ryu, H.-K., Woo, J.-M., Ling, H.**,2011 , Miniaturisation of $\lambda/4$ microstrip antenna using perturbation effect and plate loading for low-VHF-band applications, *Electronics Letters* , vol.47, no.3, pp.162-164, Feb.3 doi: 10.1049/el.2010.3647
- [15] **W.-J. Liao, S.-H. Chang, Y.-C. Chu, and W.-S. Jhong**, 2010, A beam scanning phased array for uhf rfid readers with circularly polarized patches, *J. of Electromagn. Waves and Appl.*, Vol. 24, 2383–2395
- [16] **T. Hong, L.-T. Jiang, Y.-X. Xu, S.-X. Gong, and W. Jiang**, 2010, Radiation and scattering analysis of a novel circularly polarized slot antenna, *J. of Electromagn. Waves and Appl.*, Vol. 24, 1709–1720
- [17] **T. S. Ooi , S. K. A. Rahim**,2010, 2.45 GHz and 5.8GHz compact dual band circularly polarized patch antenna”, *J. of Electromagn. Waves and Appl.*, Vol. 24, 1473–1482,
- [18] **C. Lin, F.-S. Zhang, Y. Zhu, and F. Zhang**,2010, A novel three-fed microstrip antenna for circular polarization application, *J. of Electromagn. Waves and Appl.*, Vol. 24, 1511–1520
- [19] **S. Du, Q.-X. Chu, and W. Liao**,2010, dual-band circularly polarized stacked square microstrip antenna with small frequency ratio, *J. Of Electromagn. Waves and Appl.*, Vol. 24, 1599–1608
- [20] **C.-N. Chiu, C.-C. Yang**,2010, A new board-integrated single microstripfed circularly polarized monopole antenna for global positioning satellite receivers, *J. of Electromagn. Waves and Appl.*, Vol. 24, 903–909
- [21] **X. Li, Y.-J., X.-L. Liu**, 2010, A novel design of wideband circular polarization antenna array with high gain characteristic, *J. of Electromagn. Waves and Appl.*, Vol. 24, 951–958
- [22] **C.-L. Tsai**, 2010, A study on the non-uniform rectangular ring slot antenna for broadband circular polarization operations, *J. of Electromagn. Waves and Appl.*, Vol. 24, 543–555

- [23] **C.-H. Lai**, 2009, Circularly-polarized reconfigurable microstrip antenna, *J. of Electromagn. Waves and Appl.*, Vol. 23, 195–201
- [24] **C.-L. Tsai, S.-M. Deng**, 2009, A novel shorted rectangular-loop antenna for circularly polarized wave operations, *J. of Electromagn. Waves and Appl.*, Vol. 23, 1323–1334
- [25] **X. Bai, X. M. Zhang, L. Li, Q. Yang, and J. Y. Li**, 2009, Double-sided printed four rhombic-loop antenna with parasitic loops for circular polarization, *J. of Electromagn. Waves and Appl.*, Vol. 23, 1795–1802
- [26] **J. Chen, G. Fu**, 2009, Broadband circularly polarized combinatorial slot antenna, *J. of Electromagnetic. Waves and Appl.*, Vol. 23, 2127–2134
- [27] **A.-N. Wang, W.-X. Zhang**, 2009, Design and optimization of broadband circularly polarized wide-slot antenna, *J. of Electromagn. Waves and Appl.*, Vol. 23, 2229–2236
- [28] **J. Pourahmadazar, Ch. Ghobadi, J. Nourinia, N. Felegari, and H. Shirzad**, 2011, Broadband CPW-Fed Circularly Polarized Square Slot Antenna With Inverted-L Strips for UWB Applications, *IEEE antennas and wireless propagation letters*, VOL. 10
- [29] **C. Chen, E. K. N. Yung**, 2009, Dual-Band Dual-Sense Circularly-Polarized CPW-Fed Slot Antenna With Two Spiral Slots Loaded, *IEEE transactions on antennas and propagation*, VOL. 57, NO. 6, JUNE
- [30] **Kow-Ming Chang, Ren-Jie Lin, I-Chung Deng, and Qing-Xiang Ke**, 2007, A Novel Design Of A Microstrip fed shorted Square-Ring Slot Antenna For Circular Polarization, *Microwave And Optical Technology Letters / Vol. 49, No. 7, July*
- [31] **J. Sze, C. Hsu, Z. Wei Chen, and C. Chaan Chang**, 2010, Broadband CPW-Fed Circularly Polarized Square Slot Antenna With Lightning-Shaped Feedline and Inverted-L Grounded Strips, *IEEE transactions on antennas and propagation*, VOL. 58, NO. 3, MARCH
- [32] **J. Sze, Chung-I. G. Hsu, M. Ho, Y. Ou, and M. Wu**, 2007, Design of Circularly Polarized Annular-Ring Slot Antennas Fed by a Double-Bent Microstripline, *IEEE transactions on antennas and propagation*, VOL. 55, NO. 11, NOVEMBER
- [33] **C.-J. Wang Y.-C. Lin**, 2008, New CPW-fed monopole antennas with both linear and circular polarization, *IET Microw. Antennas Propag.*, Vol. 2, No. 5, pp. 466–472
- [34] **W.H. Chen**, 2011, Axial-ratio-bandwidth Enhancement of a Microstrip-line-fed Circularly Polarized Annular-ring Slot Antenna, *IEEE Early access*
- [35] **J.-C. Wang, C.-C. Chang**, 2008, Axial-ratio bandwidth enhancement of asymmetric-CPW-fed circularly-polarised square slot antenna, *Electronics Letters* 28th August Vol. 44 No. 18
- [36] **Shi. Fu, Sh. Fang, Zh. Wang, and X. Li**, 2009, Broadband Circularly Polarized Slot Antenna Array Fed by Asymmetric CPW for L-Band Applications, *IEEE Antennas And Wireless Propagation Letters*, VOL. 8

- [37] **Chien-Jen Wang, Chih-Hsing Chen**, 2009, CPW-Fed Stair-Shaped Slot Antennas With Circular Polarization, *IEEE Transactions On Antennas And Propagation*, VOL. 57, NO. 8, AUGUST
- [38] **C.H. Chen, E.K.N. Yung and B.J. Hu**, 2007, Miniaturised CPW-fed circularly polarized corrugated slot antenna with meander line loaded, *Electronics Letters* 6th December Vol. 43 No. 25
- [39] **Kin-Lu Wong, Chien-Chin Huang, and Wen-Shan Chen**, 2002, Printed Ring Slot Antenna for Circular Polarization, *IEEE transactions on antennas and propagation*, VOL. 50, NO. 1, JANUARY
- [40] **H.Chen, and H.T.Chen**, 2004, A CPW-Fed Dual-Frequency Monopole Antenna”, *IEEE Transactions On Antennas And Propagation*, VOL. 52, NO. 4, APRIL
- [41] **J Ki.Wong**, 2001, Bandwidth Enhancement of a Microstrip-Line-Fed Printed Wide-Slot Antenna, *IEEE Transactions On Antennas And Propagation*, VOL. 49, NO. 7, JULY
- [42] **S. F. R. Chang, W. L. Chen, S. C. Chang, C. K. Tu, C. L. Wei, C. H. Chien, C. H. Tsai, J. Chen, and A. Chen**, 2005, A dual-band RF transceiver for multistandard WLAN applications, *IEEE Trans. Microw. Theory Tech.*, vol. 53, pp. 1048–1055, Mar.
- [43] **Ch.I G. Hsu, and Sh.Ch. Hsu**, 2007, Design of a Compact Dual-Band Annular-Ring Slot Antenna, *IEEE Antennas And Wireless Propagation Letters*, VOL. 6
- [44] **Christina F. Jou, Jin-Wei Wu, and Chien-Jen Wang**, 2009, Novel Broadband Monopole Antennas With Dual-Band Circular Polarization, *IEEE Transactions On Antennas And Propagation*, VOL. 57, NO. 4, APRIL

CURRICULUM VITAE



Name Surname: Sasan Ahdi Rezaeieh

Place and Date of Birth: Iran 16.08.1986

Address: Bahçeköy öğrenci yurdu

E-Mail: ahdi@itu.edu.tr

B.Sc.:IAU Urmia-Iran- Telecommunication Engineering

List of Publications and Patents:

- An Ultra Wide Band Miniaturized Monopole Antenna for Microwave Near-Field Measurement Applications, **Sasan Ahdi Rezaeieh**, Mehmet Abbak, Javad Janghi, Tuba Alpaya, Ibrahim Akduman, ISMOT 2011, June 20 - 23, Prague, Czech Republic, EU
- Broad-Band Three Layer Suspended Plate Antenna, Mehmet Abbak, **Sasan Ahdi Rezaeieh**, Ibrahim Akduman, Accepted for presentation in proceeding of TELFOR (IEEE) 2011 Belgrade Serbia Nov. 2011

PUBLICATIONS/PRESENTATIONS ON THE THESIS

- A Circularly Polarized Square Slot Antenna for Wireless Applications, **Sasan Ahdi Rezaeieh**, Mehmet Abbak, Ibrahim Akduman, Accepted for presentation in proceeding of TELFOR (IEEE) 2011 Belgrade Serbia Nov. 2011